The mechanics of active clays circulated by salts, acids and bases -Comprehensive version-

Alessandro Gajo[(1)] and **Benjamin Loret**[(2)]

[(1)] Dipartimento di Ingegneria Meccanica e Strutturale,
Università di Trento, via Mesiano 77, 38050 Trento, Italia
Alessandro.Gajo@ing.unitn.it *

[(2)] Laboratoire Sols, Solides, Structures
B.P. 53X, 38041 Grenoble Cedex, France
Benjamin.Loret@inpg.fr

July 12, 2007

Keywords: electro-chemo-mechanical couplings; pH; clays;
fluid-saturated porous media; elasto-plasticity

Abstract

An elastic-plastic model that accounts for electro-chemo-mechanical couplings in clays has been proposed in Gajo et al. [2002] and Gajo and Loret [2004]. Chemically sensitive clays are viewed as two-phase multi-species saturated porous media circulated by an electrolyte. The model can simulate elementary and complex mechanical and chemical loading paths involving changes of ionic concentrations and ionic replacements in homoionic and heteroionic active clays.

An extension that accounts for the effects of pH variations is presented here. The developments are embedded in the framework of the thermodynamics of multi-phase multi-species porous media.

Four transfer mechanisms between the solid and fluid phases are delineated: (1) hydration, (2) ion exchange, (3) acidification, (4) alkalinization. The rates of change of the various species that sorb to the clay, or desorb from it, are derived. The variation of the electrical charge of the minerals, which is a key to the electro-chemo-mechanical couplings, is addressed by the same token. These four mechanisms are seen as controlling much of the elastic and elastic-plastic behaviors of the clay mass. Depending on concentrations and ionic affinities to the minerals, these mechanisms either compete or cooperate to modify the compressibility and strength of the clay, and induce swelling (volume expansion) or chemical consolidation (volume decrease). The framework is rich enough to allow for the simulations of available laboratory experiments where clay samples are submitted to intertwined mechanical and chemical loading programmes, involving large changes in ionic strengths and pH.

*Corresponding author. Phone: 39 0461 882519 Fax: 39 0461 882599

1 Introduction

Chemically sensitive clays are viewed as two-phase multi-species saturated porous media circulated by an electrolyte. In the present work, the permeant fluid will be water, and these are the nature and concentration of the ions dissolved in the pore water that will be varied, as they might during typical processes, like contaminant extraction and stabilizing injection.

In a previous study, Gajo et al. [2002] have developed a model that incorporates the changes of compressibility and strength under modifications of pore water composition. Changes in mechanical properties are induced by transfer, namely by absorption/desorption, of cations and water between the pore fluid and the clusters of clay particles. Finite element simulations of transient laboratory experiments during which an initial 1 M NaCl solution in contact with the clay sample is totally diluted or replaced by a 1 M KCl solution have been presented in Gajo and Loret [2004].

The developments described here enrich this model, by embedding the influence of the pH of the electrolyte in the mechanical properties. The following observation may serve as a motivation. During soil remediation processes, acidification propagates through the soil from the anode towards the cathode, and it is the key mechanism that promotes desorption of cations. The acidification front is accompanied with a deformation front, so that settlements are spatially heterogeneous. Standard analyzes address the transport issues associated to remediation, and disregard settlements. While both transport and mechanical issues should be addressed, attention here is concentrated on the electro-chemo-mechanical couplings induced by pH.

In fact, the minerals of chemically sensitive clays are electrically charged. This charge is said to be *fixed*, in contrast to that of *mobile* ions. Part of the fixed charge, located on the faces of the clay units, is *permanent* and negative: it is due to isomorphous substitution of cations of charge +3 or +4 in the crystal lattice against cations of lower charge. At the time scale of interest here, the permanent charge can be considered as frozen, independently of the pore water content: ions located in the absorbed water compete to form inner and outer sphere complexes that contribute to establish electroneutrality within the volume containing the particles and the inter-layer water. This mechanism, termed ion exchange, is ruled by the relative affinity of the ions to the sites of permanent charge, referred to as X-sites. On the other hand, the charge of the edges, and of part of the faces in kaolinites, is *variable*. This variable charge is modified by pH via surface complexation mechanisms that involve the hydrogen and hydroxyl ions.

The relative weight of the variable versus permanent charges is much higher in kaolinites, about 1 or more, than in montmorillonites, about 10% to 20%. Indeed, there exists in kaolinites a value of pH, from 2 to 4, termed isoelectric point, at which the total fixed charge of clay minerals vanishes. Below this pH, the variable charge is so positive as to imply the total fixed charge to be positive as well. In montmorillonites, the variable charge can not overweigh the permanent charge, and the isoelectric point of the variable charge at clay edges ranges between 5 and 8.

The developments are embedded in the framework of the thermodynamics of multi-phase multi-species porous media. Four transfer mechanisms between the solid and fluid phases are delineated: (1) hydration, (2) ion exchange, (3) acidification, (4) alkalinization. These four mechanisms are seen as controlling partially the elastic and elastic-plastic behaviors of the clay. Ion exchange on the sites of permanent charge, surface complexation associated to acid-base reactions, and electrical shielding at increasing ionic strength of pore fluid either compete or cooperate to induce swelling or chemical consolidation. The sole ionic strength of the aqueous solution is not sufficient to describe the available laboratory data, and the time history of

individual ionic concentrations needs to be followed.

A brief review of instances where these interactions, or electro-chemo-mechanical couplings, are at work, is presented in Sect. 2. Next is introduced the two-phase multi-species framework that includes both the transport and mechanical aspects, Sect. 3. An effort is made to embed the developments in the framework of the thermodynamics of porous media. This approach has the advantage of providing a comprehensive overview of the different physical phenomena, and of structuring their interactions. The Clausius-Duhem inequality constrains strongly the various couplings, and minimizes the number of constitutive functions and parameters, Sect. 4. The transfer mechanisms between the phases are delineated, and the rates of change of the various species that sorb to the mineral, or desorb from it, are derived, Sect. 5. The variation of the electrical charge of the minerals is obtained by the same token. The four mechanisms are subsequently built in the elastic and elastic-plastic constitutive equations of the two-phase material, Sects. 6 and 7 respectively. The elastic-plastic model can be seen as a prototype, that extends the standard Cam-Clay plasticity. Other plastic models could be used as well. Still, the framework is versatile enough to allow for the simulations of laboratory experiments where clay samples are submitted to intertwined mechanical and chemical loading programmes.

While a number of geological, biological and engineered materials contain a fixed electric charge, comprehensive sets of data on the mechanical effects of pH on these materials are not available. Still, sparse information indicates unambiguously that the apparent compressibility depends strongly on the magnitude of the charge. Confined compression tests on articular cartilages by Grodzinsky et al. [1981] show that the axial stress necessary to ensure equilibrium has a minimum at the isoelectric point. A similar observation applies to the relative hydration, namely ratio of wet weight over dry weight, of bovine cornea, Huang and Meek [1999]. On cross-linked polymer chains of hydrogels that contain acidic and basic groups, De and Aluru [2004] note that an increase of pH of the aqueous solution implies swelling, which is reversible upon decrease of pH.

The above biological tissues and engineered electro-active polymers are endowed with an elastic or visco-elastic mechanical behavior. On the other hand, we are not aware of previous attempts at embodying the effects of pH in the elastic-plastic behavior of geomaterials. Moreover, the present analysis goes clearly beyond former studies by Esrig [1968], Olsen [1969] and Wan and Mitchell [1976] inter alii where the coupled effects of consolidation and electrokinetics were simply superposed, in linear analyzes, without interactions nor direct chemo-mechanical feedbacks: non-linearities have to be accounted for, as they characterize the modifications of mechanical and transport properties by the developing processes.

The presence of the ions hydrogen and hydroxyl, in addition to metallic ions, strongly affects the transport properties. Indeed, the sign of the electro-osmotic coefficient is opposite to that of the fixed electric charge. Thus, while electro-osmosis implies water to move towards the cathode above the isoelectric point, reverse osmosis takes place at very low pH below the isoelectric point of kaolinites. However, the modifications of our previous framework for generalized diffusion, Gajo et Loret [2004], Loret et al. [2004], are not envisaged here but postponed to a future work.

Notation: Compact or index tensorial notation will be used throughout this text. Tensor quantities are identified by boldface letters. Symbols '$\cdot$' and ':' between tensors of various orders denote their inner product with single and double contraction respectively. Unless stated otherwise, the convention of summation over repeated indices does <u>not</u> apply.

2 Field and laboratory observations

Electrokinetics has been used in environmental applications in various directions that take advantage, enhance or decrease some properties of clays and clayey soils: in order to assess and optimize the impermeability of barriers to contaminants, Yeung [1990], to extract pollutants from contaminated soils, or to inject at cathode negatively charged nutrients so as to enhance bioremediation, Thevanayagam and Rishindra [1998].

Electrokinetics has historically first targeted remediation, and the associated modelling of transport. However, the interactions between pore water composition and mechanics are becoming an issue. Indeed, the origins of the settlements induced by remediation have to be understood, modelled and controlled. These developments are also triggered by a more recent use of electrokinetics, namely the injection of chemicals aimed at improving mechanical properties, Alshawabkeh and Sheahan [2002].

A brief description of the laboratory and field experiments where chemo-mechanical couplings are clearly active will serve to motivate the theoretical developments proposed in this work. However the effects of pH in the remediation processes are stressed first.

Electrokinetic remediation aims at removing heavy metals (lead, cadmium, chromium, copper, strontium $\cdots$) from several types of clays, including kaolinites and montmorillonites, as well as organic pollutants dissolved in contaminated soils (acetic acid, phenol, gasoline hydrocarbons $\cdots$). A review of experimental results up to 1990 is presented by Acar [1992]. Laboratory setups to extract cadmium and copper from saturated kaolinite are described in Acar et al. [1994] and Eykholt and Daniel [1994] respectively.

A significant step forward in the understanding of electrokinetic processes is due to Acar et al. [1994]. They show that a most prominent phenomenon is the development of an acid front starting close to the anode and moving towards the cathode. An electrolytic decomposition of water in ions hydrogen and hydroxyl occurs at the electrodes. The mobility of these ions is high with respect to that of other ions and, once generated, they move in the soil by advection of the pore fluid, fickian diffusion and migration due to electrical field. The acid front created by the motion of hydrogen ions H^+ towards the cathode and the basic front created by the motion of hydroxyl ions OH^- towards the anode are not symmetric. Indeed, first, the mobility of the former is much larger, and, second, the motion of the H^+'s (resp. OH^-'s) is assisted (resp. opposed) by electro-osmosis.

The modelling of electrokinetic remediation processes accounts for advection of contaminants by water flow. Models differ in the way they include ionic mobility of the various species present in the pore fluid, and in the number of electro-chemical reactions included, Yeung and Datla [1995], Alshawabkeh and Acar [1996], but they assume a rigid solid skeleton.

Still, Di Maio and Fenelli [1997] and Di Maio [1998] have reported spectacular chemo-mechanical couplings on various homoionic and heteroionic clays of Southern Italy. They have performed oedometric tests where active clays are kept in contact with a reservoir whose chemical composition is varied in time. Replacement of deionised water in the reservoir by an electrolyte containing an increasing concentration of NaCl results in osmotic consolidation, decreased compressibility and increased strength. Replacement of deionised pore water by a solution of KCl instead of NaCl amplifies all these phenomena. The nature and initial mineralogical composition of the clays tested affect these features quantitatively but not qualitatively. Cycling over the chemistry of the reservoir initially amplifies the above effects as well but a stabilization is observed after a few cycles. The irreversibility of the strains induced by chemi-

cal cycling should be examined with care. Indeed, some symmetry in the chemical sequence is observed to unlock the strain that, in a first step, might have been thought to be plastic, Loret and Gajo [2004].

An elastic-plastic model that accounts for these chemo-mechanical couplings is proposed in Gajo et al. [2002] and finite element simulations of the phenomena involved in the oedometer tests, namely mass transfer, coupled diffusion and deformation, are described in Gajo and Loret [2004].

Note that no external electrical field is applied in the experiments of Di Maio and coworkers. In contrast, the experiments by Alshawabkeh and Sheahan [2002] to improve mechanical properties involve three types of *electrokinetic stabilization*: i) electro-osmotic consolidation where an electrical gradient, is applied, without mechanical load, in order to extract pore fluid; ii) electro-osmotic flow to draw stabilizing chemicals into the soil; iii) ionic migration with addition of an acid at the cathode, and extraction of a minimum of fluid in order to minimize advection that opposes motion of anions towards the anode. Their experiments on Boston Blue Clay, a marine illitic clay, show that modifications of transport and mechanical properties by pH may not be simultaneous. Addition of nitric acid NH_3 is observed to change the sign of the electro-osmotic conductivity and to give rise to reverse osmosis; this phenomenon is not observed for phosphoric acid H_3PO_4. On the other hand, the drained shear strength increases when the soil is acidified by phosphoric acid only: the phenomenon is attributed to (instantaneous) dissolution of soil minerals and (slower) precipitation of phosphate minerals that creates interparticular forces/*cementation*.

Quite generally, acidification tends to reduce absorbed water, enhance face-to-edge contacts, i.e. flocculation, which both are expected to decrease compressibility and increase strength. For example, Cascini and Di Maio [1994] performed oedometric tests on Vesuvium ash (clayey pozzuolana) and on a peat where the sample is in equilibrium with a reservoir of controlled chemical composition. Initial mechanical consolidation is performed with deionised water in the reservoir. Then deionised water is substituted by an electrolyte at constant load. Replacement of deionised water by a saturated solution of NaCl induces consolidation but replacement by a 5% acetic acid solution induces a still much larger consolidation of both materials.

In order to address the effects of pore water composition and pH on a Na-bentonite, Gajo and Maines [2007] have performed three types of tests, namely oedometric tests to assess the changes in compressibility and permeability, shear tests to check the changes of residual strength, and measurements of liquid limit (LL). The mechanical effects were found to be compatible with the model of ionic replacement described in Gajo et al. [2002]. In this model, the relative order of affinity of ions to the X-sites is shown to play a key role. The effects of pH can be qualitatively explained with this model if the hydrogen ions are considered to have the highest affinity to the X-sites. The present developments aim at quantifying these observations, and some of the results of Gajo and Maines [2007] will be used to test the enlarged framework.

The presence of certain minerals might make obscure the interpretation of the effects of pH on mechanical properties. Du et al. [1987] show that the dynamic shear modulus presents an extremum for some value of pH: this extremum, at pH about 7, is a minimum for a mixture of sand and kaolinite, and it is a maximum, at pH about 10, for a mixture of sand and bentonite. Torrance and Pirnat [1984] observe that the shear strength of carbonate-free Leda clay decreases monotonously as pH increases, but it displays a maximum at pH about 6 when carbonates are present. At extreme pHs, some high valence cations might be expelled from the clay mineral first to the absorbed water surrounding them, and, next to the free water.

However, the minerals are considered below to remain intact, and a description of the modifications of the structure of the clay goes beyond the present framework. The main issue targeted is the change of variable charge. The experiments performed by Gajo and Maines [2007] indicate that such an analysis is relevant for montmorillonites: even paths involving successive excursions in the acid and basic regions show a sort of reversibility, which witnesses a permanent microstructure. On the other hand, preliminary tests seem to indicate that such a conclusion does not apply to kaolinites.

Similarly, the analysis does not address a number of physico-chemical phenomena, like cementation, or formation of hydroxy-complexes and salt precipitation, that are of practical significance for a successful remediation process: these are postponed to be reported together with simulations of field processes as initial and boundary value problems.

3 The mixture framework

The clay mass is viewed as a two-phase porous medium. Each phase is composed of several species as sketched in Fig. 1 .

3.1 The two phases

Defining the phases of the mixture represents a main step of the model. There are several ways to partition species in phases in electrically charged porous media saturated by an electrolyte. The role of the nanometric structure of the solid components of the mixture is discussed and highlighted in Loret and Gajo [2004]. The phase definition adopted here follows ideas advocated in our previous works on heteroionic clays, Gajo et al. [2002].

The solid phase is constituted by the assembly of clusters of mineral sheets. The latter are bathed in an electrolytic solution, which constitutes the fluid phase. The clusters are surrounded by a fictitious membrane whose permeability is species-dependent. The sole fluid phase is in contact with the surroundings. Water and exchangeable ions *transfer* between the solid and fluid phases. The membrane is a tool that allows much flexibility. It may serve also as a barrier against anions or non-exchangeable cations. For example, chloride ions Cl^- might be considered to be mainly excluded from the clay interlayers when the clay sheets are negatively charged. This simplification is motivated by the fact that, at moderate to high pH, anions undergo electrical repulsion by the negatively charged clay sheets. This exclusion could be used for montmorillonites but it does not apply to kaolinites below the isoelectric point, where the clay minerals are positively charged. On the other hand, here, the membrane is impermeable to clay particles. Once again, this assumption may be removed in future studies to account for the dissolution of clay minerals due to acid attack for example, as sketched in Fig. 2.

The chemical compositions of bulk water and absorbed water are distinct: indeed even if a species is present at both places, its molar fractions differ. The species of each phase are gathered into sets, e.g. $\mathcal{S}$ for the solid phase. The species of the fluid phase

$$\mathcal{W} \equiv \{Na^+, Cl^-, H^+, OH^-, w = H_2O\}$$

can, both, exchange with the surroundings by diffusion, and transfer to and from the solid phase, according to specific mechanisms. However, the framework could naturally accommodate a species that communicates with the surroundings only, or that remains within the fluid phase.

The hydrogen and hydroxyl ions may establish different bonds with the clay minerals, resulting in different mechanical and electrical effects. Thus subsets of these ions will be tied to the transfer mechanism through which they enter the solid phase.

3.2 Basic entities

As a rule, a species in a phase is referred to by two indices, the index of the species and the index of the phase, the only exception being clay particles, denoted by the subscript c, and clay sites X– for ion exchange and S–O^-, S–OH and S–OH_2^+ for acid-base reactions, which unambiguously belong to the solid phase.

3.2.1 Electro-chemical potentials

A key entity that accounts for the electro-chemical properties of species k of phase $\mathcal{K}$ is the mole-based *electro-chemical potential* $g^{\rm ec}_{kK}$ [unit kg/mole×$\rm m^2/s^2$], which is work-conjugate to the mole content $\mathcal{N}_{kK}$, much like the stress $\boldsymbol{\sigma}$ is conjugate to the strain $\boldsymbol{\epsilon}$. An alternative, and equivalent, entity is the mass-based *electro-chemical potential* $\mu^{\rm ec}_{kK}$ [unit $\rm m^2/s^2$], which is work-conjugate to the mass content m_{kK}. Indeed the incremental work done by the stress $\boldsymbol{\sigma}$ in the strain $\delta\boldsymbol{\epsilon}$ and by the electro-chemical potentials in supplying, or removing, chemical species can be cast in either form,

$$\delta\Psi = \boldsymbol{\sigma} : \delta\boldsymbol{\epsilon} + \sum_{k,K} g^{\rm ec}_{kK}\,\delta\mathcal{N}_{kK} = \boldsymbol{\sigma} : \delta\boldsymbol{\epsilon} + \sum_{k,K} \mu^{\rm ec}_{kK}\,\delta m_{kK}\,. \tag{3.1}$$

Summation extends to all chemicals, whose mass is not constant.

For the species k in the fluid phase $\mathcal{W}$, the classical formula of the chemical potential, e.g. Kestin [1968], identifies (1) a purely mechanical contribution, which involves the *intrinsic pressure* of the fluid phase $p_{\rm W}$; (2) a chemical contribution, which accounts for the *molar fraction* $x_{k\rm W}$ of the species k in its phase; (3) an electrical contribution, for charged species in presence of the electrical potential $\phi_{\rm W}$ [unit Volt=kg×$\rm m^2/s^3$/A], and (4) a free enthalpy of formation $g^0_{k\rm W}$. As for the species within the solid phase $\mathcal{S}$, the mechanical contribution to the electro-chemical potential of species k is assumed to involve its intrinsic pressure $p_{k\rm S}$ to be defined by constitutive relations. In integral form,

$$g^{\rm ec}_{kK} = \underline{m}_k\,\mu^{\rm ec}_{kK} = g^0_{kK} + \int \underline{v}_k\,dp_{kK} + RT\,{\rm Ln}\,x_{kK} + \zeta_k\,F\,\phi_K\,, \tag{3.2}$$

with $p_{k\rm W} = p_{\rm W}$, $k \in \mathcal{W}$. The integration above is performed from a reference state to the current state. Therefore, g^0_{kK} serves as the mole-based value of the chemical potential in the reference state. In these formulas, $R = 8.31451\,{\rm J/mole/^\circ K}$ is the universal gas constant, $T(^\circ{\rm K})$ the absolute temperature, $\underline{m}_k$ is the molar mass of the species k, and $\underline{v}_k$ its apparent molar volume. The electrical contribution to the chemical potentials is introduced through the valence ζ_k (by convention, $\zeta_{\rm w} = 0$) and Faraday's equivalent charge F=Avogadro number × charge of an electron= 96487 Coulomb/mole (1 Coulomb=1 A×s).

3.2.2 Geometry and mass

Several measures of mass and volume are used in the constitutive equations.

The *molar fraction* x_{kK} of the species k in phase $\mathcal{K}$ is defined by the relative ratio of the mole number N_{kK} of that species within the phase $\mathcal{K}$, namely

$$x_{kK} = \frac{N_{kK}}{N_K} \quad \text{with} \quad N_K = \sum_{l\in\mathcal{K}} N_{lK}, \quad \sum_{k\in\mathcal{K}} x_{kK} = 1\,, \quad \mathcal{K} = \mathcal{S}, \mathcal{W}\,. \tag{3.3}$$

Let the initial volume of the porous medium be V_0 and $V = V(t)$ its current volume. The current volume and current mass of a generic species are denoted by V_{kK} and M_{kK} respectively, while

the current volume and mass of phase $\mathcal{K}$ are V_K and M_K. The *volume fraction* $n^{kK} = V_{kK}/V$ of a generic species, and the *apparent* density $\rho^{kK} = M_{kK}/V = n^{kK}\,\rho_k$ refer to the current volume of porous medium. On the other hand, the *mole content* $\mathcal{N}_{kK} = N_{kK}/V_0$, the *volume content* $v_{kK} = V_{kK}/V_0 = n^{kK}\,V/V_0$ and the *mass content* $m_{kK} = M_{kK}/V_0$ refer to the initial total volume V_0. These entities are linked by the relations (no sum on k)

$$m_{kK} = \mathcal{N}_{kK}\,\underline{m}_k = \rho_k\,v_{kK}\,. \tag{3.4}$$

With help of (3.4), the molar fractions x_{kK} can be expressed in terms of the mass contents. For incompressible species, the mass and volume contents are one and the same variables.

The apparent molar volume $\underline{v}_k$ and molar mass $\underline{m}_k$ of the species k are linked by the intrinsic density ρ_k, namely $\underline{m}_k = \rho_k\,\underline{v}_k$. The *molar volume* of the phase $\mathcal{K}$ is $\underline{v}_K = \sum_{k\in\mathcal{K}} x_{kK}\,\underline{v}_k$. Use will be made also of the concentration c_{kK}, which is the mole number referred to the phase rather than to the porous medium, namely

$$c_{kK} = \frac{\text{nb. of moles of species } k \text{ in phase } K}{\text{volume of phase } \mathcal{K}} = \frac{N_{kK}}{V_K} = \frac{1}{\underline{v}_k}\,\frac{n^{kK}}{n^K} = \frac{x_{kK}}{\underline{v}_K}\,,\ k\in\mathcal{K}\,. \tag{3.5}$$

The volume fractions of the phases $n^K = V_K/V = \sum_{k\in\mathcal{K}} n^{kK}$ satisfy the closure relation $n^{\mathrm{S}} + n^{\mathrm{W}} = 1$. The volume content $v_K = V_K/V_0 = n^K\,V/V_0$ and mass content $m_K = M_K/V_0$ of phase $\mathcal{K}$ are simply obtained by summation over species.

3.2.3 Electrical entities

The *electrical density* $I_{\mathrm{e}K}$ [unit Coulomb/m^3] in phase $\mathcal{K}$ is defined as

$$I_{\mathrm{e}K} = F\,\sum_{k\in\mathcal{K}} \zeta_k\,\frac{N_{kK}}{V}\,. \tag{3.6}$$

The fulfillment of *electroneutrality* in phase $\mathcal{K}$ can be expressed in various forms, e.g.

$$I_{\mathrm{e}K} = 0 \ \Leftrightarrow\ \sum_{k\in\mathcal{K}} \zeta_k\,\mathcal{N}_{kK} = 0 \ \Leftrightarrow\ \sum_{k\in\mathcal{K}} \zeta_k\,x_{kK} = 0 \ \Leftrightarrow\ \sum_{k\in\mathcal{K}} \zeta_k\,c_{kK} = 0\,. \tag{3.7}$$

Both the solid and fluid phases are assumed to be electrically neutral. This assumption is motivated by the fact that the characteristic time to restore electroneutrality is much smaller than the interphase transfer times for all ionic species. The electroneutrality condition implies the presence of a minimal number of absorbed ions $\mathcal{S}^{\pm}$, namely cations and anions respectively above and below the isoelectric point of the total fixed charge,

$$\sum_{k\in\mathcal{S}^{\pm}} \zeta_k\,\mathcal{N}_{k\mathrm{S}} = -\zeta_{\mathrm{c}}\,\mathcal{N}_{\mathrm{c}} \neq 0\,, \tag{3.8}$$

the subscript c referring to the clay particles.

4 Interacting deformation, mass transfer, diffusion and electroneutrality

The overall behavior of active clays results from the interactions between a number of physical phenomena, among which deformation, mass transfer, diffusion and electroneutrality. These phenomena interact. In addition, some of them involve their own couplings. Therefore, it is important to structure the constitutive framework so as to distinguish the different levels at which these interactions and couplings take place.

4.1 A strongly interacting two-phase multi-species mixture

The key assumptions of the two-phase model follow a *strongly interacting* model, Loret et al. [2002], namely,

(H1) The mass balance is required for each species.

(H2) Species in the fluid phase are endowed with their own velocities so as to allow them to diffuse in their phase, and to satisfy their own balance of momentum.

(H3) The velocity of any species in the solid phase is that of the latter, $\mathbf{v}_{k\mathrm{S}} = \mathbf{v}_{\mathrm{S}}$, $\forall k \in \mathcal{S}$, and therefore their balance of momentum is not required explicitly, but accounted for by the balance of momentum of the mixture as a whole.

(H4) In the fluid phase, pressure is assumed to be uniform across all species, $p_{k\mathrm{W}} = p_{\mathrm{W}}$, $\forall k \in \mathcal{W}$. In contrast, absorbed species in the solid phase are endowed, through specific constitutive equations, with their own intrinsic pressure.

(H5) Electroneutrality is required in each phase separately. Thus the fixed charges in the solid phase require the presence of counterions in the so-called outer-sphere domain and diffuse layer, namely cations above the isoelectric point, and, in kaolinites, anions below the isoelectric point.

In practice, mass balance is required for all species in the fluid phase but water, and for the fluid phase as a whole. The mass balances of the solid species are taken care of by the transfer equations.

In order to partition the motion of each species into its transfer and diffusion parts, a *volume* flux $\mathbf{J}_{kK}$ and a *mass* flux $\mathbf{M}_{kK}$ are introduced, namely

$$\mathbf{J}_{kK} = n^{kK}\,(\mathbf{v}_{kK} - \mathbf{v}_{\mathrm{S}}), \quad \mathbf{M}_{kK} = \rho^{kK}\,(\mathbf{v}_{kK} - \mathbf{v}_{\mathrm{S}}), \quad k \in \mathcal{K}\,. \tag{4.1}$$

The above fluxes are relative to the solid skeleton, and consequently, the fluxes of the species in the sole fluid phase do not vanish identically.

4.2 Transfer and diffusion of mass

Quite generally, the change of the mole number and mass of a species is due a priori to both a *transfer* between the phases, denoted by a superimposed hat, and a *diffusion*. Altogether the transfers maintain the continuing electroneutrality condition in both phases.

The mass changes of the species of the solid phase are purely reactive, and due to transfers from the fluid phase, that is $\delta m_{k\mathrm{S}} = \delta \hat{m}_{kS}$, $\forall k \in \mathcal{S}$. The constitutive equations of these mass transfers are considered in Sect. 5.

The species of the fluid phase undergo both a *mass transfer* with the solid phase and a mass exchange by diffusion with the surroundings, namely (the symbol $\delta\ /\delta t$ means derivative following the solid skeleton or phase),

$$\frac{\delta m_{k\mathrm{W}}}{\delta t} = \frac{\delta \hat{m}_{k\mathrm{W}}}{\delta t} - \mathrm{div}\ \mathbf{M}_{k\mathrm{W}}, \quad k \in \mathcal{W}\,. \tag{4.2}$$

Since the transfer concerns individual species, then $\delta \hat{m}_{k\mathrm{W}} + \delta m_{k\mathrm{S}} = 0$, and (4.2) becomes,

$$\frac{\delta m_{k\mathrm{W}}}{\delta t} = -\frac{\delta m_{k\mathrm{S}}}{\delta t} - \mathrm{div}\ \mathbf{M}_{k\mathrm{W}}\,, \quad k \in \mathcal{W}\,. \tag{4.3}$$

The framework is versatile. For example, for a species k of the fluid phase that would not exist in the solid phase, or exist but not transfer, the first term of the right-hand side of (4.3) would simply be set to zero.

4.3 Global incompressibility

In an infinitesimal strain analysis, $V/V_0 = v_{\rm S} + v_{\rm W}$ is equal to $1 + \mathrm{tr}\,\boldsymbol{\epsilon}$, tr denoting the trace operator, and the time rate of $\mathrm{tr}\,\boldsymbol{\epsilon}$ is equal to the divergence $\mathrm{div}\,\mathbf{v}_{\rm S}$ of the solid velocity field. Then

$$\mathrm{div}\,\mathbf{v}_{\rm S} = \frac{\delta v_{\rm S}}{\delta t} + \frac{\delta v_{\rm W}}{\delta t}\,. \tag{4.4}$$

Henceforth, all species are considered incompressible[1], $\delta\rho_k = 0,\ \forall k$. Dividing both sides of (4.3) by the density, summing up, and using (4.4), the change of volume of the solid skeleton, equal to that of the porous medium, is seen to be equal and opposite to the volume change of the fluid phase due to diffusion, namely

$$\mathrm{div}\ \mathbf{v}_{\rm S} + \mathrm{div}\ \mathbf{J}_{\rm W} = 0\,, \tag{4.5}$$

where $\mathbf{J}_{\rm W} = \sum_{k\in\mathcal{W}} \mathbf{J}_{k\rm W}$ is volume averaged flux of the fluid phase through the solid skeleton.

As $\mathrm{pH} \equiv -\mathrm{Ln}_{10} c_{\rm HW}$ is varying, it is appropriate to account for water dissociation

$$\mathrm{H_2O} \rightleftharpoons \mathrm{OH^-}\ +\ \mathrm{H^+} \tag{4.6}$$

defined by the dissociation constant

$$c_{\rm HW}\, c_{\rm OHW} = K^{wd} = 10^{-14}\,. \tag{4.7}$$

Water dissociation can be considered to be instantaneous relative to the other chemical reactions. In contrast to the balance of mass of water and of the ions hydrogen and hydroxyl, the overall mass balance is not affected by water dissociation.

4.4 Dissipation inequalities

In absence of thermal effects, starting from the statements of balance of mass for each species, and of momentum and energy for the phases, the Clausius-Duhem inequality for the mixture as a whole can be cast in a format that highlights mechanical, transfer and diffusion contributions, Loret and Simões [2005]. These contributions will be required to be positive individually,

$$\left\{\begin{array}{l} \delta D_1 = -\delta\Psi + \boldsymbol{\sigma} : \delta\boldsymbol{\epsilon} + \displaystyle\sum_{k,K} g^{\rm ec}_{kK}\,\delta\mathcal{N}_{kK} \geq 0\,, \\ \delta D_2 = -\displaystyle\sum_{k\in\mathcal{S}} (g^{\rm ec}_{kS} - g^{\rm ec}_{kW})\,\delta\mathcal{N}_{kK} \geq 0\,, \\ \delta D_3/\delta\, t = -\displaystyle\sum_{k\in\mathcal{W}} \nabla\mu^{\rm ec}_{k\rm W}\cdot\mathbf{M}_{k\rm W} \geq 0\,. \end{array}\right. \tag{4.8}$$

The chemo-hyperelastic behavior will be constructed in order for the first term δD_1 to exactly vanish, Sect. 6. Satisfaction of the second and third inequalities motivates generalized transfer equations, Sect. 5, and generalized diffusion equations respectively.

[1] This is in fact an approximation since the apparent molar volumes of ions vary.

5 pH-induced changes of the mineral electrical charge

Mass transfers between the fluid and solid phases affect strongly the mechanical behavior of the clays. These transfers are driven mainly by the electrical charge of the clay minerals. In turn, this electrical charge is modified by changes of the pH of the fluid phase.

The transfer mechanisms are now viewed as physico-chemical reactions. In this context, the standard approximation in chemistry which amounts to neglect the pressure contribution to the chemical potentials of solutes is adopted. The resulting information will be embedded in the coupled chemo-mechanical analysis of Sects. 6 and 7.

5.1 The transfer mechanisms

Four electrically neutral transfer mechanisms are considered. They account for ion exchange, acid-base equilibrium, and change of hydration.

Acid-base equilibrium is defined by two independent surface complexation mechanisms of acidification, and alkalinization. These two mechanisms are decomposed in two submechanisms, which individually are not electrically neutral. Acid-base equilibrium can not be described by a single mechanism, because the three sites of surface complexation undergo typical changes in terms of pH.

Ion exchange leaves the electrical charge of the clay mineral unchanged, in contrast to surface complexation. Change in hydration is not accounted for in the ion exchange and surface complexation mechanisms, but, instead, it is viewed as an independent mechanism. For practical purposes, the four mechanisms are numbered as indicated in Fig. 4.

The mechanisms, submechanisms, and the physico-chemical reactions they represent, are a priori reversible. The associated transfer rules will be naturally cast in a format that satisfies the dissipation inequality $(4.8)_2$. Indeed, let δN_K be the mole change, in the initial volume of the porous medium V_0, of a given chemical species of phase $\mathcal{K}$. For each mechanism, or submechanism, the dissipation inequality can be cast as $-\mathcal{G}_K\,\delta N_K$ in terms of the associated electro-chemical affinity $\mathcal{G}_K$. A superimposed hat denoting the part of an entity that undergoes transfer, as opposed to diffusion, one has $\delta\hat{N}_{\rm W}+\delta N_{\rm S}=0$. Consequently, the total incremental dissipation expresses as $-\mathcal{G}\,\delta N_{\rm S}$, in terms of the change of mole number of the solid phase $N_{\rm S}$, and of the electro-chemical affinity $\mathcal{G}=\mathcal{G}_{\rm S}-\mathcal{G}_{\rm W}$ of the physico-chemical reaction. Thus a linear transfer rule expresses via a characteristic transfer time $\tau>0$ as,

$$\frac{\delta N_{\rm S}}{\delta t}=-\frac{1}{\tau}\,\frac{\mathcal{G}}{RT}\,. \tag{5.1}$$

An equilibrium is reached when the affinity $\mathcal{G}$ vanishes.

[2] Furthermore, once the various contributions to the affinity are gathered, an equilibrium constant is shown to emanate from a linear combination of the enthalpies of formation that contribute to the electro-chemical potentials (3.2).

---

[2] *The rate of transfer of mass content*: The dissipation per unit initial volume can equivalently be written as $-\mathcal{M}\,\delta m_{\rm S}$ in terms of the mass content of the solid phase and of the mass-based electro-chemical affinity $\mathcal{M}$ such that $\mathcal{G}=\underline{m}\,\mathcal{M}$. In terms of these entities, the transfer rule takes the form,

$$\frac{\delta m_{\rm S}}{\delta t}=-\frac{1}{\tau}\,\frac{\underline{m}^2}{V_0}\,\frac{\mathcal{M}}{RT}\,. \tag{5.2}$$

For a transfer which is electrically neutral, the work done by the electrical potential vanishes, and the electro-chemical affinity in (5.1) is replaced by the chemical affinity.

In our previous analyzes, the electrical potential was phase-wise homogeneous, and discontinuous along the inter-phase. A more realistic analysis would account for the progressive change of the electrical potential from the surface of the clay particle to the bulk water. Sposito [1984] and others, e.g. Petrangeli Papini and Majone [2002], delineate three degrees of refinement. This macroscopic analysis is not sophisticated enough as to define a smooth nanometric variation of the entities across the absorbed water. Simply, a piecewise spatial variation of the electrical potential is introduced, as sketched in Fig. 3. The homogeneous scheme and refined scheme are referred to as single layer (SL) and double layer (DL) schemes respectively.

Furthermore, the sodium and hydrogen ions play different mechanical roles according to the chemicals they bind or sorb to, and/or their spatial locations in the absorbed water. This information is recorded in the analysis according to the transfer mechanism they participate.

5.2 Exchange of water

As already mentioned, exchange of water is associated to all transfer mechanisms. Thus, viewing water exchange as an independent mechanism is adopted as a simplification. The dissipation in the volume V_0 expresses in terms of the chemical affinity of the hydration mechanism

$$\mathcal{G}_1 = g_{\mathrm{wS}} - g_{\mathrm{wW}}\,, \tag{5.3}$$

as $-\mathcal{G}_1\,\delta N_{1\mathrm{S}}$, where $\delta N_{1\mathrm{S}} \equiv \delta N_{\mathrm{wS}} = -\delta \hat{N}_{\mathrm{wW}}$. Thus a linear transfer law, characterized by the transfer time $\tau_1 > 0$, that satisfies the dissipation inequality, has the form

$$\frac{\delta N_{1\mathrm{S}}}{\delta t} = -\frac{1}{\tau_1}\Big(\frac{v_{\mathrm{w}}}{RT}(p_{\mathrm{wS}} - p_{\mathrm{W}}) + \mathrm{Ln}\,\frac{x_{\mathrm{wS}}}{x_{\mathrm{wW}}}\Big)\,. \tag{5.4}$$

5.3 Ion exchange

Ion exchange concerns the permanent charge. Ions solvated in the outer sphere and in the diffuse layer can be exchanged with ions in the fluid phase, depending on their relative concentrations and relative affinities to the clay sites. In the ion exchange mechanism, as indicated on Fig. 4, a sodium cation Na^+ competes with a hydrogen ion H^+ for the clay site X,

$$\mathrm{X{-}Na}^+ \;+\; \underbrace{\mathrm{H}^+}_{\text{fluid phase}} \;\rightleftharpoons\; \mathrm{X{-}H}^+ \;+\; \underbrace{\mathrm{Na}^+}_{\text{fluid phase}}\quad. \tag{5.5}$$

Let $N_{2\mathrm{S}} \equiv N^{(2)}_{\mathrm{HS}}$ be the number of hydrogen ions that participate to ion exchange. Continuing electroneutrality requires $\delta N^{(2)}_{\mathrm{HS}} = -\delta N^{(2)}_{\mathrm{NaS}} = -\delta \hat{N}^{(2)}_{\mathrm{HW}} = \delta \hat{N}^{(2)}_{\mathrm{NaW}}$. Thus the work done in the volume V_0 during the exchange expresses via the electro-chemical potentials in the following form,

$$\begin{aligned}
&\text{in the solid phase}: \quad g^{\mathrm{ec}}_{\mathrm{NaS}}\delta N^{(2)}_{\mathrm{NaS}} + g^{\mathrm{ec}}_{\mathrm{HS}}\delta N^{(2)}_{\mathrm{HS}} \;&=\; (-g^{\mathrm{ec}}_{\mathrm{NaS}} + g^{\mathrm{ec}}_{\mathrm{HS}})\,\delta N_{2\mathrm{S}}\,,\\
&\text{in the fluid phase}: \quad g^{\mathrm{ec}}_{\mathrm{NaW}}\delta \hat{N}^{(2)}_{\mathrm{NaW}} + g^{\mathrm{ec}}_{\mathrm{HW}}\delta \hat{N}^{(2)}_{\mathrm{HW}} \;&=\; (g^{\mathrm{ec}}_{\mathrm{NaW}} - g^{\mathrm{ec}}_{\mathrm{HW}})\,\delta N_{2\mathrm{S}}\,.
\end{aligned} \tag{5.6}$$

The dissipation contributed by this mechanism is thus $-\mathcal{G}_2\,\delta N_{2\mathrm{S}}$ with $\mathcal{G}_2$ the chemical affinity,

$$\mathcal{G}_2 = -g^{\mathrm{ec}}_{\mathrm{NaS}} + g^{\mathrm{ec}}_{\mathrm{HS}} + g^{\mathrm{ec}}_{\mathrm{NaW}} - g^{\mathrm{ec}}_{\mathrm{HW}}\,. \tag{5.7}$$

In line with the rule (5.1), a linear transfer law that governs the rate of variation of the mole number N_{2S} of the hydrogen ions that participate to ion exchange involves a transfer time $\tau_2 > 0$ and an equilibrium constant K_2^{eq},

$$\frac{\delta N_{2S}}{\delta t} = -\frac{1}{\tau_2} \operatorname{Ln} \frac{x_{HS}^{(2)}}{x_{NaS}^{(2)}} \frac{x_{NaW}}{x_{HW}} \frac{1}{K_2^{eq}} . \tag{5.8}$$

The equilibrium constant was shown to derive from the enthalpies of formation in Gajo et al. [2002]. The simulations presented in Sect. 9 require three ions to participate to ion exchange. The extension presents no difficulty and it is sketched in Appendix A.

5.4 Surface complexation

Surface complexation results from the competition, sketched on Fig. 4, between hydroxyl and hydrogen ions for three types of sites S–O^-, S–OH and S–OH_2^+.

Each surface complexation mechanism is decomposed in two parts: one reaction represents the acidification process, or alkalinization process, and a second reaction occurs so as to maintain electroneutrality. The neutralizing ions remain solvated in the outer layer. Since the electrical potential is varying in the diffuse layer, the dissipation induced by the transfers of the neutralizing ions is more difficult to estimate, as it depends on the exact position of these ions in the diffuse layer. However, this dissipation is expected to be small, and, in a tentative approach, it will be neglected relative to the dissipation associated to the first part of the acidification and alkalinization processes. Indications on the submechanisms intended to re-establish electrical neutrality are provided in Sect. 5.6.

5.4.1 The acidification submechanism

Acidification of the fluid phase implies hydrogen ions to migrate toward the solid phase and to change the termination S–OH to S–OH_2^+,

$$\underbrace{S-OH_2^+}_{\text{clay site}} \rightleftharpoons \underbrace{S-OH}_{\text{clay site}} + \underbrace{H^+}_{\text{fluid phase}} . \tag{5.9}$$

Let $N_{3S} \equiv N_{SOH_2}$. Since $\delta N_{SOH_2} = -\delta \hat{N}_{HW}^{(3)}$, the work done in the volume V_0 during these exchanges is,

$$\begin{aligned} &\text{in the solid phase :} \;\; g_{SOH}^{ec} \delta N_{SOH}^{(3)} + g_{SOH_2}^{ec} \delta N_{SOH_2} = (-g_{SOH}^{ec} + g_{SOH_2}^{ec})\, \delta N_{3S} , \\ &\text{in the fluid phase :} \;\; g_{HW}^{ec}\, \delta \hat{N}_{HW}^{(3)} = -g_{HW}^{ec}\, \delta N_{3S} , \end{aligned} \tag{5.10}$$

so that the dissipation due to this mechanism expresses as $-\mathcal{G}_3\, \delta N_{3S}$ via the electro-chemical affinity $\mathcal{G}_3$,

$$\mathcal{G}_3 = -g_{SOH}^{ec} + g_{SOH_2}^{ec} - g_{HW}^{ec} . \tag{5.11}$$

A linear transfer law for the rate of variation of the mole number of sites SOH_2 for this mechanism involves the transfer time $\tau_3 > 0$ and the equilibrium constant K_3^{eq},

$$\frac{\delta N_{3S}}{\delta t} = -\frac{1}{\tau_3} \operatorname{Ln} \frac{\{SOH_2\}}{\{SOH\}} \frac{K_3^{eq}}{x_{HW}} e^{\frac{F[\phi]}{RT}} , \tag{5.12}$$

with

$$[\phi] \equiv \phi_{\rm S} - \phi_{\rm W}\,. \tag{5.13}$$

Here $\{{\rm Y}\} = N_{\rm Y}/A_{\rm c}$ denotes the number of sites Y per area $A_{\rm c}$ of clay mineral, and

$$\delta\{{\rm SOH_2}\} = -\delta\{{\rm SOH}\}^{(3)} = \delta N_{\rm 3S}/A_{\rm c}\,. \tag{5.14}$$

5.4.2 The alkalinization submechanism

Alkalinization of the fluid phase implies hydroxyl ions to migrate toward the solid phase and to change the termination S–OH to S–O^-,

$$\underbrace{{\rm S-O^-}}_{\text{clay site}}\ (+{\rm H_2O}) \rightleftharpoons \underbrace{{\rm S-OH}}_{\text{clay site}} + \underbrace{{\rm OH^-}}_{\text{fluid phase}}\quad . \tag{5.15}$$

Let $N_{\rm 4S} \equiv N_{\rm SO}$. The work done in the volume V_0 expresses in terms of electro-chemical potentials, since $\delta N_{\rm SO} = -\delta\hat{N}^{(4)}_{\rm OHW}$, as

$$\begin{aligned} &\text{in the solid phase}: \ g^{\rm ec}_{\rm SOH}\delta N^{(4)}_{\rm SOH} + g^{\rm ec}_{\rm SO}\delta N_{\rm SO} \qquad\quad = (-g^{\rm ec}_{\rm SOH} + g^{\rm ec}_{\rm SO})\,\delta N_{\rm 4S}\,,\\ &\text{in the fluid phase}: \ g^{\rm ec}_{\rm OHW}\delta\hat{N}^{(4)}_{\rm OHW} = -g^{\rm ec}_{\rm OHW}\delta N_{\rm 4S}\,. \end{aligned} \tag{5.16}$$

Thus the dissipation due to this mechanism is $-\mathcal{G}_4\,\delta N_{\rm 4S}$ in terms of the electro-chemical affinity,

$$\mathcal{G}_4 = -g^{\rm ec}_{\rm SOH} + g^{\rm ec}_{\rm SO} - g^{\rm ec}_{\rm OHW}\,. \tag{5.17}$$

A linear transfer law that indicates the rate of variation of the mole number of sites SO^- for this mechanism involves the transfer time $\tau_4 > 0$ and the equilibrium constant K_4^{eq},

$$\frac{\delta N_{\rm 4S}}{\delta t} = -\frac{1}{\tau_4}\,{\rm Ln}\,\frac{\{{\rm SO}\}}{\{{\rm SOH}\}}\frac{K_4^{eq}}{x_{\rm OHW}}e^{-\frac{F[\phi]}{RT}}\,, \tag{5.18}$$

and

$$\delta\{{\rm SO}\} = -\delta\{{\rm SOH}\}^{(4)} = \delta N_{\rm 4S}/A_{\rm c}\,. \tag{5.19}$$

5.4.3 Alternative description of alkalinization

Alkalinization of the fluid phase may alternatively be seen as implying hydrogen ions to migrate toward the fluid phase, changing as well the termination S–OH to S–O^-,

$$\underbrace{{\rm S-OH}}_{\text{clay site}} \rightleftharpoons \underbrace{{\rm S-O^-}}_{\text{clay site}} + \underbrace{{\rm H^+}}_{\text{fluid phase}}\quad . \tag{5.20}$$

Let $N_{\overline{4}{\rm S}} \equiv N_{\rm SO}$. Since $\delta N_{\rm SO} = \delta\hat{N}^{(\overline{4})}_{\rm HW}$, the work done in the volume V_0 during the exchanges can be expressed via the electro-chemical potentials,

$$\begin{aligned} &\text{in the solid phase}: \ g^{\rm ec}_{\rm SOH}\delta N^{(\overline{4})}_{\rm SOH} + g^{\rm ec}_{\rm SO}\delta N_{\rm SO} \ = (-g^{\rm ec}_{\rm SOH} + g^{\rm ec}_{\rm SO})\,\delta N_{\overline{4}{\rm S}}\,,\\ &\text{in the fluid phase}: \ g^{\rm ec}_{\rm HW}\delta\hat{N}^{(\overline{4})}_{\rm HW} = g^{\rm ec}_{\rm HW}\delta N_{\overline{4}{\rm S}}\,, \end{aligned} \tag{5.21}$$

so that the dissipation contributed by this mechanism, denoted by the index $\overline{4}$, expresses as $-\mathcal{G}_{\overline{4}}\,\delta N_{\overline{4}{\rm S}}$ in terms of the electro-chemical affinity,

$$\mathcal{G}_{\overline{4}} = -g^{\rm ec}_{\rm SOH} + g^{\rm ec}_{\rm SO} + g^{\rm ec}_{\rm HW}\,. \tag{5.22}$$

A linear transfer law that indicates the rate of variation of the mole number of sites SO^- for this mechanism involves the transfer time $\tau_{\overline{4}}>0$ and the equilibrium constant $K_{\overline{4}}^{eq}$,

$$\frac{\delta N_{\overline{4}S}}{\delta t} = -\frac{1}{\tau_{\overline{4}}} \mathrm{Ln}\, \frac{\{SO\}}{\{SOH\}} \frac{x_{HW}}{K_{\overline{4}}^{eq}} e^{\frac{-F[\phi]}{RT}}\,, \tag{5.23}$$

and

$$\delta\{SO\} = -\delta\{SOH\}^{(\overline{4})} = \delta N_{\overline{4}S}/A_c\,. \tag{5.24}$$

Note the relation linking the equilibrium constants attached to the alkalinization reactions,

$$K_4^{eq}\, K_{\overline{4}}^{eq} = K^{wd}\, \underline{v}_w^2\,. \tag{5.25}$$

5.5 The modified electrical charge of the mineral

The *fixed* electrical charge of clay minerals contains two parts, a *permanent* charge $N_{ep}F$ due to isomorphous substitution, and a *variable* charge $N_{ev}F$ associated to surface complexation. N_{ep} is negative while N_{ev} may be either positive or negative. With M_c and N_c denoting the mass and number of moles of clay minerals contained in the volume V_0, the permanent and variable *algebraic* charge densities per unit mass of clay are equal respectively to $\sigma_{ep} = N_{ep}F/M_c$ and $\sigma_{ev} = N_{ev}F/M_c$. The valence of the clay minerals is defined as $\zeta_c = (N_{ep} + N_{ev})/N_c$.

The variable electrical charge,

$$N_{ev}F = (\,\{SOH_2\} - \{SO\}\,)\, A_c\, F, \tag{5.26}$$

is modified by the acidification and alkalinization processes. The variation of the number of sites SOH_2 is calculated by (5.12),(5.14) and that of the sites SO^- by (5.18),(5.19), or (5.23),(5.24), and

$$\delta N_{ev} = \delta N_{SOH_2} - \delta N_{SO} = \delta N_{3S} - \delta N_{4S}\,. \tag{5.27}$$

The ions involved in ion exchange are monovalent, so that their total number N_{ie} is equal to the number -N_{ep} defining the permanent charges[3]. Since the integrity of the clay is maintained, the number of active sites for ion exchange is constant,

$$N_{HS}^{(2)} + N_{NaS}^{(2)} = N_{ie} = -N_{ep}\,, \tag{5.28}$$

as well as the total number of sites of surface complexation,

$$N_{SO} + N_{SOH} + N_{SOH_2} = N_{sc}\,. \tag{5.29}$$

Remark 5.1 From thermodynamics to the empirical Langmuir isotherm

The chemical reactions considered in this thermodynamic analysis imply a competitive Langmuir isotherm: the latter is described by an empirical expression that gives the proportion of bound species (or of occupied sites) in terms of the concentrations of the dissolved species.

Let us first consider a non competitive Langmuir scheme with the hydrogen ion as the single free species. The adsorption site Y is thus either free, or occupied in the form HY. The concentration $\{c\} = \{c_Y\} + \{c_{HY}\}$ of the total number of sites is constant, hydrogen appears in dissolved form, with concentration c_{H_f}, and bound form with concentration per area

[3]This relation would not hold if for example ions X^{2+} and H^+ were involved. Then $-N_{ep} = 2\,N_{XS} + N_{HS}$ but $N_{ie} = N_{XS} + N_{HS}$.

$\{c_{\rm HY}\}$. The adsorption is described by the reaction, Y + $H^+ \rightleftharpoons$ HY with the equilibrium constant $K^{eq} = \{c_{\rm HY}\}/\{c_{\rm Y}\}\, c_{{\rm H}_f}$. The concentration of bound hydrogen is thus given in terms of the concentration of free (dissolved) hydrogen through a relation that has the form of a Langmuir isotherm, $\{c_{\rm HY}\} = K^{eq}\, c_{{\rm H}_f}\, \{c\}/(1 + K^{eq} c_{{\rm H}_f})$. The concentration of free sites is $\{c_{\rm Y}\} = \{c\} - \{c_{\rm HY}\} = \{c\}/(1 + K^{eq} c_{{\rm H}_f})$.

Actually, the acid-base reactions involve here two species, the hydrogen and the hydroxyl ions, that compete for the sites SOH, so that the model is similar to a competitive Langmuir scheme.

In the present description, the acid-base reactions and the ion exchange reaction present a noteworthy difference: some of the acid-base sites SOH may be free, while the X-sites are always occupied.

5.6 Dependent and independent variables

Before embarking in the development of elastic and elastic-plastic constitutive equations, it is worth to summarize the degrees of dependence between the variables that have been introduced to describe the various transfer mechanisms.

Indeed, some chemicals are involved in more than one transfer mechanism, some play the same role in these mechanisms, but others play different roles. One independent variable is defined for each mechanism,

$$
\begin{aligned}
&\delta N_{\rm 1S} = \delta N_{\rm wS} = -\delta \hat{N}_{\rm wW}\,,\\
&\delta N_{\rm 2S} \equiv \delta N^{(2)}_{\rm HS} = -\delta \hat{N}^{(2)}_{\rm HW} = -\delta N^{(2)}_{\rm NaS} = \delta \hat{N}^{(2)}_{\rm NaW}\,,\\
&\delta N_{\rm 3S} \equiv \delta N_{\rm SOH_2} = \delta N^{(3)}_{\rm HS} = -\delta \hat{N}^{(3)}_{\rm HW} = -\delta N^{(3)}_{\rm SOH} = \delta N_{\rm ClS} = -\delta \hat{N}_{\rm ClW}\,,\\
&\delta N_{\rm 4S} \equiv \delta N_{\rm SO} = \delta N^{(4)}_{\rm OHS} = -\delta \hat{N}_{\rm OHW} = -\delta N^{(4)}_{\rm SOH} = \delta N^{(4)}_{\rm NaS} = -\delta \hat{N}^{(4)}_{\rm NaW}\,,\\
&\delta N_{\overline{4}\rm S} \equiv \delta N_{\rm SO} = -\delta \hat{N}^{(\overline{4})}_{\rm HS} = \delta \hat{N}^{(\overline{4})}_{\rm HW} = -\delta N^{(\overline{4})}_{\rm SOH} = \delta N^{(\overline{4})}_{\rm NaS} = -\delta \hat{N}^{(\overline{4})}_{\rm NaW}\,.
\end{aligned}
\tag{5.30}
$$

The total variations of the fluid species, due to the transfers, can be expressed in terms of these independent variables ($i = 1$ for mechanism 4, and 0 for mechanism $\overline{4}$),

$$
\begin{aligned}
&\delta \hat{N}_{\rm wW} = -\delta N_{\rm 1S}\,,\\
&\delta \hat{N}_{\rm HW} = -\delta N_{\rm 2S} - i\,\delta N_{\rm 3S} + (1-i)\,\delta N_{\overline{4}\rm S}\,,\\
&\delta \hat{N}_{\rm OHW} = -i\,\delta N_{\rm 4S}\,,\\
&\delta \hat{N}_{\rm NaW} = \delta N_{\rm 2S} - i\,\delta N_{\rm 4S} - (1-i)\,\delta N_{\overline{4}\rm S}\,,\\
&\delta \hat{N}_{\rm ClW} = -\delta N_{\rm ClS} = -\delta N_{\rm 3S}\,,
\end{aligned}
\tag{5.31}
$$

where $\delta N_{\rm 1S}$ is given by (5.4), $\delta N_{\rm 2S}$ by (5.8), $\delta N_{\rm 3S}$ by (5.12), $\delta N_{\rm 4S}$ by (5.18), and $\delta N_{\overline{4}\rm S}$ by (5.23).

6 Chemo-hyperelastic constitutive equations

Electro-chemo-mechanical couplings, like electrical shielding, occur essentially in the clay clusters. The presence of cations in between the negatively charged parallel clay platelets *shields*

the repulsive forces of electrical nature between the platelets. The larger the cation concentration, the smaller the distance between the platelets, and, at a macroscopic scale, the smaller the volume of the clay. Along this point of view, the macroscopic mechanical properties of the clay depend on the state of the clay clusters, that is on mass contents in the solid phase. On the other hand, the mere presence of ions in the water phase does not affect directly the mechanical behavior of the porous medium, these ions just flow through. Their amount is governed by an equation of mass conservation and a flow equation.

Therefore, to develop the electro-chemo-mechanical constitutive equations, the fluid phase is treated as a whole: its chemical composition is formally ignored, a point of view which of course is not adopted in the diffusion analysis. This is along this line that have been developed a model for homoionic clays in Loret et al. [2002], Gajo and Loret [2003], later extended to heteroionic clays in Gajo et al. [2002], Gajo and Loret [2004].

The spatial variation of the electrical potential, Fig. 3, allows a refinement to be introduced. Indeed, only the ions, located in a close vicinity of the clay minerals, and that undergo the solid electrical potential, will be assumed to contribute to the mechanical properties.

The constitutive equations are provided for the following conjugate variables:

- a stress-strain couple attached to the mechanical state of the solid phase;
- a pressure-volume couple attached to the mechanical state of the fluid phase;
- as many couples of electro-chemical affinity-mole content as there are independent ionic transfer mechanisms.

In fact, the compatibility condition, eqn (4.4), reduces the number of unknowns and equations by one, and introduces effective generalized stresses.

Given a reference state, and a process which is reversible from that reference state to the current state, the elastic, or reversible, part of a generalized strain is by convention equal to the total entity. This rule applies to strains, volume, mole contents, and to entities derived consistently from the latter, e.g. mass contents and molar fractions.

6.1 The formal constitutive relations

The mechanical potential per unit initial volume of porous medium Φ is taken as the elastic energy of the porous medium Ψ from which the electro-chemical effects in the fluid phase $\Psi_{\rm W}$ and remote diffuse layer Ψ_{dl} are disregarded. The latter energy is contributed by the chlorine and sodium ions that participate to the second submechanisms of the acid-base equilibrium.

Thanks to the Gibbs-Duhem relation, Sect. 2.3 in Gajo et al. [2002], the differential of the electro-chemical energy of the fluid phase per initial unit volume of the porous medium can be cast in the form,

$$\delta\Psi_{\rm W} = \sum_{k\in\mathcal{W}} g^{(\rm ec)}_{kW}\,\delta\mathcal{N}_{k\rm W} - p_{\rm W}\,\delta v_{\rm W}\,, \tag{6.1}$$

the electrical contribution vanishing due to electroneutrality of the fluid phase, eqns (3.6),(3.7).

With the definitions (3.1) and (6.1), the elastic potential is seen to be contributed by the work done in the volume V_0 by the deformation of the porous medium, and by the four submechanisms described in Sect. 5 by eqns (5.3),(5.6),(5.10), and (5.16) or (5.21),

$$\delta\Phi = \boldsymbol{\sigma} : \delta\boldsymbol{\epsilon} + p_{\rm W}\,\delta v_{\rm W} + \sum_{n=1,4} \mathcal{G}_{n\rm S}\,\delta\mathcal{N}_{n\rm S}\,. \tag{6.2}$$

The formulation simplifies due to the compatibility relation (4.4), which holds in both the elastic and elastic-plastic regimes. Upon elimination of the volume change of the fluid phase,

the elastic potential expresses in terms of Terzaghi's *effective* stress $\bar{\boldsymbol{\sigma}}$, and of the associated affinities[4] $\overline{\mathcal{G}}_{n\mathrm{S}}$, $n \in [1,4]$,

$$\bar{\boldsymbol{\sigma}} = \boldsymbol{\sigma} + p_{\mathrm{W}}\,\mathbf{I}\,, \quad \overline{\mathcal{G}}_{n\mathrm{S}} = \mathcal{G}_{n\mathrm{S}} - \underline{v}_n\, p_{\mathrm{W}}, \quad n = 1,4\,, \tag{6.3}$$

where $\mathbf{I}$ is the second order identity tensor. The $\underline{v}_n$'s are calculated with help of (4.4) and (5.30) as $\underline{v}_1 = \underline{v}_{\mathrm{w}}$, $\underline{v}_2 = \underline{v}_{\mathrm{H}} - \underline{v}_{\mathrm{Na}}$, $\underline{v}_3 = \underline{v}_{\mathrm{H}} + \underline{v}_{\mathrm{Cl}}$, $\underline{v}_4 = \underline{v}_{\mathrm{OH}} + \underline{v}_{\mathrm{Na}}$. Then (6.2) becomes

$$\delta\Phi = \bar{\boldsymbol{\sigma}} : \delta\boldsymbol{\epsilon} + \sum_{n=1,4} \overline{\mathcal{G}}_{n\mathrm{S}}\, \delta\mathcal{N}_{n\mathrm{S}}\,. \tag{6.4}$$

In the standard Cam-Clay model in which chemical interactions are absent, the elastic moduli depend on the stress state. To recover this property, a partial Legendre transform is performed which changes Φ to $\bar{\boldsymbol{\sigma}} : \boldsymbol{\epsilon} - \Phi$, so as to retrieve the stress, rather than the strain, as independent variable,

$$\delta\Phi(\bar{\boldsymbol{\sigma}}, \mathcal{N}_{\mathrm{S}}) = \boldsymbol{\epsilon} : \delta\bar{\boldsymbol{\sigma}} - \sum_{n=1,4} \overline{\mathcal{G}}_{n\mathrm{S}}\, \delta\mathcal{N}_{n\mathrm{S}}\,. \tag{6.5}$$

In terms of the independent and dependent sets of variables $\{\bar{\boldsymbol{\sigma}}, \mathcal{N}_{\mathrm{S}}\}$ and $\{\boldsymbol{\epsilon}, \overline{\mathcal{G}}_{\mathrm{S}}\}$ respectively,

$$\mathcal{N}_{\mathrm{S}} = \cup_{n=1}^{4} \mathcal{N}_{n\mathrm{S}}, \quad \overline{\mathcal{G}}_{\mathrm{S}} = \cup_{n=1}^{4} \overline{\mathcal{G}}_{n\mathrm{S}}\,, \tag{6.6}$$

the constitutive relations can be cast in the format,

$$\boldsymbol{\epsilon} = \frac{\partial\Phi}{\partial\bar{\boldsymbol{\sigma}}}\,, \quad \overline{\mathcal{G}}_{n\mathrm{S}} = -\frac{\partial\Phi}{\partial\mathcal{N}_{n\mathrm{S}}}\,,\ n \in [1,4]\,. \tag{6.7}$$

6.2 Elastic potential

To complete the elastic equations, the potential Φ has to be built. The chemical, chemo-mechanical, formation, and electric contributions to Φ are addressed in turn.

6.2.1 Chemical contribution

The chemical parts of the four affinities in (6.7) are obtained by defining the purely chemical contribution of the elastic potential as

$$\begin{aligned}\varphi_{\mathrm{ch}}(\mathcal{N}_{\mathrm{S}}) = \frac{RT}{V_0}\Big(\quad & N_{\mathrm{S}}\,\mathrm{Ln}N_{\mathrm{S}} - N_{\mathrm{c}}\,\mathrm{Ln}N_{\mathrm{c}} - N_{\mathrm{wS}}\,\mathrm{Ln}N_{\mathrm{wS}} \\ & - N^{(2)}_{\mathrm{HS}}\,\mathrm{Ln}N^{(2)}_{\mathrm{HS}} - N^{(2)}_{\mathrm{NaS}}\,\mathrm{Ln}N^{(2)}_{\mathrm{NaS}} \\ & - N_{\mathrm{SOH_2}}\,\mathrm{Ln}N_{\mathrm{SOH_2}} - N_{\mathrm{SOH}}\,\mathrm{Ln}N_{\mathrm{SOH}} - N_{\mathrm{SO}}\,\mathrm{Ln}N_{\mathrm{SO}}\Big)\,.\end{aligned} \tag{6.8}$$

The total number of moles N_{S} is defined as[5]

$$N_{\mathrm{S}} = N_{\mathrm{c}} + \underbrace{N_{\mathrm{wS}}}_{=N_{1\mathrm{S}}} + \underbrace{N^{(2)}_{\mathrm{HS}} + N^{(2)}_{\mathrm{NaS}}}_{=N_{ie}} + \underbrace{N_{\mathrm{SOH_2}} + N_{\mathrm{SOH}} + N_{\mathrm{SO}}}_{=N_{sc}}\,. \tag{6.9}$$

Thus

$$\delta N_{\mathrm{S}} = \delta N_{1\mathrm{S}}\,. \tag{6.10}$$

[4] If the pressure terms are neglected in the chemical potentials of ions, then $\overline{\mathcal{G}}_{n\mathrm{S}} = \mathcal{G}_{n\mathrm{S}}$, $n \in [2,4]$.

[5] Note that 1. the surface complexation sites are counted, not the ions that fix on them; 2. the ions of the outer layer are not accounted for, on the ground that they do not participate to the mechanical behavior.

6.2.2 Chemo-mechanical contribution

To recover the standard Cam-Clay model in the limit of inert soils, the elasticity will be assumed to be logarithmic in the effective mean-stress and linear in shear. Moreover, the bulk modulus is taken here to depend on chemistry. While the framework allows for a chemistry-dependent shear modulus G, this possibility is not exploited, due to insufficient data, and the shear modulus is kept constant.

At this point, it is instrumental to record the decomposition of the strain and of the effective stress into their spherical and deviator parts, namely $\boldsymbol{\epsilon} = \frac{1}{3}\,\mathrm{tr}\boldsymbol{\epsilon}\,\mathbf{I} + \mathrm{dev}\,\boldsymbol{\epsilon}$, and $\bar{\boldsymbol{\sigma}} = -\overline{p}\,\mathbf{I} + \mathbf{s}$, with $\overline{p} = -\frac{1}{3}\,\mathrm{tr}\bar{\boldsymbol{\sigma}}$ the effective mean stress, and $q = (\frac{3}{2}\,\mathbf{s}:\mathbf{s})^{\frac{1}{2}}$ the shear stress.

The chemo-mechanical contribution to the elastic potential is postulated in the format,

$$\varphi_{\mathrm{ch-mech}}(\bar{\boldsymbol{\sigma}}, \mathcal{N}_{\mathrm{S}}) = -\overline{p}\,\mathrm{tr}\,\boldsymbol{\epsilon}^{\mathrm{el}}_{\kappa} + \kappa\, F(\overline{p}) + \frac{q^2}{6\,G}\,. \tag{6.11}$$

Here $\kappa = \kappa(\mathcal{N}_{\mathrm{S}})$ is the generalized Cam-Clay elastic coefficient: in practice the chemical dependence is introduced via molar fractions, Loret et al. [2002]. $F(\overline{p})$ is the function that introduces a logarithmic dependence in mean-stress,

$$F(\overline{p}) = \overline{p}\,\mathrm{Ln}\,\frac{\overline{p}}{\overline{p}_{\kappa}} - \overline{p}\,, \quad \frac{dF}{d\overline{p}} = \mathrm{Ln}\,\frac{\overline{p}}{\overline{p}_{\kappa}}\,, \tag{6.12}$$

and $\mathrm{tr}\boldsymbol{\epsilon}_{\kappa}$ is the value of the elastic volume change when the effective mean-stress varies from the convergence stress $\overline{p}_{\kappa}$ to a small reference value $\overline{p}_0$ while the pore fluid is deionised water,

$$\mathrm{tr}\boldsymbol{\epsilon}_{\kappa} = -\kappa^{\mathrm{dw}}\,\mathrm{Ln}\,\frac{\overline{p}_{\kappa}}{\overline{p}_0} \quad \text{with} \quad \kappa^{\mathrm{dw}} = \kappa(\mathcal{N}_{\mathrm{S}}^{\mathrm{dw}})\,. \tag{6.13}$$

An estimation of the chemical content of clay clusters, denoted by the symbol $^{\mathrm{dw}}$ when pore water is deionised, is proposed in Appendix D of Gajo et al. [2002].

6.2.3 Enthalpies of formation

The contribution of the enthalpies of formation, which generate the equilibrium constants, is simply

$$\varphi_{\mathrm{cf}}(\mathcal{N}_{\mathrm{S}}) = -\sum_{k\in\mathcal{S}} g^0_{k\mathrm{S}}\,\mathcal{N}_{k\mathrm{S}} = -\sum_{n\in[2,4]} \mathcal{G}^0_{n\mathrm{S}}\,\mathcal{N}_{n\mathrm{S}}\,. \tag{6.14}$$

6.2.4 Electrical contribution

According to the constant capacitance model, the clay is behaving as a capacitor, of constant capacitance G_e [unit Farad F=Coulomb C/Volt V]. The difference of electrical potentials between the two surfaces of the capacitor expresses in terms of the electrical variable charge as

$$\phi_{\mathrm{S}} - \phi_{\mathrm{W}} = \frac{M_{\mathrm{c}}}{G_e}\,\sigma_{ev} = \frac{F\,V_0}{G_e}\,\mathcal{N}_{ev}\,. \tag{6.15}$$

Thus the electrical contribution to the elastic potential is postulated in the format

$$\varphi_{\mathrm{e}}(\mathcal{N}_{\mathrm{S}}) = -F\,\phi_{\mathrm{W}}\,\mathcal{N}_{ev} - \frac{F^2\,V_0}{2\,G_e}\,\mathcal{N}^2_{ev}\,. \tag{6.16}$$

The mole content of the variable electrical charge $\mathcal{N}_{ev} = N_{ev}/V_0$ is given by (5.27) as $\mathcal{N}_{3\mathrm{S}} - \mathcal{N}_{4\mathrm{S}}$.

6.3 The complete chemo-hyperelastic relations

Upon summation of the four contributions to the elastic potential, the constitutive equations (6.7) can be recast in the following form,

$$\mathrm{tr}\boldsymbol{\epsilon} = \mathrm{tr}\boldsymbol{\epsilon}_\kappa - \kappa\,\mathrm{Ln}\frac{\overline{p}}{\overline{p}_\kappa}\,, \quad \mathrm{dev}\boldsymbol{\epsilon} = \frac{\mathbf{s}}{2\,G} \tag{6.17}$$

$$\overline{\mathcal{G}}_{1\mathrm{S}} = -F(\overline{p})\,\frac{\partial\kappa}{\partial\mathcal{N}_{1\mathrm{S}}} + RT\,\mathrm{Ln}\,x_{\mathrm{wS}} \tag{6.18}$$

$$\overline{\mathcal{G}}_{2\mathrm{S}} = \mathcal{G}^0_{2\mathrm{S}} - F(\overline{p})\,\frac{\partial\kappa}{\partial\mathcal{N}_{2\mathrm{S}}} + RT\,\mathrm{Ln}\,\frac{x^{(2)}_{\mathrm{HS}}}{x^{(2)}_{\mathrm{NaS}}} \tag{6.19}$$

$$\overline{\mathcal{G}}_{3\mathrm{S}} = \mathcal{G}^0_{3\mathrm{S}} - F(\overline{p})\,\frac{\partial\kappa}{\partial\mathcal{N}_{ev}} + RT\,\mathrm{Ln}\,\frac{\{\mathrm{SOH_2}\}}{\{\mathrm{SOH}\}} + F\,\phi_{\mathrm{S}} \tag{6.20}$$

$$\overline{\mathcal{G}}_{4\mathrm{S}} = \mathcal{G}^0_{4\mathrm{S}} + F(\overline{p})\,\frac{\partial\kappa}{\partial\mathcal{N}_{ev}} + RT\,\mathrm{Ln}\,\frac{\{\mathrm{SO}\}}{\{\mathrm{SOH}\}} - F\,\phi_{\mathrm{S}} \tag{6.21}$$

The enthalpies of formation $\mathcal{G}^0_{n\mathrm{S}}$, $n \in [2,4]$, give rise to equilibrium constants. The electrochemical affinities above can be checked to be consistent with the solid part of the entities derived in Sect. 5, namely (5.3), (5.7), (5.11), and (5.17), to within the fact that now, due to the existence of an elastic potential, mechanical coupling terms appear in the form of a derivative of the elastic coefficient κ. It has been anticipated that κ depends on the mechanisms of acidification and alkalinization through the electrical charge only. Still, the mechanical contribution to the sole chemical potential of water in (6.18) is significant.

In actual calculations, the rate transfer formulas are still valid if the definitions of the pressure term and equilibrium constants are formally modified as follows:

$$\underline{v}_{\mathrm{w}}\,(p_{\mathrm{wS}} - p_{\mathrm{W}}) \quad \overset{\text{modified to}}{\rightarrow} \quad -F(\overline{p})\,\frac{\partial\kappa}{\partial\mathcal{N}_{1\mathrm{S}}} \tag{6.22}$$

$$RT\,\mathrm{Ln}\,\frac{1}{K^{eq}_2} = \mathcal{G}^0_{2\mathrm{S}} - F(\overline{p})\,\frac{\partial\kappa}{\partial\mathcal{N}_{2\mathrm{S}}} \Rightarrow \frac{1}{K^{eq}_2} \quad \overset{\text{modified to}}{\rightarrow} \quad \frac{1}{K^{eq}_2} \times \exp\Big(-\frac{F(\overline{p})}{RT}\,\frac{\partial\kappa}{\partial\mathcal{N}_{2\mathrm{S}}}\Big) \tag{6.23}$$

$$RT\,\mathrm{Ln}\,K^{eq}_3 = \mathcal{G}^0_{3\mathrm{S}} - F(\overline{p})\,\frac{\partial\kappa}{\partial\mathcal{N}_{ev}} \Rightarrow K^{eq}_3 \quad \overset{\text{modified to}}{\rightarrow} \quad K^{eq}_3 \times \exp\Big(-\frac{F(\overline{p})}{RT}\,\frac{\partial\kappa}{\partial\mathcal{N}_{ev}}\Big) \tag{6.24}$$

$$RT\,\mathrm{Ln}\,\frac{1}{K^{eq}_4} = \mathcal{G}^0_{4\mathrm{S}} + F(\overline{p})\,\frac{\partial\kappa}{\partial\mathcal{N}_{ev}} \Rightarrow \frac{1}{K^{eq}_4} \quad \overset{\text{modified to}}{\rightarrow} \quad \frac{1}{K^{eq}_4} \times \exp\Big(\frac{F(\overline{p})}{RT}\,\frac{\partial\kappa}{\partial\mathcal{N}_{ev}}\Big) \tag{6.25}$$

7 Chemo-plastic constitutive equations

In generic loading paths, the generalized strains are contributed by an elastic, or reversible, part and a plastic, or irreversible, part,

$$\boldsymbol{\epsilon} = \boldsymbol{\epsilon}^{\rm el} + \boldsymbol{\epsilon}^{\rm pl}\,, \quad \mathcal{N}_{n\rm S} = \mathcal{N}_{n\rm S}^{\rm el} + \mathcal{N}_{n\rm S}^{\rm pl},\ n \in [1,4]\,. \tag{7.1}$$

In this context, the relations of the previous section are seen as involving the elastic, rather than the total, part of the strains.

Plasticity is driven by the solid skeleton, and a plastic strain $\boldsymbol{\epsilon}^{\rm pl}$ goes unquestioned. Other generalized plastic strains result *from* the plasticity of the solid skeleton. For example, in a standard poroplasticity model with incompressible constituents, a 'plastic' volume content of pore fluid, proportional to the plastic strain $\boldsymbol{\epsilon}^{\rm pl}$ is required so that the incompressibility constraint (4.5) be satisfied.

The structure of the elastic-plastic framework is motivated by the mechanical dissipation inequality. The hardening-softening rule is contributed a priori by both mechanics, via the plastic strain, and chemistry, via the chemical state variables.

7.1 The generalized flow rule

Since the elastic constitutive equations are chemo-hyperelastic, the contribution to the mechanical dissipation $(4.8)_1$ is of purely plastic origin, and, indeed,

$$\delta D_1 = -\overline{p}\,{\rm tr}\,\delta\boldsymbol{\epsilon}^{\rm pl} + \mathbf{s} : {\rm dev}\,\delta\boldsymbol{\epsilon}^{\rm pl} + \sum_{n=1,4}\overline{\mathcal{G}}_{n\rm S}\,\delta\mathcal{N}_{n\rm S}^{\rm pl}\,, \tag{7.2}$$

which motivates the generalized normality flow rule in terms of the plastic potential $g = g(\overline{p}, q, \overline{\mathcal{G}}_{\rm S})$, and of the incremental plastic multiplier $\delta\Lambda$,

$${\rm tr}\,\delta\boldsymbol{\epsilon}^{\rm pl} = -\delta\Lambda\,\frac{\partial g}{\partial \overline{p}}\,, \quad {\rm dev}\,\delta\boldsymbol{\epsilon}^{\rm pl} = \delta\Lambda\,\frac{\partial g}{\partial q}\,\frac{3}{2}\frac{\mathbf{s}}{q}\,, \quad \delta\mathcal{N}_{n\rm S}^{\rm pl} = \delta\Lambda\,\frac{\partial g}{\partial \overline{\mathcal{G}}_{n\rm S}},\ n \in [1,4]\,. \tag{7.3}$$

In the applications below, the plastic potential turns out to be independent on the chemical affinities, so that the plastic strain is the sole non vanishing generalized plastic strain. In general, the other generalized plastic strains are implied by the use of a generalized normality rule. The motivation, physical interpretation in the mineral structure and control of these entities remain to be addressed.

7.2 Mechanical and chemical hardening-softening

The yield function f is given the same arguments as g plus ${\rm tr}\boldsymbol{\epsilon}^{\rm pl}$ which allows for hardening and softening. The Modified Cam-Clay model is used as a prototype, namely

$$f = f(\overline{p}, q, \overline{\mathcal{G}}_{\rm S}, {\rm tr}\boldsymbol{\epsilon}^{\rm pl}) = \frac{q^2}{M^2\,\overline{p}} + \overline{p} - p_{\rm c}\,, \tag{7.4}$$

with $M = M(\overline{\mathcal{G}}_{\rm S})$ and $p_{\rm c} = p_{\rm c}(\overline{\mathcal{G}}_{\rm S},\ {\rm tr}\boldsymbol{\epsilon}^{\rm pl})$. Notice that the major symmetry of the elastic-plastic incremental relations holds iff the flow rule is associative, namely $f = g$.

The lines of volume changes during mechanical loadings have a slope λ and converge to a point $\overline{p}_\lambda$,

$${\rm tr}\,\boldsymbol{\epsilon} = {\rm tr}\,\boldsymbol{\epsilon}_\lambda - \lambda\,{\rm Ln}\,\frac{\overline{p}}{\overline{p}_\lambda}\,, \quad {\rm tr}\,\boldsymbol{\epsilon}_\lambda \equiv -\lambda^{\rm dw}\,{\rm Ln}\,\frac{\overline{p}_\lambda}{\overline{p}_0}\,, \tag{7.5}$$

with $\lambda = \lambda(\overline{\mathcal{G}}_{\rm S})$, $\lambda^{\rm dw} = \lambda(\overline{\mathcal{G}}_{\rm S}^{\rm dw})$, while the unloading curves are defined by eqns (6.13),(6.17) with $\kappa = \kappa(\mathcal{N}_{\rm S}^{\rm el})$ and $\kappa^{\rm dw} = \kappa(\mathcal{N}_{\rm S}^{\rm el,dw})$. The actual expressions used for $\kappa = \kappa(\mathcal{N}_{\rm S}^{\rm el})$ and $\lambda = \lambda(\overline{\mathcal{G}}_{\rm S})$ are provided respectively in Appendices B and D.

Combining the elastic and plastic volumetric changes provides the preconsolidation stress $p_{\rm c}$. In order to reduce the chemical dependence of the preconsolidation stress $p_{\rm c}$ to a single type of parameter, namely the electro-chemical affinities $\overline{\mathcal{G}}_{\rm S}$, a slight modification is introduced, and the chemical dependence of κ is expressed as $\tilde{\kappa} = \tilde{\kappa}(\overline{\mathcal{G}}_{\rm S})$. This transformation requires a particular structure of the electro-chemical affinities, namely the set $\mathcal{N}_{\rm S}^{\rm el}$ has to be calculated in terms of the set $\overline{\mathcal{G}}_{\rm S}$ in a tractable format[6]. The resulting preconsolidation stress,

$$(\lambda - \tilde{\kappa}) \operatorname{Ln} \frac{p_{\rm c}}{\overline{p}_0} = -\operatorname{tr} \boldsymbol{\epsilon}^{\rm pl} + (\lambda - \lambda^{\rm dw}) \operatorname{Ln} \frac{\overline{p}_\lambda}{\overline{p}_0} - (\tilde{\kappa} - \tilde{\kappa}^{\rm dw}) \operatorname{Ln} \frac{\overline{p}_\kappa}{\overline{p}_0} \,, \tag{7.6}$$

appears as a modification of the standard preconsolidation stress of the Cam-Clay model. The latter is recovered when both $\overline{p}_\kappa$ and $\overline{p}_\lambda$ are equal and $\lambda - \tilde{\kappa}$ is independent of chemical content of the solid phase. Purely chemical loadings and unloadings are then elastic.

[6]The required partial inversion $\mathcal{N}_{\rm S}^{\rm el} = \mathcal{N}_{\rm S}^{\rm el}(\overline{\mathcal{G}}_{\rm S})$ is provided in Appendix C.

8 Material parameters and initial data

Material parameters pertain to an Na-bentonite tested by Gajo and Maines [2007], whose index properties, composition and mechanical characteristics are very similar to the natural Na-bentonite, referred to as Ponza clay by Di Maio [1998].

A slight modification of the scheme presented so far is required. Indeed, the liquid limit of a pure Na-montmorillonite is about 700%. However, the experimental values of the liquid limit of the tested clay samples displayed on Fig. 6 are lower. Metallic ions other than sodium are concluded to be present and to participate to the ion exchange process. As the simplest possibility, three monovalent cations are considered to compete for the X-sites, e.g. ions sodium, potassium and hydrogen respectively. The presence of ions potassium requires an additional independent mole content associated to an electro-chemical affinity, and the number of transfer equations and equilibrium equations is increased by one. The modifications required by the presence of these three ions are sketched in Appendix A.

8.1 Material parameters

8.1.1 Molar masses and molar volumes

The apparent molar volumes of dissolved species are not constant, even under isothermal conditions. The apparent molar volumes of electrically neutral species, like NaCl and KCl, depend on their own molalities or concentrations, Lobo [1990]. In a solution, due to electrostriction, a charged ion is attracted so strongly by counterions that, at low concentration, the ionic link implies a reduction in volume with respect to the two independent species. The apparent molar volume of some ions can result to be negative. As the concentration increases, the phenomenon is counteracted by the repulsion between ions whose electrical charges are of the same sign.

The apparent molar volumes reported in Table 1 represent a reasonable approximation at low ionic concentrations.

Table 1. Molar masses (gm) and apparent molar volumes (cm^3)

species	molar mass	molar volume
H_2O	18	18
Na^+	23	2.8
K^+	39.1	12.8
H^+	1	4.1
OH^-	17	-7.8
Cl^-	35.5	14
clay	382	119.375

8.1.2 Parameters linked to the electrical charge

Permanent charge and variable charge

A characteristics of montmorillonites is their cation exchange capacity (CEC) defined as the permanent charge per unit mass, namely N_{ep}/M_c. The CEC is usually expressed in meq/100gm of clay=centimole/kg. It can also be expressed in Coulomb/m^2 as $F\,N_{ep}/A_c$. The specific area A_c/M_c ranges from 700×10^3 to $840\times10^3\,m^2$/kg for montmorillonites, but is much less for kaolinites, namely from 10×10^3 to $20\times10^3\,m^2$/kg. For a montmorillonite of molar mass 382 gm, a typical CEC of -100 meq/100gm=-1 mole/kg implies a permanent valence ζ_{cp}=-0.382. For the

bentonites analysed here, these numbers are assumed to be slightly lower according to Gajo et al. [2002],

$$\frac{N_{ep}}{M_{\rm c}} = -0.863872\,\text{mole/kg}, \quad \zeta_{cp} = \frac{N_{ep}}{N_{\rm c}} = -0.33\,. \tag{8.1}$$

The variable electrical charge in the volume V_0 varies in the range $[-F\,N_{sc}, F\,N_{sc}]$. Thus the total charge of the clay mass varies from $F\,(-|N_{ep}|+N_{sc})$ at low pH to $F\,(-|N_{ep}|-N_{sc})$ at high pH. At low pH, the ratio of the variable versus permanent charge is N_{sc}/N_{ep}, while it is just the opposite at high pH. This ratio is moderate for montmorillonites, but larger for kaolinites, typically,

$$\frac{N_{sc}}{|N_{ep}|} = 0.1 - 0.2 \text{ for montmorillonites}, \quad 1.0 - 2.0 \text{ for kaolinites}\,. \tag{8.2}$$

Capacitance

The smaller the capacitance, the smoother the variations in terms of pH of the electrical charge and of the number of surface sites, as indicated by Figs. 5-(a)-(b). The value selected for the areal capacitance is in the range quoted in the literature, e.g. Majone et al. [1996].

The plots of Fig. 5 have been obtained by solving the equilibrium equations (8.7) below, for a clay exposed to a fluid phase of increasing pH. The number of the sites S–OH_2^+ decreases monotonously, and the number of the sites SO^- increases monotonously as the pH of the fluid phase increases. The number of the sites S–OH has a maximum at a finite pH. With help of the relations (4.7),(5.29), and equilibria (5.12),(5.18), this extremum can be shown to occur at zero electrical variable charge, and thus to be independent of the capacitance in view of (6.15). The corresponding pH is usually called isoelectric point of the variable charge. The values corresponding to this extremum depend only on the constants defining the acid-base equilibrium,

$$\frac{N_{\rm SOH}}{N_{sc}} = \frac{1}{1+2\,\alpha}, \quad \frac{N_{\rm SOH_2}}{N_{sc}} = \frac{N_{\rm SO}}{N_{sc}} = \frac{\alpha}{1+2\,\alpha}, \quad \text{pH} = -\frac{1}{2}\text{Ln}_{10}\frac{K_3^{eq}}{\underline{v}_{\rm w}}\,\frac{K_4^{eq}}{\underline{v}_{\rm w}}\,, \tag{8.3}$$

where, via (5.25),

$$\alpha^2 = \frac{K_4^{eq}}{K_3^{eq}}\,. \tag{8.4}$$

For the constants listed in Table 3, $\alpha = 0.132$, and the variable charge vanishes at pH=6.60. [7]

Table 2. Electrical properties of the clay

specific area $A_{\rm c}/M_{\rm c}$ (m^2/kg)	700×10^3
specific permanent charge $N_{ep}/M_{\rm c}$ (mole/kg)	-0.863872
specific nb of surface sites $N_{sc}/M_{\rm c}$ (mole/kg)	0.08801
areal capacitance G_e/A_c (F/m^2)	6.66

[7] Moreover, the number of sites S–OH and S–OH_2^+ are equal for

$$\frac{N_{\rm SOH}}{N_{sc}} = \frac{N_{\rm SOH_2}}{N_{sc}} = \frac{1}{2+\alpha^2}, \quad \frac{N_{\rm SO}}{N_{sc}} = \frac{\alpha^2}{2+\alpha^2}, \quad \text{pH} = -\text{Ln}_{10}\frac{K_3^{eq}}{v_{\rm w}^{\rm M}} - \frac{F^2\,N_{sc}}{G_e RT}\,\frac{1-\alpha^2}{2+\alpha^2}\,. \tag{8.5}$$

Similarly, the number of sites S–OH and SO are equal for

$$\frac{N_{\rm SOH}}{N_{sc}} = \frac{N_{\rm SO}}{N_{sc}} = \frac{1}{2+\alpha^2}, \quad \frac{N_{\rm SOH_2}}{N_{sc}} = \frac{\alpha^2}{2+\alpha^2}, \quad \text{pH} = -\text{Ln}_{10}\alpha^2\,\frac{K_3^{eq}}{v_{\rm w}^{\rm M}} + \frac{F^2\,N_{sc}}{G_e RT}\,\frac{1-\alpha^2}{2+\alpha^2}\,. \tag{8.6}$$

8.1.3 Equilibrium constants

The relative affinities of the three ions Na^+, K^+ and H^+ for the X-sites may be characterized by the two equilibrium constants defined in Appendix A. The constant K_2^{eq} associated to the ion exchange $Na^+ \rightleftharpoons H^+$ is the product of these constants.

The prescription of the isoelectric point of the variable charge and of the associated relative number of SOH sites, as indicated by eqns (8.3)-(8.4) and shown on Fig. 5, suffices to define the surface complexation constants K_3^{eq} and $K_{\overline{4}}^{eq}$, from which K_4^{eq} is obtained via (5.25).

Table 3. Equilibrium constants for ion exchange and surface complexation

K_2^{H-K}	K_2^{K-Na}	K_3^{eq}	$K_{\overline{4}}^{eq}$
50	5	3.42×10^{-8}	5.856×10^{-10}

8.1.4 Chemo-mechanical coefficients

The identification procedure of the chemo-mechanical coefficients at given pH is described in Gajo et al. [2002]. The Cam-Clay coefficient κ varies between a maximum value κ^{dw} in presence of deionised water to a minimum value κ^{sat} at high ionic strength. The variation is strong at low ionic strength, where the initial slope is controlled by the coefficient κ_3. Note that the dependence of electrical shielding on individual ions decreases so as to vanish as the ionic strength increases. The elastic parameters selected for the clays tested are given in Table 4. Moreover, the difference $\lambda - \kappa$ is assumed constant and equal to 0.098 and the convergence stresses $\overline{p}_\kappa$, eqn (6.13), and $\overline{p}_\lambda$, eqn (7.5), are both equal to 2 200 kPa. Thus there is no chemical hardening and, therefore, chemical loadings and unloadings at constant effective stress are reversible. The effect of pH expresses linearly through the relative variable electric charge N_{ev}/N_{sc}, which is equal to +1 at high acidity, and to -1 at high alkalinity.

Table 4. Mechanical parameters

coefficient	Na^+	K^+	H^+
κ^{dw} at low pH	0.060	0.013	0.020
κ^{dw} at high pH	0.115	0.015	0.030
κ^{sat}	0.010	0.010	0.010
κ_3	15	15	25

8.2 Initial configuration

The clay sample is put in contact with a reservoir of deionised water at atmospheric pressure. Establishment of equilibrium, under a mechanical load of 20 kPa, implies some modification of the chemical composition of the reservoir, which, in practice, has always a finite size. The overall initial volumes and initial compositions of the fluid phase and reservoir are shown in Tables 5-7. They are computed by requiring the electro-chemical affinities $\overline{\mathcal{G}}_{1S}$ to $\overline{\mathcal{G}}_{4S}$ to be in equilibrium with their counterparts in the fluid phase,

$$\overline{\mathcal{G}}_{nS} = \overline{\mathcal{G}}_{nW}, \quad n \in [1, 4]\,. \tag{8.7}$$

Typical of bentonites, the fluid phase results alkaline with a pH=9, while metallic ions appear in the form of traces only, Table 6. Since the fixed electric charge remains in the solid phase, the chemical composition of the reservoir and fluid phase are identical.

A part of water, referred to as irreversibly bound water, is closely tied to the mineral and does not evaporate at 105°C, while the remaining part, referred to as reversibly bound water, is

modified mainly by a changing chemical environment. The void ratio in the two phase context is equal to $e_0^* = V_{\rm W}/V_{\rm S}$. On the other hand, the traditional void ratio $e_0 = (V_{\rm W}+V_{\rm rbw})/(V_{\rm S}-V_{\rm rbw})$ excludes the volume $V_{\rm rbw}$ of the reversibly bound water from the solid part.

The total number of sites of exchangeable cations is chosen so as to neutralize the negative permanent charge of the clay, namely $N_{ie} = -N_{ep}$. The total number of complexation sites N_{sc} is fixed as a proportion of N_{ep} as indicated by (8.2). The relative number of each ion participating to the ion exchange process and of the three surface sites is obtained as the solution of the equilibrium (8.7). The number of neutralizing ions in the diffuse layer is then deduced as indicated in Fig. 4, namely $N_{\rm Cl} = N_{\rm SOH_2}$, $N_{\rm Na} = N_{\rm SO}$. The resulting initial chemical composition of the solid phase is displayed by Table 7. The specific gravity of the clay 204.851/84.084=2.436 is thus close to the minimum quoted in the literature. Note also that the moderately alkaline environment of bentonites (pH=9) is associated to the negative relative variable charge $N_{ev}/N_{sc} = -0.548$ as can be checked on Fig. 5.

Table 5. Overall initial volumes and mechanical state

total initial volume V_0 (liter)	1000
initial volume of solid phase $V_{\rm S}$ (liter)	174.1
initial volume of fluid phase $V_{\rm W}$ (liter)	825.9
traditional void ratio e_0	10.93
void ratio e_0^*	4.75
preconsolidation stress p_{c0} (kPa)	20
water pressure $p_{\rm W} - p_{\rm atm}$ (kPa)	0

Table 6. Initial partition of ionic species in the *fluid phase* of volume $V_{\rm W}$

species	mmole nb.
cation Na^+	8.1577600
cation K^+	0.2719250
cation H^+	0.0008259
anion OH^-	8.2590000
anion Cl^-	0.1715120

Table 7. Initial partition of species and sites in the *solid phase*

species or site	mass (kg)	volume (liter)	nb of moles	charge
clay mineral	170.9952	53.436	447.631	-147.7180
cation $Na^{+(2)}$	2.8503	0.3470	123.926	+123.9260
cation $K^{+(2)}$	0.8076	0.2645	20.6547	+20.6547
cation $H^{+(2)}$	0.0031	0.01271	3.1	+3.1000
site SOH_2^+	-	-	0.084507	+0.0845
site SOH	-	-	6.61766	0
site SO^-	-	-	8.34783	-8.3478
anion $Cl^{-(3)}$	0.003	0.0012	0.084507	-0.0845
cation $Na^{+(\overline{4})}$	0.192	0.0234	8.34783	+8.3478
irreversibly bound water	30	30	1666.67	0
reversibly bound water	90	90	5000	0

9 Simulations

The constitutive model is used to simulate purely mechanical, purely chemical and mixed chemo-mechanical loading processes. The chemical composition of the reservoir in contact with the clay sample is controlled. The chemical loading information carries to the clay through the transfer equations

$$\frac{\delta N_{n\mathrm{S}}}{\delta t} = -\frac{1}{\tau_n}\frac{\mathcal{G}_n}{RT}\,, \tag{9.1}$$

where $\mathcal{G}_n = \mathcal{G}_{n\mathrm{S}} - \mathcal{G}_{n\mathrm{W}}$ is the chemical affinity of the mechanism $n \in [1,4]$. The fluid part $\mathcal{G}_{n\mathrm{W}}$ of the chemical affinity, defined in explicit form in Sect. 5, is controlled since the chemical compositions of the fluid phase and reservoir are identical in the present framework. The solid part $\mathcal{G}_{n\mathrm{S}}$ is provided by the constitutive equations of Sect. 6.

The present simulations address only equilibrium paths. The granularity of the time scale is much larger than any of the transfer times, so that the chemical affinities $\mathcal{G}_n$, $n \in [1,4]$, are zero at any point of the scale of observation. A comprehensive analysis, where the transient spatial heterogeneities induced by diffusion are accounted for, will be presented in a finite element framework.

9.1 The liquid limit as a mechanical indicator

Gajo and Maines [2007] report experimental variations of the liquid limit of a Na-bentonite as a function of pore water composition and pH. They bath a specified amount of dry clay in a large volume of solution thus obtaining a suspension. The ratio between the weight of solution and the weight of the clay is usually fifteen. This notwithstanding, for the smaller ionic strengths, a correction of pH would have been anyway necessary for maintaining the pH of surnatant equal to the initial value of the solution. Actually, the correction was performed only for hydrochloric acid.

Experimental data show that the liquid limit essentially decreases as the ionic strength increases, Fig. 6. This general trend should be mitigated. Indeed, first the data are clearly ion-dependent. For instance, the same concentration of HCl and KCl is accompanied by distinct liquid limits. Moreover, the liquid limit initially increases at small concentration of NaOH and KOH.

The ionic dependence of the Cam-Clay coefficient κ and liquid limit are assumed to follow similar trends. The validity of this assertion is checked by comparing experimental data and model simulations on various chemical and mixed chemo-mechanical loading paths.

9.2 Swelling and chemical consolidation under purely chemical loading paths

9.2.1 Ion exchange, surface complexation and electrical shielding

Three ion-induced mechanical effects have been built in the model:

(1) *ion exchange*: the competition for the X-sites of the clay is controlled by the relative order of the affinities of ions, quantified by free enthalpies of formation and equilibrium constants. This relative order, namely $H^+ > K^+ > Na^+$ according to Table 3, does not carry over to mechanical stiffnesses, for which $K^+ > H^+ > Na^+$ according to Table 4. Thus replacement of a site X-Na by a site X-H or X-K leads to volume contraction. Ionic replacements are a priori reversible, as stressed in Loret and Gajo [2004] based on the experiments of Di Maio and Fenelli [1997] and Gajo and Maines [2007]. Still under large confining stresses, they may well contribute to induce plasticity. Acid-base reactions which

may impart edge-to-face friction are traditionally expected to induce more irreversibility, but macroscopic data to substantiate or invalidate this statement are currently lacking. Therefore chemical hardening and softening have been neglected in the simulations;
(2) *surface complexation*: adsorption of ions H^+ onto the surface sites leads to contraction while adsorption of ions OH^- leads to volume expansion, as suggested by the experimental data of evolutions of the liquid limit shown on Fig. 6. Still, the pH-induced effects on mechanical properties of clayey materials may not be always monotonous, because surface complexation can be concomitant with other mechanisms, like ion exchange; Reasons that can be advocated are the dissolution of clay minerals in some sand-clay mixtures as indicated in Sect. 2, or the various configurations adopted by the clay sheets in kaolinites;
(3) *electrical shielding*: screening of electrical repulsion between charged particles by ions solvated in the diffuse layer leads to volume contraction. At this point, it is worth issuing a warning. Indeed, observation of experimental results of ionic replacements, at moderate to large concentrations only, might incorrectly suggest that the induced mechanical effects are roughly ion-independent. Still, a more careful observation of volume changes at low ionic strength shows opposite. This point of view, indirectly motivated by the data displayed on Fig. 6, is reflected in the elastic parameters shown in Table 4.

Changes in compliances, and equivalently volume changes, described by the model under various modifications of chemical composition of pore water are shown on Fig. 7-(a). These changes are dictated by the following phenomena:

(4) at small identical concentrations, NaOH induces larger swelling than NaCl. Indeed, at increasing concentration of NaOH, ion exchange and surface complexation cooperate to induce swelling. On the other hand, surface complexation is not triggered by changes in NaCl concentration. Note that displacement of ions H^+ by ions Na^+ is progressive due to the larger affinity of the former ions to the X-sites;
(5) at small identical concentrations, KOH induces contraction while NaOH induces swelling. Indeed, unlike for NaOH, at increasing concentration of KOH, ion exchange and surface complexation compete to control the volume change, ionic exchange leading to contraction and surface complexation inducing swelling, and the former mechanism definitely dominates;
(6) the exposures to KOH and KCl yield practically identical liquid limits, even if the pH is higher for KOH. In fact, the initial pH is already 9 and the range of variation of the elastic parameter associated to the ions K^+ is small for pH above 9, Table 4;
(7) at increasing concentration of hydrochloric acid HCl, ion exchange and surface complexation cooperate to induce contraction. Note that volume change is rapid, again due to the large affinity of the ions hydrogen to the X-sites;
(8) as the ionic strength of the solution increases, the volume decreases, because the coefficients κ^{sat} are smaller than the coefficients κ^{dw}. The final volumes are equal because the κ^{sat}'s are considered here to be independent of ions and of pH, Table 4.

A spectacular illustration of the various ion-induced mechanisms is displayed on Fig. 8, where a H-clay is exposed to either NaOH or NaCl. The H-clay is obtained by exposing first the Na-bentonite to a solution of HCl, resulting in a significant contraction.

Subsequent exposure to NaOH annihilates this volume change by reversing the surface complexation mechanism and the ion exchange mechanism, which cooperate to induce swelling. On the other hand, during exposure to small concentrations of NaCl, the ion exchange mechanism is activated like for NaOH, while the surface complexation mechanism is not activated. At

larger ionic strength, electrical shielding wipes out anyway the possible differences attached to individual ions.

9.2.2 An artefact of the experimental setup

The experimental setup used in standard chemical loadings introduces an artefact, even for equilibrium paths. The key parameter is the relative size, or mass, of the reservoir in contact with the sample and of the sample itself.

Indeed, when for example the concentration of K^+ is increased in the reservoir, these ions diffuse to the fluid phase, and next they transfer to the solid phase. They may displace ions present at X-sites, e.g. ions Na^+. The latter transfer to the fluid phase and next diffuse to the reservoir. This phenomenon introduces a modification of the chemical composition of the reservoir. The smaller the reservoir, the larger will be the additional concentration due to the displaced ions.

Consequently the variation of the coefficient κ for a finite reservoir is, at small ionic strength, expected to be smaller than for an infinite reservoir. Indeed, exposure to an ion displaces other ions, and their presence in the reservoir counterbalances the influence of the primary ion. For example, exposure of the Na-bentonite to ions sodium would intrinsically imply a significant swelling at small ionic strength. Displacement of ions potassium or hydrogen by ions sodium and their diffusion to the reservoir will reduce this swelling. Conversely, exposure of the clay to ions potassium implies a contraction, which is moderated by the displacement of ions sodium.

Still the effect of counterbalance advocated above applies to ions for which the order of affinities to the X-sites carries over to the mechanical stiffnesses. This property does not hold for ions hydrogen and potassium. Therefore, exposure to ions hydrogen in a finite reservoir will displace ions potassium, which will induce more contraction than in an infinite reservoir.

Simulations in Fig. 7 illustrate this artefact. Fig. 7-(a) involves an infinite reservoir, and thus provides an intrinsic material response. The use of a reservoir whose mass is fifteen times larger than that of the clay yields results which are significantly different, Fig. 7-(b).

9.2.3 Complex variation of the chemical composition of the reservoir

A standard test begins by exposing the clay sample to a reservoir of deionised water, and to submit it to a purely mechanical oedometric consolidation. Once equilibrium is reached, the load is kept constant and a purely chemical complex loading is imposed. The test shown on Fig. 9 intertwines increases of ionic strength of the reservoir, via either HCl or NaOH, to 0.1 or 0.5 M, and restoration of a quasi-deionised fluid. In the experimental process, modification of the chemical composition of the reservoir is performed only once a steady volumetric strain is reached. This stage is assumed to be associated with a uniform mechanical and chemical state of the clay sample. Since it involves coupled electro-mechanical diffusion, the complete process depends on several characteristic times. The point is analysed in detail in Gajo and Loret [2003],[2004]. The transient period, before steady state is reached, is inherently inhomogeneous. The present analysis being local, only steady states can be simulated by the constitutive equations. Thus the x-axis of the model simulations of Fig. 9-(b) can be thought of as a fictitious time.

The experimental process and simulations reported in Fig. 9 deserve the following comments:

(1) exposure to hydrochloric acid is accompanied by a significant contraction due to the simultaneous effects of the ion exchange and surface complexation mechanisms, as already observed in Fig. 8;

(2) subsequent refreshment of the reservoir does not succeed to displace the hydrogen ions (endowed with the highest affinity to the X-sites), and thus the contractive strain is not unlocked, even if the latter should not be understood as irreversible, as it can be seen in the subsequent loading. Still some swelling is observed due to decrease of electrical shielding and to a more negative variable charge. In fact, the phenomenon is also displayed in Fig. 13 (exposure to deionised water from point E to point F');
(3) subsequent exposure to a small concentration of NaOH leads to significant unlocking of the contraction, corresponding to the peak in the experimental results, and to the dotted curve in the simulations. This swelling is due to the concomitant effects of ion exchange (increased number Na-X sites) and surface complexation (more negative variable charge). Similarly to Fig. 8, further increase of the concentration of NaOH to 0.1 M introduces electrical shielding which limits the actual swelling;
(4) the second refreshment of the reservoir leads this time to complete unlocking of the contraction induced by HCl. Indeed the ion exchange repartition dominated by Na^+ has been recovered as explained in point (3). Thus the elastic Cam-Clay parameter is maximum and close to its value for a deionised water with traces of ions sodium;
(5) the above sequence is repeated four times. The experimental results show some significant difference in the first cycle, at the exposures to deionised water. This is probably due to the fact that the clay was not initially 'washed' and some salt was initially deposited and passed in the solution when the clay was first exposed to deionised water. The simulations involve only elasticity, and thus the four cycles repeat unchanged. In the fifth cycle, the concentration of NaOH is increased to 0.5 M, so that electrical shielding wipes out completely the transient swelling, associated to the peak. Subsequent exposure to deionised water unlocks the initial volume, as in point (4).

Thus the model provides a qualitatively correct description of chemically induced contraction and swelling of this complex loading path. However the experimental volume change increases progressively during the first cycles until a stabilization can be reached. Indeed, several washings with sodium hydroxyde seem necessary to displace metallic ions out of the clay sites to the pore water, and next to the reservoir where they can be disposed of. The details of the experimental setup and procedure are thought to play a significant role in this transient effect, that the constitutive model, local in nature, is not intended to capture.

Similar cyclic modifications of the chemical composition of the reservoir, but with larger concentrations and with KOH instead of HCl, are displayed on Fig. 10:
(1) the first contraction after exposure to NaOH is clearly due to electrical shielding, while the second contraction after exposure to KOH is due to both electrical shielding and ion exchange;
(2) refreshment of the reservoir after exposure to KOH does not succeed in displacing the ions K^+, whose affinity to the X-sites is larger than that of ions Na^+, so that the swelling is limited. However subsequent exposure to NaOH displaces this time almost totally the ions K^+;
(3) therefore a subsequent refreshment is able to unlock the contraction by removing electrical shielding due to sodium ions, and the situation is quite similar to that obtained at the end of point (4) above;
(4) similarly only electrical shielding and its inverse effect are at work in the last cycle of exposure to NaCl and deionised water.

9.3 Mechanical and chemo-mechanical paths

9.3.1 Mechanical tests at given chemical composition of the reservoir

Oedometric consolidation and swelling tests of samples in equilibrium with a finite reservoir of fixed chemical composition are shown on Fig. 11. The samples tested have been obtained by mixing a clay mass in a solution of given chemical composition. These reconstituted samples are known to behave slightly differently, from a quantitative point of view, from samples whose composition is modified by exposure to a reservoir at that chemical composition, Di Maio and Fenelli [1997]. Still the qualitative effects of various ions are quite similar. Deionised water, NaOH, and HCl correspond to decreasing compliance, and smaller void ratio.

9.3.2 Intertwined mechanical and chemical tests

The analysis assumes that the clay mineral does not undergo irreversible modifications in its structure due to the changes in pH. It has been argued in Loret and Gajo [2004] that many seemingly locked strains due to chemical loadings could be removed if the subsequent loadings respect some symmetry properties. Quite generally, a single elementary cycle, namely, exposure to a solution followed by exposure to deionised water, displays some residual volume change, due to a temporary modification of the internal repartition and amount of ions.

A very small residual volume change is shown on the test depicted Fig. 12, unlike on Fig. 14.

In the mixed mechanical and chemical test displayed on Fig. 12, a clay sample is exposed successively to deionised water, HCl at 0.1 M, deionised water and finally NaOH at 0.1 M. Note that the contraction and swelling at equilibrium are approximately equal and are in agreement with the simulation shown in Fig. 8: in fact at this ionic strength of 0.1 M, the volume changes due to HCl and NaOH displayed by the latter plot are exactly opposite. Moreover the initial over-swelling at the start of the re-exposure to NaOH is quite visible on the simulations of Fig. 12-(b).

The evolutions of the concentrations of the ions involved in the ion exchange mechanism, and of the variable charge are displayed on Fig. 13. Exposure of the clay to hydrochloric acid displaces completely the ions sodium and potassium. In turn, exposure to sodium hydroxide displaces the hydrogen ions and reverses the sign of the variable charge, points F'F" on Fig. 13-(b). Still, the potassium ions do not re-appear, as they have been expelled in the reservoir. Therefore the volume change due to chemical reloading should be larger: in fact it is, but the effect is small because the ion sensitivity is small at the considered ionic strength.

The mixed chemo-mechanical loading displayed on Fig. 14 involves exposure to NaOH at a higher concentration. Consequently, electrical shielding wipes out the initial swelling, and contraction results. Upon re-exposure to deionised water, the variable charge remains negative at its maximum as indicated on Fig. 15, and swelling results by removal of electrical shielding induced by ions sodium, that is by the decrease of the ionic strength in the diffuse layer (an information not reported in Fig. 15).

Note that the swelling upon re-exposure to deionised water is slightly larger than the contraction induced by exposure to NaOH, due to the displacement of the ions potassium and hydrogen from the X-sites. However, the model can not capture the amplitude of the phenomenon shown by the experiment. This phenomenon is so far not completely understood. It seems to indicate that the chemical unloading is accompanied by plasticity, a characteristic not shown in the other experiments reported here. This possibility is not ruled out by the constitutive framework, eqn (7.6), and in fact it has been discussed and illustrated in Loret et al. [2002] and Gajo et al. [2002]. While these works address isotropic chemical hardening/softening, more

sophisticated chemo-mechanical couplings can be envisaged. Data to substantiate qualitatively and quantitatively these features are needed. Still, experiments are hampered by difficulties of their own. Indeed, the modifications of the standard oedometric apparatus to accommodate the circulation of an electrolyte instead of deionised water are relatively simple. On the other hand, cyclic experiments may last for months. Such a long characteristic period of time results from the low permeability of active clays and height of the oedometric sample.

9.4 Hydraulic conductivity

The hydraulic conductivity reported in Fig. 16-(a) along the oedometric compression paths of a sample in contact with a reservoir of controlled chemical composition has been measured in Gajo and Maines [2007]. The oedometric paths are shown on Figs. 12 and 14. The permeability decreases by more than two orders of magnitude as the mechanical load increases from 20 to 1200 kPa while the traditional void ratio e changes from 12 to 2. The influence of the pore water composition increases as the void ratio decreases.

When permeability is expressed via the Kozeny-Carman relation in terms of e, the model prediction is twice the data, Fig. 16-(b). A much better prediction is obtained by using the void ratio e^* associated to the present two phase framework.

10 Outlook

A number of fluid-saturated porous materials, whether geological, biological or engineered, develop special properties through the existence of fixed electrical charges. A part of this charge is variable and affected by the pH of the electrolyte which bathes the materials. For example, the fixed charge attached to proteoglycans in knee articular cartilages is widely viewed as minimizing the static and dynamic strains due to body weight and motion. The proteoglycans in the cornea are thought to optimize the spatial distribution of water and transparency. On another perspective, the engineering of ionic polymer composites aims at maximizing the mechanical response to external chemical excitations, like change in pH, in view of improving their performance as actuators or artificial muscles. The swelling of clays is taken advantage of in the construction industry, and its low permeability is used to build barriers that prevent the diffusion of toxic chemicals and contain nuclear wastes.

While the nanometric scale of the phenomena involved is not explicitly retained, the present multi-phase multi-species framework takes into account, at a macroscopic level, of the key electro-chemo-mechanical couplings that control the constitutive behavior of these materials. In fact, at a material point, this behavior is regulated by three phenomena, deformation, chemical reactions, and generalized diffusion. At the level of a structure, for example in an oedometric test or in situ, these three phenomena interact strongly.

Indeed, even in the simplest laboratory experiments, where a sample is brought in contact with a reservoir of controlled chemical composition, the chemical excitation penetrates the sample from part of the boundary via diffusion and strong spatial heterogeneities develop. Conditions for a configuration with uniform fields to exist are to be scrutinized. Even so, the length of the transient period is governed by several characteristic times which involve both material properties, geometrical components and boundary conditions.

Initial and boundary value problems of this kind have been addressed via the finite element method in Gajo and Loret [2003],[2004]. The next step is thus to extend these efforts which involve mechanics, chemical reactions and transport phenomena, so as to incorporate the pH-dependent constitutive behavior developed here.

References

[1] Acar Y.B. (1992). Electrokinetic soil processing. A review of the state of the art. In *Grouting, soil improvement and geosynthetics*, R.H. Borden, R.D. Holtz and I. Juran eds., American Society of Civil Engineeers, New York, Geotechnical Special Publication No 30, **2**, 1420-1432.

[2] Acar Y.B., Hamed J., Alshawabkeh A.N. and Gale R.J. (1994). Removal of cadmium(II) from saturated kaolinite by application of electric current. *Géotechnique*, **44**, 239-254.

[3] Alshawabkeh A.N. and Acar Y.B. (1996). Elektrokinetic remediation. II: Theoretical model. *J. of the Geotechnical Engng. Div.*, Transactions of the ASCE, **122**(3), 186-196.

[4] Alshawabkeh A.N. and Sheahan Th. (2002). Stabilizing fine grained soils by phosphate electrogrouting. *J. Transportation Research Board*, **1787**, 53-60.

[5] Cascini L. and Di Maio C. (1994). Emungimento delle acque sotteranee e cedimenti nell'abitato di Sarno: analisi preliminare. *Rivista Italiana di Geotecnica*, **3**.

[6] De S.K. and Aluru N.R. (2004). A chemo-electro-mechanical mathematical model for simulation of pH sensitive hydrogels. *Mech. Materials*, **36**, 395-410.

[7] Di Maio C. (1998). Discussion on Exposure of bentonite to salt solution: osmotic and mechanical effects. *Géotechnique*, **48**(3), 433-436.

[8] Di Maio C. and Fenelli G. (1997). Influenza delle interazioni chimico-fisiche sulla deformabilità di alcuni terreni argillosi. *Rivista Italiana di Geotecnica*, **1**, 695-707.

[9] Du B.L., Mikroudis G.K. and Fang H.F. (1987). Effect of pore fluid pH on the dynamic shear modulus of clay. *ASTM Special Technical Publication*, **933**, 226-239.

[10] Esrig M.L. (1968). Consolidation and electrokinetics. *J. of the Soil Mechanics and Foundation Div.*, Transactions of the ASCE, **94**(4), 899-921.

[11] Eykholt G.R. and Daniel D.E. (1994). Impact of system chemistry on electro-osmosis in contaminated soil. *J. of the Geotechnical Engng. Div.*, Transactions of the ASCE, **120**, 797-815.

[12] Gajo A., Loret B. and Hueckel T. (2002). Electro-chemo-mechanical couplings in saturated porous media: elastic-plastic behaviour of heteroionic expansive clays. *Int. J. Solids Structures*, **39**, 4327-4362.

[13] Gajo A. and Loret B. (2003). Finite element simulations of chemo-mechanical coupling in elastic-plastic homoionic expansive clays. *Computer Methods in Applied Mechanics and Engineering*, **192**(31-32), 3389-3530.

[14] Gajo A. and Loret B. (2004). Transient analysis of ionic replacement in elastic-plastic expansive clays. *Int. J. Solids Structures*, **41**(26), 7493-7531.

[15] Gajo A. and Maines M. (2007). Mechanical effects induced on a natural active clay by aqueous solutions of inorganic acids and bases. Géotechnique, in press.

[16] Gajo A. and Loret B. (2007). The mechanics of active clays circulated by salts, acids and bases. Comprehensive version. Report to be available at the site http://www.unitn.it/ricerca/pubblicazioni.htm maintained by University of Trento, Italy.

[17] Grodzinsky A., Roth V., Myers E., Grossman W. and Mow V.C. (1981). The significance of electromechanical and osmotic forces in the nonequilibrium swelling behavior of articular cartilage in tension. *J. of Biomechanical Engng.*, **103**, 221-231.

[18] Huang Y. and K.M. Meek (1999). Swelling studies on the cornea and sclera: the effects of pH and ionic strength. *Biophysical J.*, **77**, 1655-1665.

[19] Kestin J. (1968). *A Course in Thermodynamics*. Blaisdell Publishing Co., Waltham, Massachusetts.

[20] Lobo V.M.M. (1990). *Handbook of Electrolyte Solutions*. Elsevier Publishing Company, Amsterdam, two volumes.

[21] Loret B., Hueckel T. and Gajo A. (2002). Chemo-mechanical coupling in saturated porous media: elastic-plastic behaviour of homoionic expansive clays. *Int. J. Solids Structures*, **39**, 2773-2806.

[22] Loret B. and Gajo A. (2004). Multi-phase multi-species mixtures CISM Courses and Lectures *Chemo-Mechanical Couplings in Geomechanics and Biomechanics* n° 462, Udine, Italia, edited by B. Loret and J.M. Huyghe, Springer Wien New York (2004), 149-164.

[23] Loret B., Gajo A. and Simões F.M.F. (2004). A note on the dissipation due to the generalized diffusion with electro-chemo-mechanical couplings in heteroionic clays. *Eur. J. Mechanics-A/Solids*, **23**(5), 763-782.

[24] Loret B. and F.M.F. Simões (2005). A framework for deformation, generalized diffusion, mass transfer and growth in multi-species multi-phase biological materials, *Eur. J. Mechanics-A/Solids*, **24**(5),757-781.

[25] Majone M., Petrangeli Papini M. and Rolle E. (1996). Modeling lead adsorption on clays by models with and without electrostatic terms. *J. of Colloid and Interface Science*, **179**, 412-425.

[26] Olsen H.W. (1969). Simultaneous fluxes of liquid and charge in saturated kaolinite. *Soil Science Society of America J.*, **33**, 338-344.

[27] Petrangeli Papini M. and Majone M. (2002). Modeling of heavy metal adsorption at clay surfaces. *Encyclopedia of Surface and Colloid Science*, Marcel Dekker, 3483-3498.

[28] Sposito G. (1984). *The surface chemistry of soils*, Oxford University Press, New York.

[29] Thevanayagam S. and Rishindran T. (1998). Injection of nutrients and TEAs in clayey soils using electrokinetics. *J. of the Geotechnical and GeoEnvironmental Engng. Div.*, Transactions of the ASCE, **124**(4), 330-338.

[30] Torrance J.K. and Pirnat M. (1984). Effect of pH on the rheology of marine clay from the site of the South Nation River, Canada, Landslide of 1971. *Clays and Clay Minerals*, **32**(5), 384-390.

[31] Wan T.Y and Mitchell J.K. (1976). Electro-osmotic consolidation of soils. *J. of the Geotechnical Engng. Div.*, Transactions of the ASCE, **102**(5), 473-491.

[32] Yeung A.T. (1990). Electrokinetic barrier to contaminant transport through compacted clay, PhD Dissertation, University of California, Berkeley, 260 pp.

[33] Yeung A.T. and Datla S. (1995). Fundamental formulation of electrokinetic extraction of contaminants from soil. *Canadian Geotechnical J.*, **32**, 569-583. Discussion, *Canadian Geotechnical J.*, **33**, 682-684.

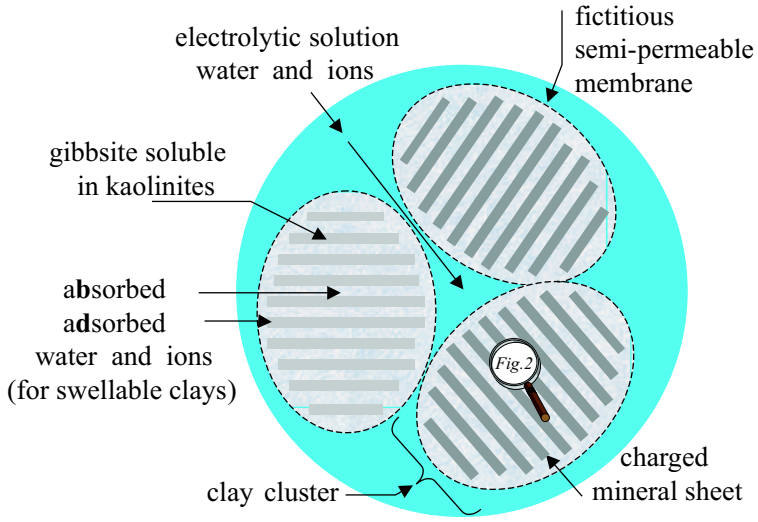

Figure 1 Clay minerals are grouped into clusters, in local contact with each others. Altogether, clusters form the skeleton of the clay, referred to as solid phase. The clusters are bathed in an electrolytic solution, referred to as the fluid phase, whose composition can be changed by external agents. Thus the domain of influence of the electrically charged clay particles does not cover the total porous medium. For a spatially homogeneous clay mass in equilibrium with a reservoir, the chemical composition of the water adsorbed to the particles is distinct from those of the fluid phase and reservoir, which are identical. In swellable clays, water and ions exchange between the two phases.

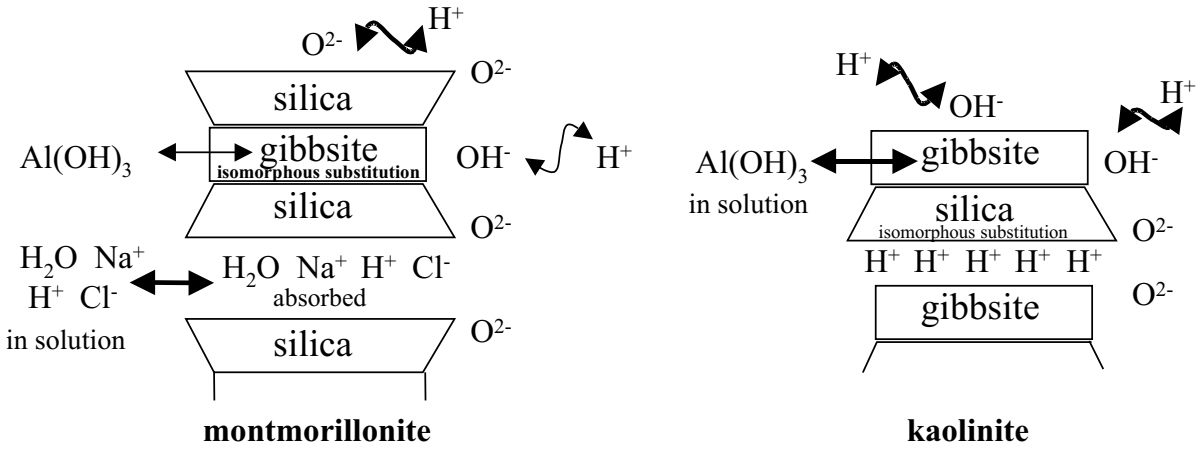

Figure 2 Standard sketches of the three main sheet structures of clays. This representation is not at scale and it does not indicate the height-to-width ratios, which are much smaller for montmorillonites than for kaolinites. A low height-to-width ratio implies large specific surface and intense ion exchange. The nature and amount of ions that adsorb on the surface of clay sheets, or absorb in the interlayer space, depend on the clay type. The thickness of the arrows is proportional to the intensity of the exchange. A large height-to-width ratio implies strong edge effects, dominated by pH: the clay minerals, and consequently the electrical charge, undergo large changes in clays sensitive to pH like kaolinites, where in addition acid-base reactions take place on some faces. For montmorillonites, both ion exchange and change of the electrical charge are significant.
Hydrogen ions can replace other exchangeable cations, even of higher valence, leading to modifications of the mineral structure, like dissolution of gibbsite. This phenomenon is not accounted for in this analysis.

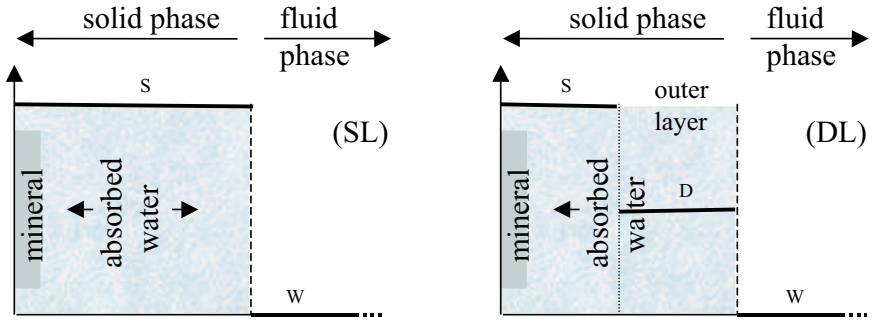

Figure 3 As a refinement of the single layer scheme (SL), where the electrical potential ϕ is uniform in the whole absorbed water, the double layer scheme (DL) considers a piecewise spatial variation, that allows the electrical potential in the outer layer to be endowed with an intermediate value. The double layer scheme is to be viewed as a (crude) attempt to represent the actual nonlinear variation of the electrical potential in the absorbed water.

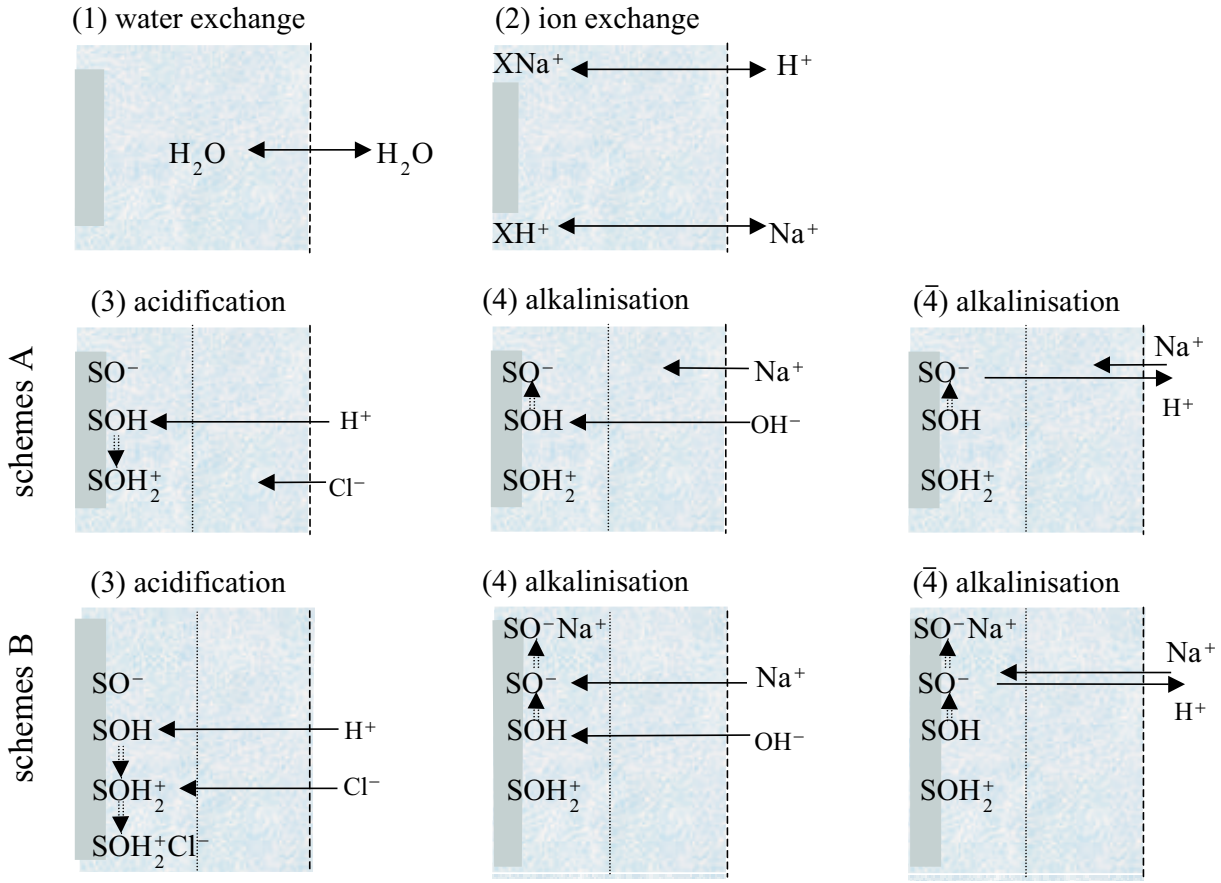

Figure 4 The four exchange mechanisms between the solid and fluid phases. In schemes A, accompanying ions intended to ensure electroneutrality of the phases stay in the outer layer, while, in schemes B, they sorb to the charged clay sites to form inner sphere complexes. The electrical potential that ions in the absorbed water undergo can be tracked by their position, according to Fig. 3. Exchange of water (1) and ion exchange (2) leave the electrical charge of the clay mineral unchanged, in contrast to surface complexation, (3), (4) or ($\overline{4}$). Even if the later reactions are shown one-sided, they are in fact reversible. Sketches (4) and ($\overline{4}$) are two possible representations of alkalinization of the fluid phase. While ionic exchanges and surface complexations both involve water exchange, the phenomenon has been isolated as an independent transfer mechanism (1).

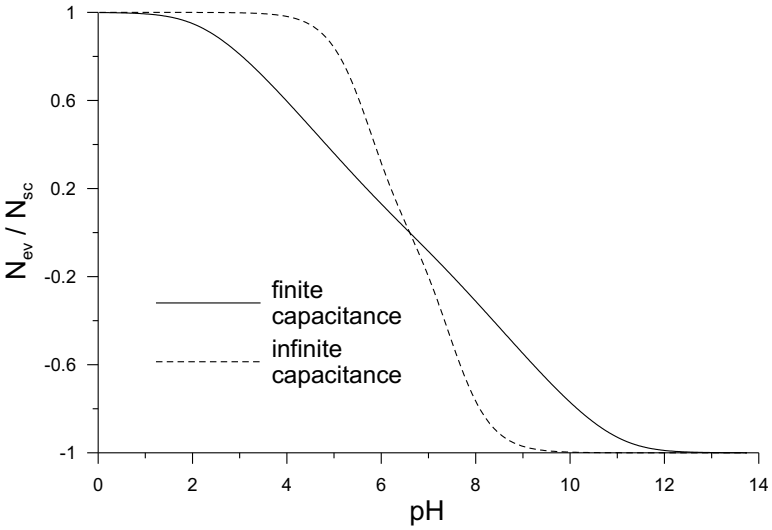

(a) Relative electrical charge N_{ev}/N_{sc}

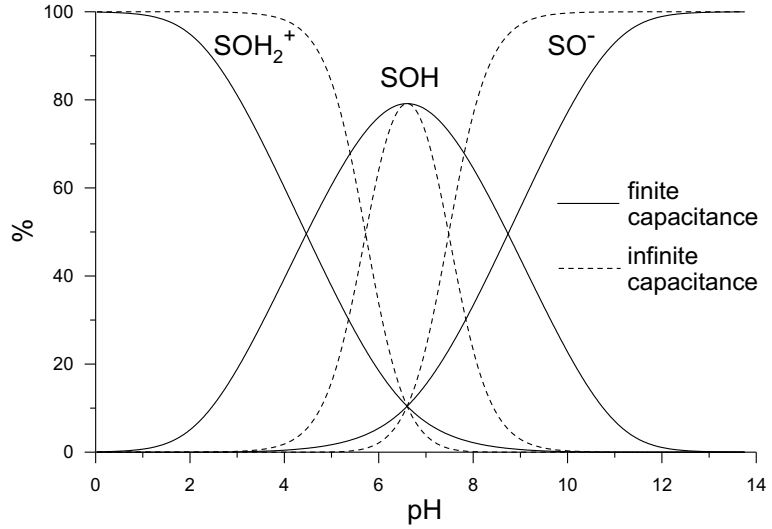

(b) Variation of the relative number of the three surface sites

Figure 5 Variation of the number of surface sites in terms of the pH of the fluid phase. The capacitance just affects the smoothness of the curves, and not the extremum values of the site numbers. As expected, the number of sites S–OH_2^+ decreases, and the number of sites S–O^- increases, as the fluid phase becomes alkaline. The value of the pH at which both the variable charge vanishes and the number of sites S–OH is maximum depends only on the equilibrium constants associated to the acid-base reactions, as indicated by the relations (8.3)-(8.4).

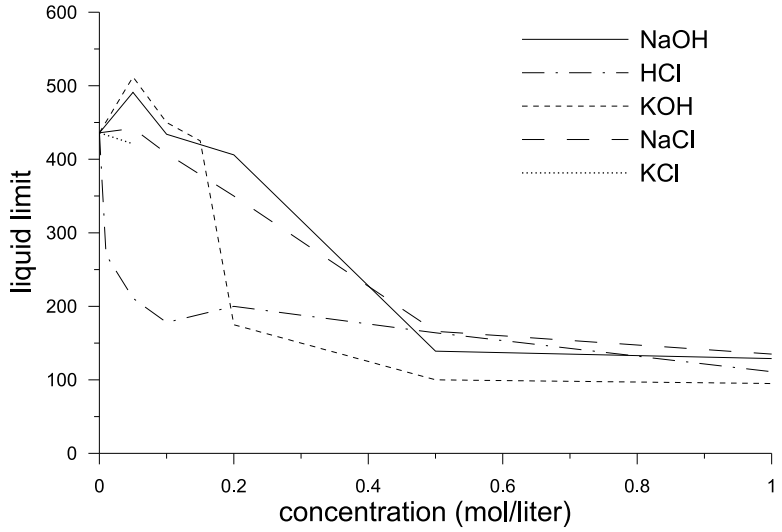

(a) Natural clay

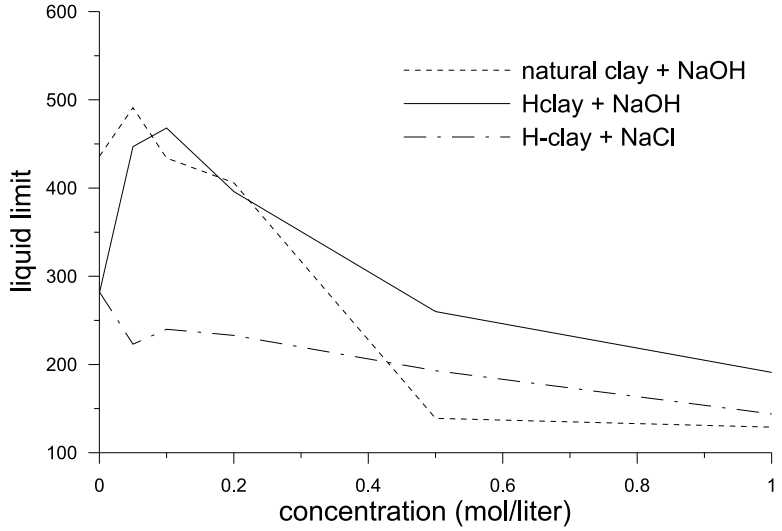

(b) H-clay

Figure 6 Evolution of the liquid limit (LL) for a Na-bentonite clay (a), and a H-clay (b) as function of the pore water composition, from Gajo and Maines [2005]. Some solutions imply a non monotonous variation of the LL as the concentration increases. Thus the total ionic strength has a significant influence, but individual ions have clearly distinct effects at low strength. A qualitative and quantitative interpretation of these effects involves three ion-induced mechanical effects, namely ion exchange, surface complexation and electrical shielding.

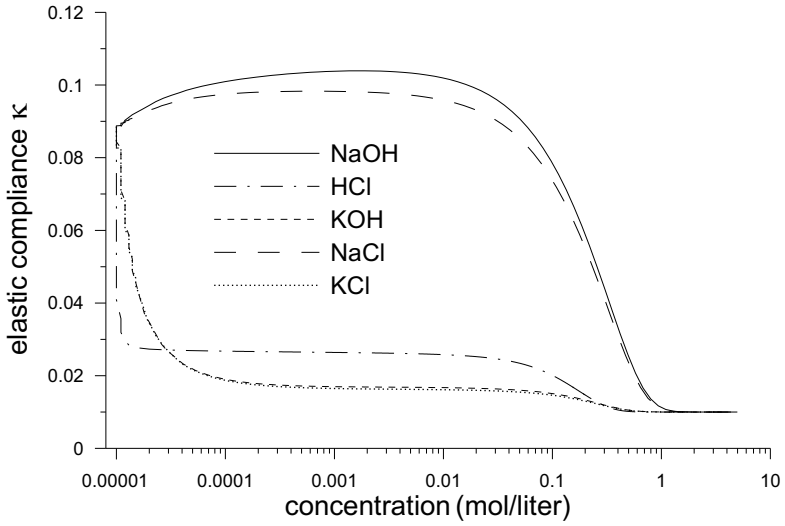

(a) Reservoir of infinite volume

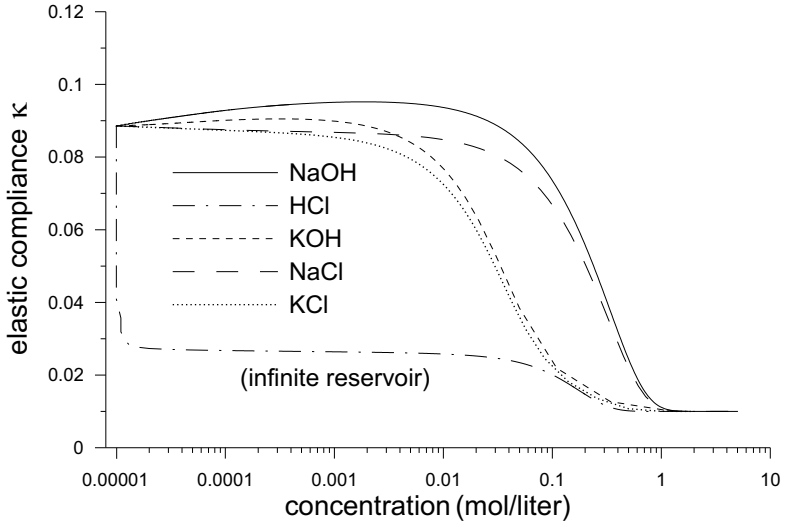

(b) Reservoir of finite volume

Figure 7 When a clay sample is put in contact with a reservoir of varying chemical composition, the ratio of the volumes of the reservoir and of the sample affects the ionic concentration at equilibrium, being the result of adsorption/desorption mechanisms. Thus only tests performed with an infinitely large reservoir (a) display the intrinsic ionic influence on the elastic coefficient κ, which controls the elastic volume variation. Tests with a finite reservoir, with a mass fifteen times larger than the sample, do not deliver intrinsic material properties (b).

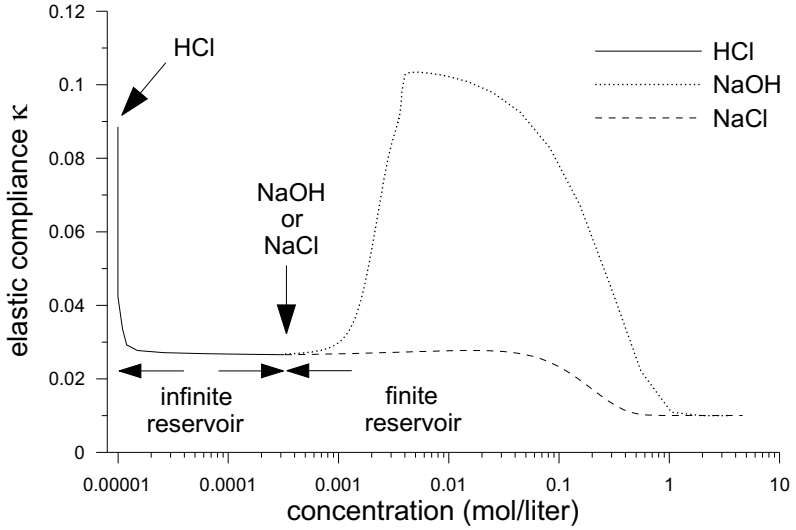

Figure 8 The dramatic opposite effects on the volumetric mechanical properties of the ions hydrogen and hydroxyl are highlighted by submitting a H-clay to either sodium chloride NaCl or sodium hydroxyde NaOH.

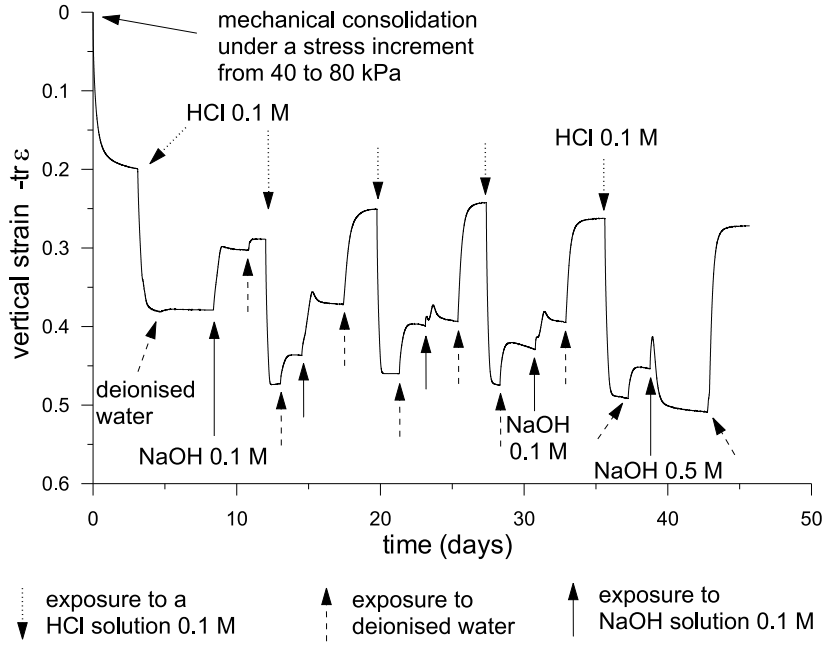

(a) Experimental data

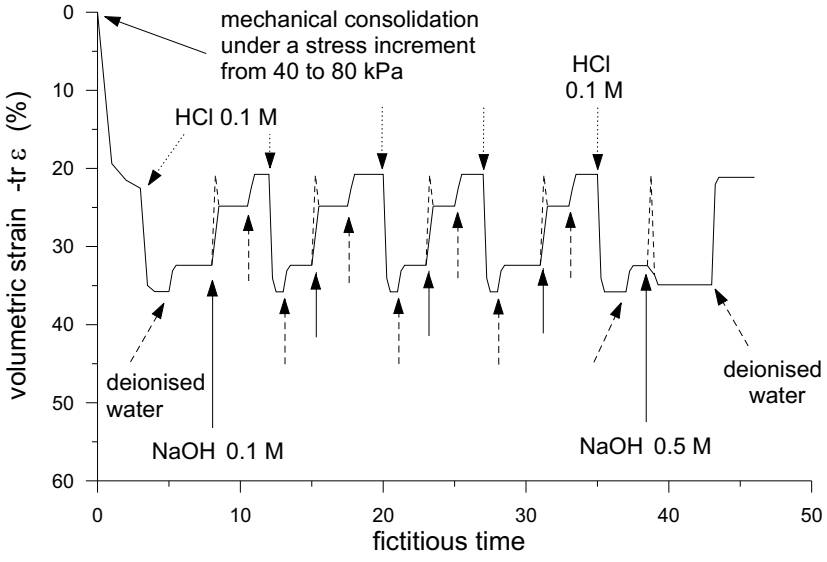

(b) Simulations

Figure 9 The Na-bentonite initially in equilibrium with a reservoir of deionised water is first consolidated with a load of 80 kPa. Once equilibrium is reached, the load is kept constant while the chemical composition of the reservoir is modified by successively increasing the concentration of HCl or NaOH to 0.1 M or 0.5 M and refreshing its water. (a) Experimental data by Gajo and Maines [2005]; (b) Model simulations.

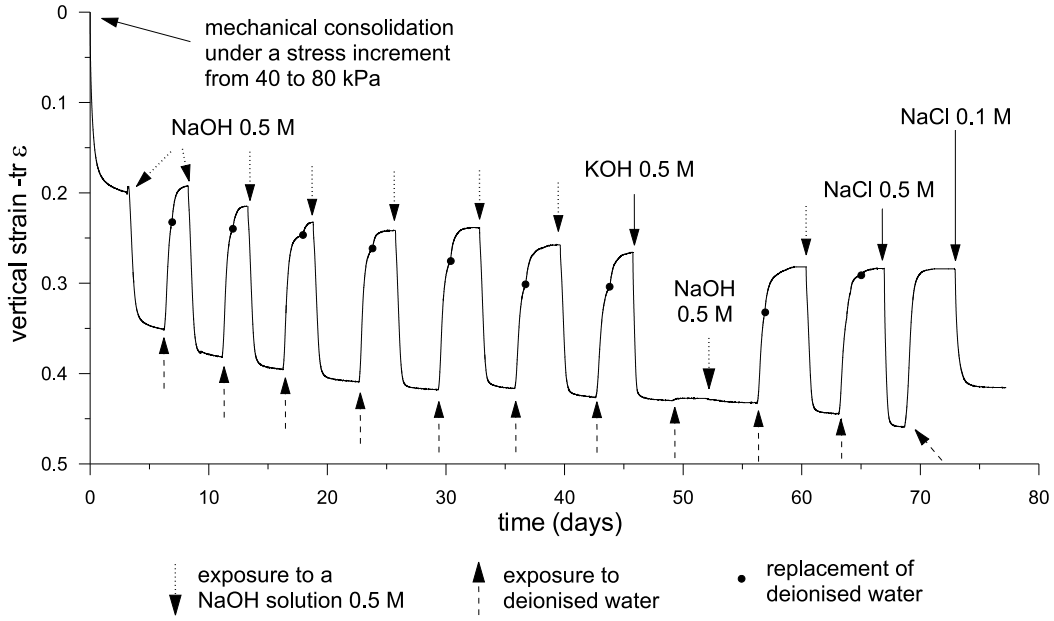

(a) Experimental data

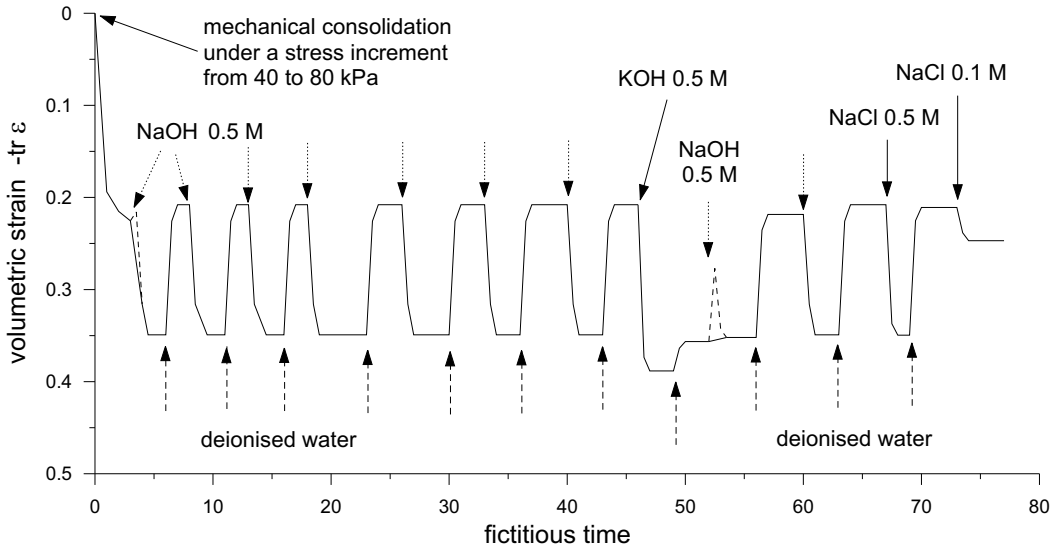

(b) Simulations

Figure 10 The Na-bentonite initially in equilibrium with a reservoir of deionised water is first consolidated with a load of 80 kPa, as in Fig. 9. The subsequent chemical loading sequence involves however larger concentrations and sodium hydroxyde instead of hydrochloric acid. (a) Experimental data by Gajo and Maines [2005]; (b) Model simulations.

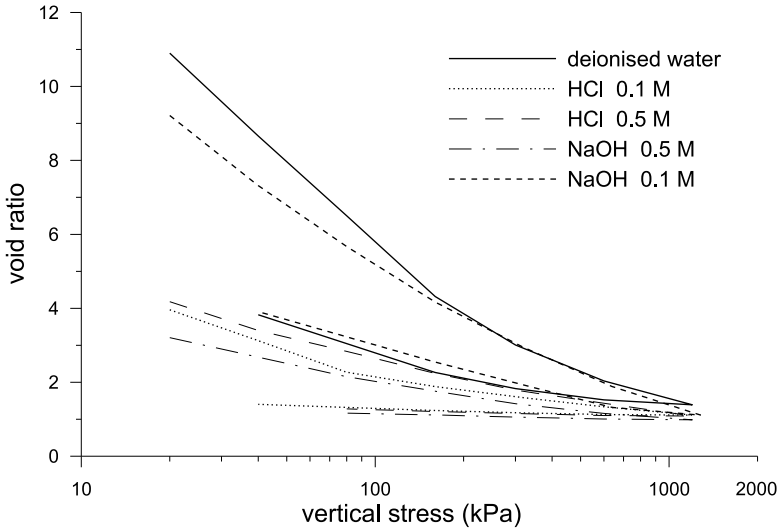

(a) Experimental data

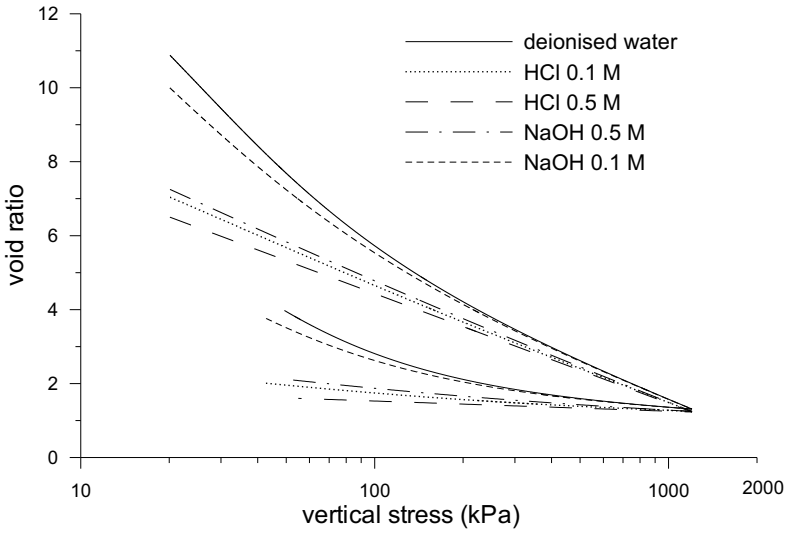

(b) Model simulations

Figure 11 Oedometric consolidation and swelling tests at given pore water composition. (a) Experimental data by Gajo and Maines [2005] on samples prepared in suspensions of given chemical composition; (b) Model simulations.

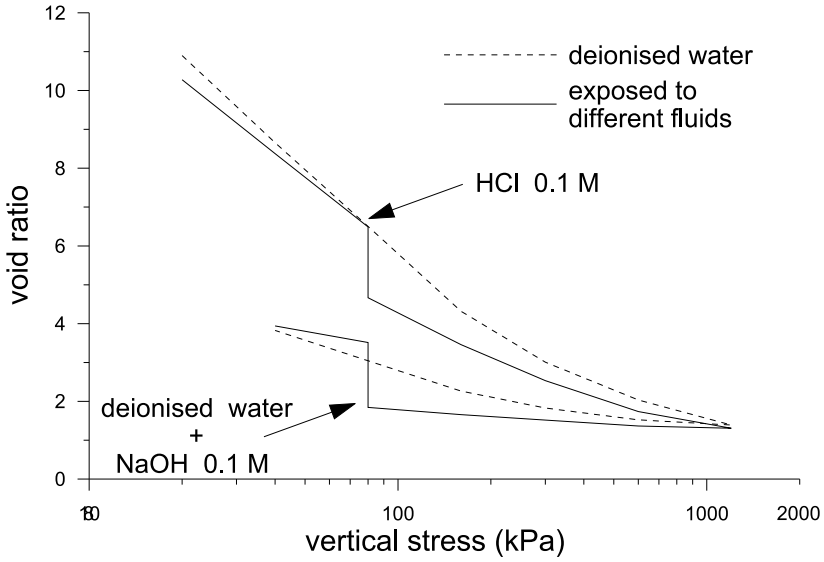

(a) Experimental data

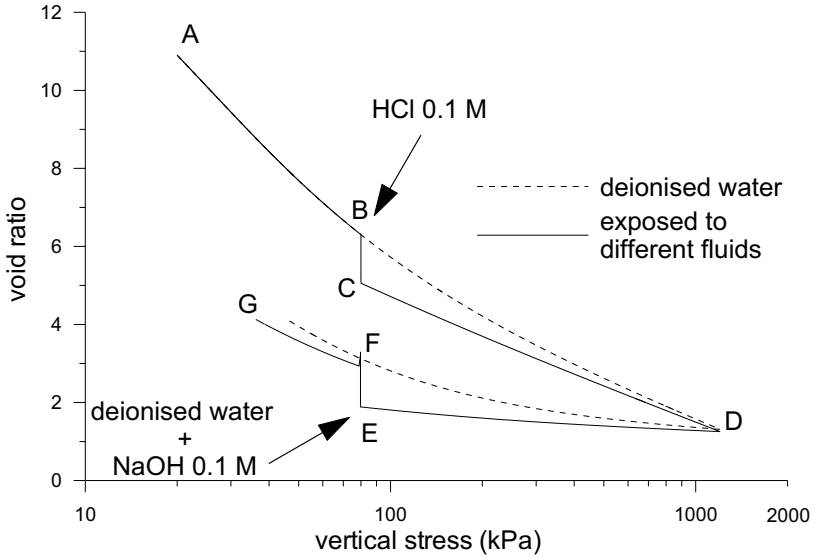

(b) Simulations

Figure 12 Mixed mechanical and chemical loading paths. (a) Experimental data by Gajo and Maines [2005]; (b) model simulations. The purely mechanical oedometric compression test with deionised water is shown for comparison purposes.

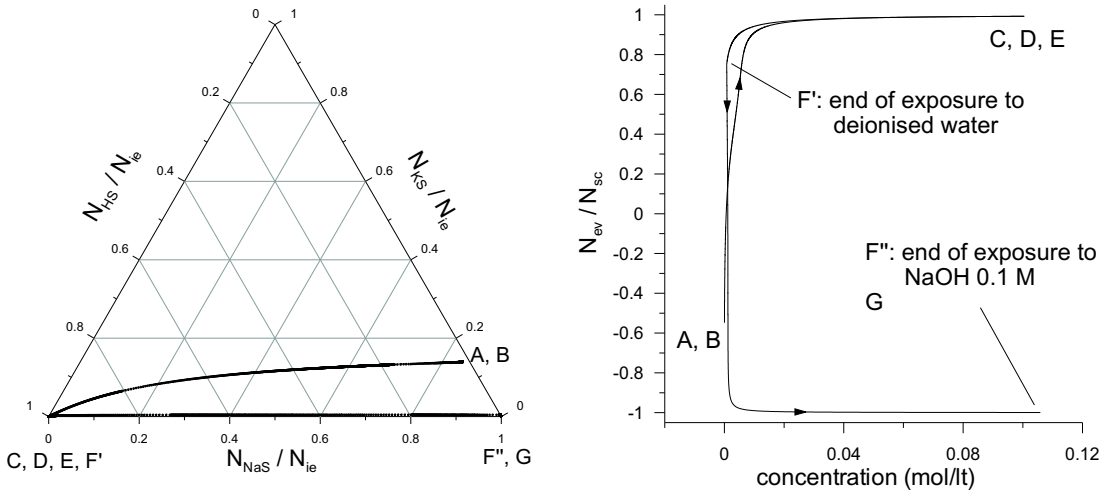

(a) Ion exchange mechanism

(b) Surface charge

Figure 13 Evolution of the concentrations of ions involved in the ion exchange mechanism (a) and of the variable charge (b) associated to the simulations of the mixed mechanical and chemical loading path shown in Fig. 12-(b). The points A to G are indicated on this figure.

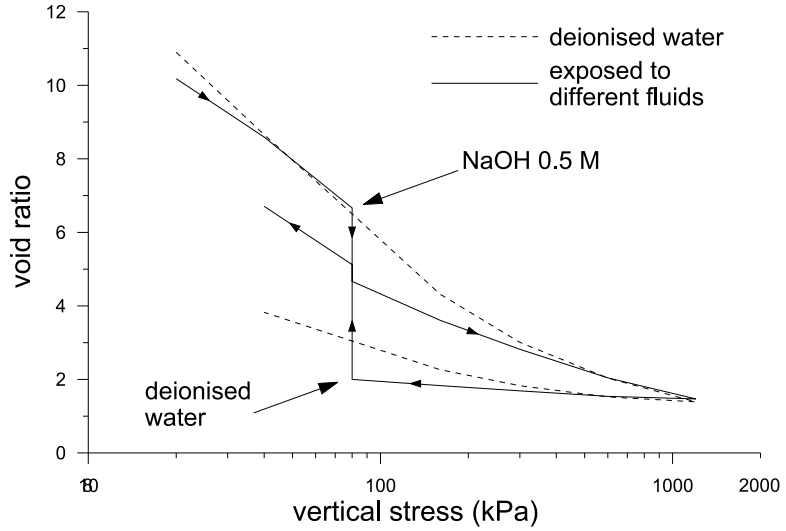

(a) Experimental data

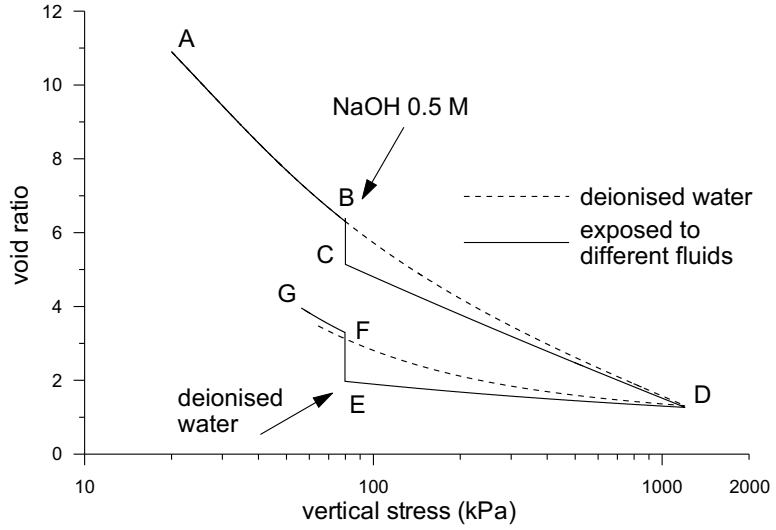

(b) Model simulations

Figure 14 Mixed mechanical and chemical loading paths. (a) Experimental data by Gajo and Maines [2005]; (b) model simulations.

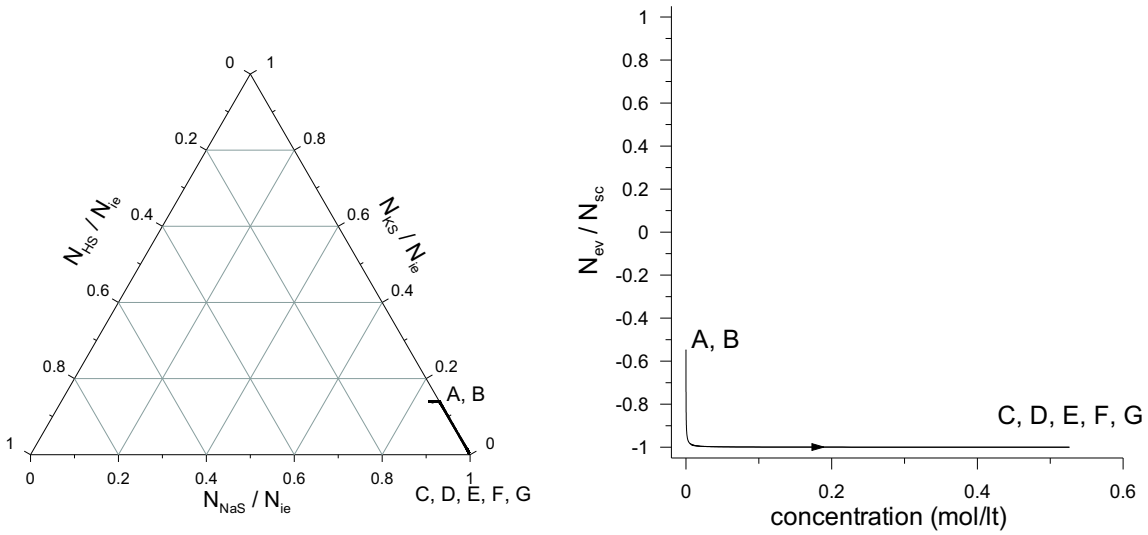

(a) Ion exchange mechanism

(b) Surface charge

Figure 15 Evolution of the concentrations of ions involved in the ion exchange mechanism (a) and of the variable charge (b) associated to the simulations of the mixed mechanical and chemical loading path shown in Fig. 14-(b). The points A to G are indicated on this figure.

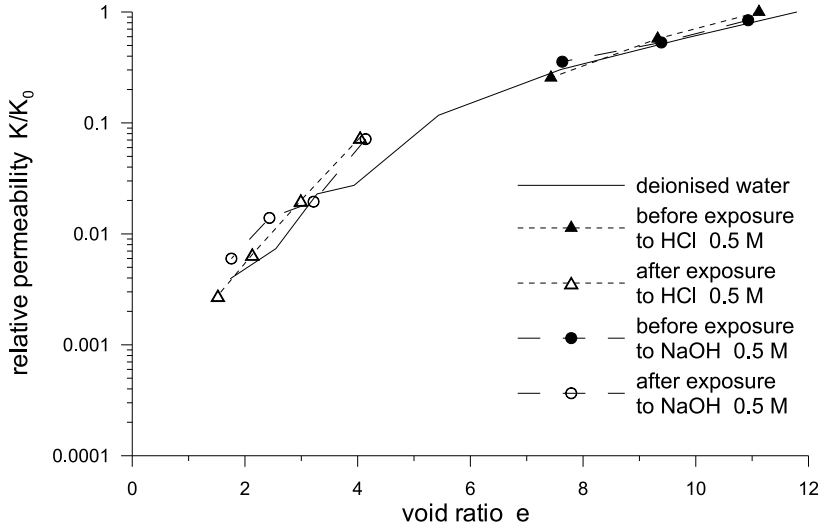

(a) Natural clay. Experimental data

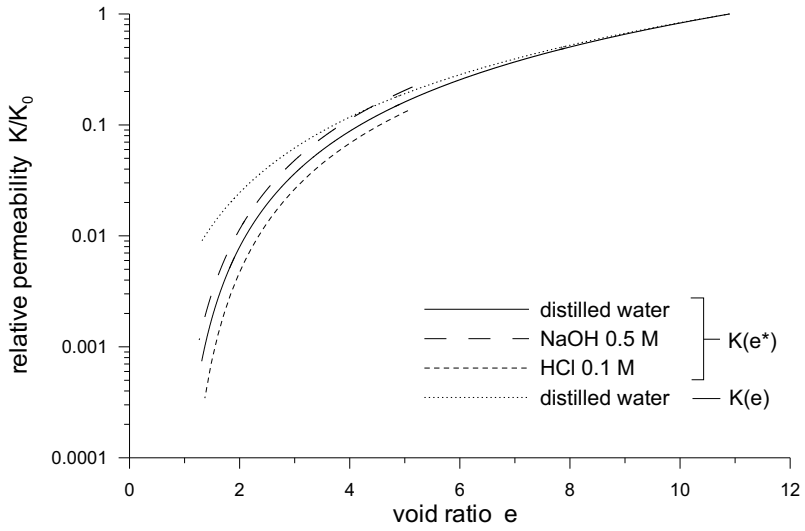

(b) Simulations

Figure 16 Evolution of the hydraulic conductivity during oedometric compression tests at given pore water composition. (a) Experimental data by Gajo and Maines [2005]; (b) model predictions in terms of the void ratios e or e^*.

Appendix A: Ion exchange with three ions Na^+, K^+, and H^+

The liquid limit (LL) of a pure Na-montmorillonite is about 700%. Since the experimental values of the LL is lower, ions other than sodium are concluded to be present and to participate to the ion exchange process. The simple tentative possibility is to consider that three monovalent cations compete for the clay sites X:

$$\begin{aligned} \mathrm{XK^+} \;+\; \underbrace{\mathrm{H^+}}_{\text{fluid phase}} \;&\rightleftharpoons \mathrm{XH^+} \;+\; \underbrace{\mathrm{K^+}}_{\text{fluid phase}} \;, \\ \mathrm{XNa^+} \;+\; \underbrace{\mathrm{K^+}}_{\text{fluid phase}} \;&\rightleftharpoons \mathrm{XK^+} \;+\; \underbrace{\mathrm{Na^+}}_{\text{fluid phase}} \;. \end{aligned} \tag{A.1}$$

The transfer relations replacing (5.8) are, assuming identical transfer times,

$$\begin{aligned} \frac{\delta N_{\mathrm{HS}}}{\delta t} &= -\frac{1}{\tau_2}\,\mathrm{Ln}\,\frac{x^{(2)}_{\mathrm{HS}}}{x^{(2)}_{\mathrm{KS}}}\,\frac{x_{\mathrm{KW}}}{x_{\mathrm{HW}}}\,\frac{1}{K^{(2)}_{\mathrm{H-K}}}\,, \\ \frac{\delta N_{\mathrm{KS}}}{\delta t} &= -\frac{1}{\tau_2}\,\mathrm{Ln}\,\frac{x^{(2)}_{\mathrm{KS}}}{x^{(2)}_{\mathrm{NaS}}}\,\frac{x_{\mathrm{NaW}}}{x_{\mathrm{KW}}}\,\frac{1}{K^{(2)}_{\mathrm{K-Na}}}\,. \end{aligned} \tag{A.2}$$

Note that K_2^{eq} is equal to the product of the two constants $K_2^{\mathrm{H-K}}$ and $K_2^{\mathrm{K-Na}}$. The number of sites for ion exchange is still constant, and (5.28) is replaced by

$$N^{(2)}_{\mathrm{HS}} + N^{(2)}_{\mathrm{NaS}} + N^{(2)}_{\mathrm{KS}} = N_{ie}\,. \tag{A.3}$$

The relative weights $\tilde{\omega}_k = N^{(2)}_{k\mathrm{S}}/N_{ie}$, k=H,Na,K, in terms of chemical affinities, of the three ions are needed for the interpolation of the mechanical compliances. They are obtained as a generalization of eqn (C.2),

$$\frac{N^{(2)}_{\mathrm{HS}}}{N^{(2)}_{\mathrm{KS}}} \simeq \exp\Big(\frac{\mathcal{G}_{\mathrm{H-K}} - \mathcal{G}^0_{\mathrm{H-K}}}{RT}\Big), \quad \frac{N^{(2)}_{\mathrm{KS}}}{N^{(2)}_{\mathrm{NaS}}} \simeq \exp\Big(\frac{\mathcal{G}_{\mathrm{K-Na}} - \mathcal{G}^0_{\mathrm{K-Na}}}{RT}\Big)\,. \tag{A.4}$$

Appendix B: Chemical interpolation of the elastic coefficient κ

To estimate the effects of pore water composition on the elastic coefficient κ, a first step consists in calculating the elastic molar fractions $x^{\rm el}_{k\rm S}$, $k \in \mathcal{S}$, from the set $\mathcal{N}^{\rm el}_{\rm S}$.

With this preliminary step in mind, the coefficient κ depends on the chemical content in two ways:
- a first dependence is postulated, at given electric charge, with respect to the molar fractions of absorbed water and of the ions involved in ion exchange,

$$\mathcal{I}_{ie} = \{{\rm H}^{+(2)}, {\rm Na}^{+(2)}\}\,, \tag{B.1}$$

- a second dependence is introduced with respect to the electrical charge of the clay mineral, that is with respect to the set

$$\mathcal{I}_{sc} = \{{\rm SOH}_2^+, {\rm SO}^-\}\,. \tag{B.2}$$

B1. Interpolation over individual ionic planes of $\mathcal{I}_{ie}$

We consider in turn the hypothetical extreme situations where the molar fraction of one ion, say cation ${\rm Na}^{+(2)}$, is dominant in both phases. We get measures or approximations of the values of $\kappa^{\rm dw}_{\rm Na}$ and $\kappa^{\rm sat}_{\rm Na}$ corresponding respectively to a deionised and salt-saturated pore water. Then, the chemical influence of absorbed water on κ is introduced through interpolation between these two situations. The same calibration is performed on the other k-plane where the molar fraction of the ion $k \in \mathcal{I}_{ie}$ dominates.

The notations $(x^{\rm el}_{l\rm S})^{k\rm sat}$ and $(x^{\rm el}_{l\rm S})^{k\rm dw}$ refer to the molar fractions of species k, the pore water solution being k-saturated and deionised water respectively. The influence of absorbed water is introduced via the scaling functions $\theta_k(x^{\rm el}_{\rm wS})$,

$$\theta_k(x^{\rm el}_{\rm wS}) = \frac{x^{\rm el}_{\rm wS} - (x^{\rm el}_{\rm wS})^{k\rm dw}}{(x^{\rm el}_{\rm wS})^{k\rm sat} - (x^{\rm el}_{\rm wS})^{k\rm dw}}\,, \quad k \in \mathcal{I}_{ie}\,. \tag{B.3}$$

The elastic coefficient κ_k on the plane k is assumed in the form

$$\kappa_k = \kappa_k(x^{\rm el}_{\rm wS}) = \kappa_{1k}\,\Phi(\kappa_{3k}\theta_k) + \kappa_{2k}, \quad k \in \mathcal{I}_{ie}. \tag{B.4}$$

For definiteness, we take

$$\Phi(0) = 0, \quad \Phi'(0) \equiv \frac{d\Phi}{dy}(y=0) = 1\,. \tag{B.5}$$

For example, Φ may be the hyperbolic tangent tanh and then $\Phi'(y) = 1 - \tanh^2(y)$.

The coefficients κ_{1k}, κ_{2k} and κ_{3k} are obtained from the measurable quantities $\kappa^{\rm dw}_k$ and $\kappa^{\rm sat}_k$ and from the slope $d\kappa/dx^{\rm el}_{\rm wS}(x^{\rm el}_{\rm wS} = (x^{\rm el}_{\rm wS})^{k\rm dw})$, namely

$$\kappa_{2k} = \kappa^{\rm dw}_k\,, \quad \kappa_{1k} = \frac{\kappa^{\rm sat}_k - \kappa^{\rm dw}_k}{\Phi(\kappa_{3k})}\,, \quad k \in \mathcal{I}_{ie}, \tag{B.6}$$

and

$$\frac{\kappa_{3k}}{\Phi(\kappa_{3k})} = \frac{(x^{\rm el}_{\rm wS})^{k\rm sat} - (x^{\rm el}_{\rm wS})^{k\rm dw}}{\kappa^{\rm sat}_k - \kappa^{\rm dw}_k}\,\frac{d\kappa}{dx^{\rm el}_{\rm wS}}((x^{\rm el}_{\rm wS})^{k\rm dw})\,, \quad k \in \mathcal{I}_{ie}. \tag{B.7}$$

B2. Interpolation over the ions of $\mathcal{I}_{ie}$

A second interpolation is performed that weighs the relative number of moles of the ions in $\mathcal{I}_{ie}$.

The individual influence of the cations is defined by the weighting function ω_k,

$$\omega_k = \frac{\mathcal{N}^{\rm el}_{k\rm S}}{\mathcal{N}_{ie}}\,, \quad k \in \mathcal{I}_{ie}; \quad \sum_{k\in\mathcal{I}_{ie}} \omega_k = 1\,, \tag{B.8}$$

such that the coefficient κ at given electric charge (state (a)) is

$$\kappa_{\rm (a)} = \kappa_1\,\Phi(\kappa_3\,\theta) + \kappa_2, \tag{B.9}$$

with

$$\kappa_1 = \sum_{k\in\mathcal{I}_{ie}} \omega_k\,\kappa_{1k}, \quad \kappa_2 = \sum_{k\in\mathcal{I}_{ie}} \omega_k\,\kappa_{2k}, \quad \kappa_3\theta = \sum_{k\in\mathcal{I}_{ie}} \omega_k\,\kappa_{3k}\theta_k. \tag{B.10}$$

B3. Interpolation over the electric charge of the clay particle

The mineral electrical charge is characterized by the relative site number $\xi_{ev} = \mathcal{N}_{ev}^{\rm el}/\mathcal{N}_{sc} \in [-1,1]$ which depends on the set $\mathcal{N}_{\rm S}^{\rm el}$ as described in Sect. 5.5. The complete expression of the elastic coefficient is obtained by interpolation of its values $\kappa_{\rm (a)}$ and $\kappa_{\rm (b)}$ at low and high pH through the function $z(\xi_{ev})$,

$$\kappa = Z(\xi_{ev})\,\kappa_{\rm (a)}, \quad Z(\xi_{ev}) \equiv (1 - z(\xi_{ev}))\,R + z(\xi_{ev}), \quad R \equiv \frac{\kappa_{\rm (b)}}{\kappa_{\rm (a)}}\,. \tag{B.11}$$

The interpolation may tentatively be taken linear,

$$z(\xi_{ev}) = \frac{\xi_{ev} - \xi_{ev}^{\rm (b)}}{\xi_{ev}^{\rm (a)} - \xi_{ev}^{\rm (b)}}\,. \tag{B.12}$$

A non monotonous function may be chosen instead, for example to highlight the fact that the electric repulsion between particles is minimum at the isoelectric point.

B4. Useful derivatives

The differential $d\kappa$ is calculated as follows:

$$d\kappa = \overbrace{Z\,\underbrace{d\kappa_{\rm (a)}}_{\rm (B.14)}}^{\text{mechanisms 1,2}} + \overbrace{\kappa_{\rm (a)}\,\underbrace{\frac{\partial Z}{\partial \xi_{ev}}\,d\xi_{ev}}_{\rm (B.17)(B.21)(B.27)}}^{\text{mechanisms 3,4}} \tag{B.13}$$

1. Term $d\kappa_{\rm (a)}$ under mechanisms 1 (water exchange) and 2 (ion exchange):

$$\begin{aligned} d\kappa_{\rm (a)}|_{\xi_{ev}} &= \frac{\partial \kappa_{\rm (a)}}{\partial x_{\rm wS}^{\rm el}}\,dx_{\rm wS}^{\rm el} + \sum_{k\in\mathcal{I}_{ie}} \frac{\partial \kappa_{\rm (a)}}{\partial \mathcal{N}_{k\rm S}^{\rm el}}\,d\mathcal{N}_{k\rm S}^{\rm el} \\ &= (\sum_{k\in\mathcal{I}_{ie}} B_k)\,dx_{\rm wS}^{\rm el} + \frac{A_{\rm H} - A_{\rm Na}}{\mathcal{N}_{ie}}\,d\mathcal{N}_{2\rm S}^{\rm el}\,, \end{aligned} \tag{B.14}$$

with

$$A_k = \kappa_{1k}\Phi(\kappa_3\theta) + \kappa_{2k} + \kappa_1\kappa_{3k}\,\theta_k\,\Phi'(\kappa_3\theta), \quad B_k = \kappa_1\kappa_{3k}\,\omega_k\,\frac{d\theta_k}{dx_{\rm wS}^{\rm el}}\,\Phi'(\kappa_3\theta)\,, \quad k \in \mathcal{I}_{ie}\,, \tag{B.15}$$

and

$$\frac{d\theta_k}{dx_{\rm wS}^{\rm el}} = \frac{1}{(x_{\rm wS}^{\rm el})^{k\rm sat} - (x_{\rm wS}^{\rm el})^{k\rm dw}}, \quad k \in \mathcal{I}_{ie}\,. \tag{B.16}$$

2. Term $dZ(\xi_{ev})$:

$$\frac{\partial Z}{\partial \xi_{ev}} = (1 - R)\,\underbrace{\frac{dz}{d\xi_{ev}}}_{\text{Sect. B3}}\,. \tag{B.17}$$

Partial derivatives of molar fractions are needed to calculate

$$d\kappa = \sum_{n=1,3/4} \frac{\partial \kappa}{\partial \mathcal{N}_{n\rm S}^{\rm el}}\,d\mathcal{N}_{n\rm S}^{\rm el}\,, \tag{B.18}$$

with

$$\frac{\partial \kappa}{\partial \mathcal{N}_{n\rm S}^{\rm el}} = Z\,(\sum_{k\in\mathcal{I}_{ie}} B_k)\,\underbrace{\frac{\partial x_{\rm wS}^{\rm el}}{\partial \mathcal{N}_{1\rm S}^{\rm el}}\,I_{n1}}_{(B.22)/(B.28)} + Z\,\frac{A_{\rm H} - A_{\rm Na}}{\mathcal{N}_{ie}}\,I_{n2} + \kappa_{\rm (a)}\,\frac{\partial Z}{\partial \xi_{ev}}\,\underbrace{\frac{d\xi_{ev}}{\partial \mathcal{N}_{n\rm S}^{\rm el}}}_{(B.21)/(B.27)}, \quad n \in [1, 3/4]\,. \tag{B.19}$$

For the ion exchange mechanism,

$$d\,\frac{x_{\rm HS}^{\rm el2}}{x_{\rm NaS}^{\rm el2}} = d\,\frac{\mathcal{N}_{2\rm S}^{\rm el}}{\mathcal{N}_{ie} - \mathcal{N}_{2\rm S}^{\rm el}} = \frac{\mathcal{N}_{ie}}{(\mathcal{N}_{ie} - \mathcal{N}_{2\rm S}^{\rm el})^2}\,d\mathcal{N}_{2\rm S}^{\rm el}\,. \tag{B.20}$$

The relations (B.21) and (B.22) below differ for a single and two acid-base mechanisms.

B5. Elastic stiffness for two acid-base mechanisms, n=4

$$d\xi_{ev} = \frac{1}{\mathcal{N}_{\rm c}} \left(d\mathcal{N}^{\rm el}_{3\rm S} - d\mathcal{N}^{\rm el}_{4\rm S} \right). \tag{B.21}$$

Eqn (6.9) et seq. yields

$$dx^{\rm el}_{\rm wS} = (1 - x^{\rm el}_{\rm wS}) \, \frac{d\mathcal{N}^{\rm el}_{1\rm S}}{\mathcal{N}^{\rm el}_{\rm S}} \, . \tag{B.22}$$

$$\begin{bmatrix} -d\overline{p} \\ d\overline{\mathcal{G}}_{1\rm S} \\ d\overline{\mathcal{G}}_{2\rm S} \\ d\overline{\mathcal{G}}_{3\rm S} \\ d\overline{\mathcal{G}}_{4\rm S} \end{bmatrix} = \begin{bmatrix} B_{pp} & B_{p1} & B_{p2} & B_{p3} & B_{p4} \\ B_{1p} & B_{11} & B_{12} & B_{13} & B_{14} \\ B_{2p} & B_{21} & B_{22} & B_{23} & B_{24} \\ B_{3p} & B_{31} & B_{32} & B_{33} & B_{34} \\ B_{4p} & B_{41} & B_{42} & B_{43} & B_{44} \end{bmatrix} \begin{bmatrix} d{\rm tr}\boldsymbol{\epsilon}^{\rm el} \\ d\mathcal{N}^{\rm el}_{1\rm S} \\ d\mathcal{N}^{\rm el}_{2\rm S} \\ d\mathcal{N}^{\rm el}_{3\rm S} \\ d\mathcal{N}^{\rm el}_{4\rm S} \end{bmatrix}, \tag{B.23}$$

with

$$B_{pp} = \frac{\overline{p}}{\kappa}, \quad B_{pn} = B_{np} = \frac{\overline{p}}{\kappa} \underbrace{\frac{dF}{d\overline{p}}}_{(6.12)} \underbrace{\frac{\partial \kappa}{\partial \mathcal{N}^{\rm el}_{n\rm S}}}_{(B.19)}, \quad n \in [1,4] \, , \tag{B.24}$$

and

$$\begin{aligned} B_{nm} = B_{mn} \;=\; & -F \frac{\partial^2 \kappa}{\partial \mathcal{N}^{\rm el}_{n\rm S} \, \partial \mathcal{N}^{\rm el}_{m\rm S}} + \frac{\overline{p}}{\kappa} \left(\frac{dF}{d\overline{p}} \right)^2 \frac{\partial \kappa}{\partial \mathcal{N}^{\rm el}_{n\rm S}} \frac{\partial \kappa}{\partial \mathcal{N}^{\rm el}_{m\rm S}} \\ & + \underbrace{\frac{RT}{\mathcal{N}^{\rm el}_{\rm S}} \frac{1 - x^{\rm el}_{\rm wS}}{x^{\rm el}_{\rm wS}}}_{(B.22)} I_{n1} I_{m1} \\ & + \underbrace{RT \frac{\mathcal{N}_{ie}}{\mathcal{N}^{\rm el2}_{\rm NaS} \, \mathcal{N}^{\rm el}_{2\rm S}}}_{(B.20)} I_{n2} I_{m2} \\ & + \left(\frac{RT}{\mathcal{N}^{\rm el}_{\rm SOH_2}} + \frac{RT}{\mathcal{N}^{\rm el}_{\rm SOH}} + \frac{F^2 V_0}{G_e} \right) I_{n3} I_{m3} + \left(\frac{RT}{\mathcal{N}^{\rm el}_{\rm SOH}} + \frac{RT}{\mathcal{N}^{\rm el}_{\rm SO}} + \frac{F^2 V_0}{G_e} \right) I_{n4} I_{m4} \\ & + \left(\frac{RT}{\mathcal{N}^{\rm el}_{\rm SOH}} - \frac{F^2 V_0}{G_e} \right) \left(I_{n3} I_{m4} + I_{n4} I_{m3} \right), \quad m, n \in [1,4] \, . \end{aligned} \tag{B.25}$$

with

$$\mathcal{N}^{\rm el2}_{\rm NaS} = \mathcal{N}_{ie} - \mathcal{N}^{\rm el}_{2\rm S}, \quad \mathcal{N}^{\rm el}_{\rm SOH_2} = \mathcal{N}^{\rm el}_{3\rm S}, \quad \mathcal{N}^{\rm el}_{\rm SO} = \mathcal{N}^{\rm el}_{4\rm S}, \quad \mathcal{N}^{\rm el}_{\rm SOH} = \mathcal{N}_{sc} - \mathcal{N}^{\rm el}_{3\rm S} - \mathcal{N}^{\rm el}_{4\rm S} \, . \tag{B.26}$$

B6. Elastic stiffness for a single acid-base mechanism, n=3

$$d\xi_{ev} = \frac{2}{\mathcal{N}_{\rm c}}\, d\mathcal{N}_{\rm 3S}^{\rm el}\,. \tag{B.27}$$

Eqn (F.11) et seq. yields

$$dx_{\rm wS}^{\rm el} = (1 - x_{\rm wS}^{\rm el})\, \frac{d\mathcal{N}_{\rm 1S}^{\rm el}}{\mathcal{N}_{\rm S}^{\rm el}}\,. \tag{B.28}$$

$$\begin{bmatrix} -d\overline{p} \\ d\overline{\mathcal{G}}_{\rm 1S} \\ d\overline{\mathcal{G}}_{\rm 2S} \\ d\overline{\mathcal{G}}_{\rm 3S} \end{bmatrix} = \begin{bmatrix} B_{pp} & B_{p1} & B_{p2} & B_{p3} \\ B_{1p} & B_{11} & B_{12} & B_{13} \\ B_{2p} & B_{21} & B_{22} & B_{23} \\ B_{3p} & B_{31} & B_{32} & B_{33} \end{bmatrix} \begin{bmatrix} d{\rm tr}\boldsymbol{\epsilon}^{\rm el} \\ d\mathcal{N}_{\rm 1S}^{\rm el} \\ d\mathcal{N}_{\rm 2S}^{\rm el} \\ d\mathcal{N}_{\rm 3S}^{\rm el} \end{bmatrix}, \tag{B.29}$$

with

$$B_{pp} = \frac{\overline{p}}{\kappa}, \quad B_{pn} = B_{np} = \frac{\overline{p}}{\kappa} \underbrace{\frac{dF}{d\overline{p}}}_{(6.12)} \underbrace{\frac{\partial \kappa}{\partial \mathcal{N}_{n\rm S}^{\rm el}}}_{(B.19)}, \quad n \in [1,3]\,, \tag{B.30}$$

and[8]

$$\begin{aligned} B_{nm} = B_{mn} \;=\; & -F\, \frac{\partial^2 \kappa}{\partial \mathcal{N}_{n\rm S}^{\rm el}\, \partial \mathcal{N}_{m\rm S}^{\rm el}} + \frac{\overline{p}}{\kappa} \left(\frac{dF}{d\overline{p}}\right)^2 \frac{\partial \kappa}{\partial \mathcal{N}_{n\rm S}^{\rm el}}\, \frac{\partial \kappa}{\partial \mathcal{N}_{m\rm S}^{\rm el}} \\ & + \underbrace{\frac{RT}{\mathcal{N}_{\rm S}^{\rm el}} \frac{1 - x_{\rm wS}^{\rm el}}{x_{\rm wS}^{\rm el}}}_{(B.28)}\, I_{n1} I_{m1} \\ & + RT\, \frac{\mathcal{N}_{ie}}{\mathcal{N}_{\rm NaS}^{\rm el2}\, \mathcal{N}_{\rm 2S}^{\rm el}}\, I_{n2} I_{m2} \\ & + \left(\frac{RT}{\mathcal{N}_{\rm SOH_2}^{\rm el}} + \frac{RT}{\mathcal{N}_{\rm SO}^{\rm el}} + 4\, \frac{F^2 V_0}{G_e}\right) I_{n3} I_{m3}\,, \quad m,n \in [1,3]\,, \end{aligned} \tag{B.31}$$

with

$$\mathcal{N}_{\rm NaS}^{\rm el2} = \mathcal{N}_{ie} - \mathcal{N}_{\rm 2S}^{\rm el}, \quad \mathcal{N}_{\rm SOH_2}^{\rm el} = \mathcal{N}_{\rm 3S}^{\rm el}, \quad \mathcal{N}_{\rm SO}^{\rm el} = \mathcal{N}_{sc} - \mathcal{N}_{\rm 3S}^{\rm el}\,. \tag{B.32}$$

[8]Note that the coefficients 2 in (F.12) disappear in the relations below because of the 2 in (F.7).

Appendix C: Inversion of the elastic constitutive relations

While the elastic coefficient κ depends on chemistry via the numbers of moles, or the mole contents $\mathcal{N}^{\rm el}_{\rm S}$, a formal simplification arises in the elastic-plastic model when κ, then noted $\tilde\kappa$, is expressed in terms of the set $\overline{\mathcal{G}}_{\rm S}$ of electro-chemical affinities. Therefore, a partial inversion of the elastic constitutive relations is required. We examine in turn the various relations.

1. $x^{\rm el}_{\rm wS} = x^{\rm el}_{\rm wS}(\overline{\mathcal{G}}_{\rm 1S})$.

The chemical dependence of κ in $\mathcal{N}^{\rm el}_{\rm 1S} = \mathcal{N}^{\rm el}_{\rm wS}$ is realized through the molar fraction $x^{\rm el}_{\rm wS}$. The inversion of (6.18) yields,

$$x^{\rm el}_{\rm wS} = \phi^{(1)}(\overline{\mathcal{G}}_{\rm 1S}) = \exp\Big(\frac{1}{RT}\,(\overline{\mathcal{G}}_{\rm 1S} + F(\overline{p})\,\frac{\partial\kappa}{\partial\mathcal{N}^{\rm el}_{\rm 1S}})\Big) \Rightarrow \frac{d\phi^{(1)}}{d\overline{\mathcal{G}}_{\rm 1S}} = \frac{\phi^{(1)}}{RT}\,. \tag{C.1}$$

Given $x^{\rm el}_{\rm wS} = \mathcal{N}^{\rm el}_{\rm 1S}/\mathcal{N}^{\rm el}_{\rm S}$ where $\mathcal{N}^{\rm el}_{\rm S}$ is defined as indicated by (6.9), the number of moles of water $\mathcal{N}^{\rm el}_{\rm 1S}$ is readily deduced.

2. $\mathcal{N}^{\rm el}_{\rm 2S} = \mathcal{N}^{\rm el}_{\rm 2S}(\overline{\mathcal{G}}_{\rm 2S})$.

In practice the chemical dependence of κ in $\mathcal{N}^{\rm el}_{\rm 2S}$ is realized through $x^{\rm el2}_{\rm HS}/x^{\rm el2}_{\rm NaS}$. The inversion of (6.19) yields readily this ratio, as well as $\mathcal{N}^{\rm el}_{\rm 2S}$,

$$\frac{x^{\rm el2}_{\rm HS}}{x^{\rm el2}_{\rm NaS}} = \frac{\mathcal{N}^{\rm el}_{\rm 2S}}{\mathcal{N}_{ie} - \mathcal{N}^{\rm el}_{\rm 2S}} = \phi^{(2)}(\overline{\mathcal{G}}_{\rm 2S}) = \exp\Big(\frac{\overline{\mathcal{G}}_{\rm 2S} - \mathcal{G}^0_{\rm 2S}}{RT} + \frac{F(\overline{p})}{RT}\,\frac{\partial\kappa}{\partial\mathcal{N}^{\rm el}_{\rm 2S}}\Big) \Rightarrow \frac{d\phi^{(2)}}{d\overline{\mathcal{G}}_{\rm 2S}} = \frac{\phi^{(2)}}{RT}\,. \tag{C.2}$$

Two acid-base mechanisms:

3-4. $\mathcal{N}^{\rm el}_{\rm 3S} = \mathcal{N}^{\rm el}_{\rm 3S}(\overline{\mathcal{G}}_{\rm 3S}, \overline{\mathcal{G}}_{\rm 4S})$, $\mathcal{N}^{\rm el}_{\rm 4S} = \mathcal{N}^{\rm el}_{\rm 4S}(\overline{\mathcal{G}}_{\rm 3S}, \overline{\mathcal{G}}_{\rm 4S}) \Rightarrow \mathcal{N}^{\rm el}_{ev} = \mathcal{N}^{\rm el}_{\rm 3S} - \mathcal{N}^{\rm el}_{\rm 4S} = \mathcal{N}^{\rm el}_{ev}(\overline{\mathcal{G}}_{\rm 3S}, \overline{\mathcal{G}}_{\rm 4S})$.

The inversion of these two quantities can not be made in explicit form. One may proceed as follows. First, let

$$a = \frac{F^2\,V_0}{G_e RT}\,\mathcal{N}_{sc}, \quad b = a\,\frac{\mathcal{N}_{ep}}{\mathcal{N}_{sc}} + \frac{F}{RT}\,\phi_{\rm W} - \frac{F(\overline{p})}{RT}\,\frac{\partial\kappa}{\partial\mathcal{N}^{\rm el}_{ev}}\,, \tag{C.3}$$

and

$$E = \exp(a\,\frac{\mathcal{N}^{\rm el}_{ev}}{\mathcal{N}_{sc}}), \quad E_3 = \exp\Big(-\frac{\overline{\mathcal{G}}_{\rm 3S} - \mathcal{G}^0_{\rm 3S}}{RT} + b\Big), \quad E_4 = \exp\Big(+\frac{\overline{\mathcal{G}}_{\rm 4S} - \mathcal{G}^0_{\rm 4S}}{RT} + b\Big)\,. \tag{C.4}$$

Using (5.29),(6.15),(6.20) and (6.21), then

$$\frac{\mathcal{N}^{\rm el}_{\rm 3S}}{\mathcal{N}_{sc}} = \frac{1}{1 + E_3\,E + E_3\,E_4\,E^2}\,, \quad \frac{\mathcal{N}^{\rm el}_{\rm SOH}}{\mathcal{N}_{sc}} = \frac{E_3\,E}{1 + E_3\,E + E_3\,E_4\,E^2}\,, \quad \frac{\mathcal{N}^{\rm el}_{\rm 4S}}{\mathcal{N}_{sc}} = \frac{E_3\,E_4\,E^2}{1 + E_3\,E + E_3\,E_4\,E^2}\,. \tag{C.5}$$

The number of electrical variable charge per unit initial volume $\mathcal{N}^{\rm el}_{ev} = \mathcal{N}^{\rm el}_{\rm 3S} - \mathcal{N}^{\rm el}_{\rm 4S} \in [-\mathcal{N}_{sc},\ \mathcal{N}_{sc}]$ can be shown to be solution of the implicit equation

$$\frac{\mathcal{N}^{\rm el}_{ev}}{\mathcal{N}_{sc}} = \frac{1 - E_3\,E_4\,E^2}{1 + E_3\,E + E_3\,E_4\,E^2}\,. \tag{C.6}$$

Note that

$$\begin{aligned}&\Big(\frac{1}{E_3\,E} + 1 + E_4\,E + a\,\frac{\mathcal{N}^{\rm el}_{ev}}{\mathcal{N}_{sc}} + 2\,a\,(\frac{\mathcal{N}^{\rm el}_{ev}}{\mathcal{N}_{sc}} + 1)\,E_4\,E\Big)\,d\mathcal{N}^{\rm el}_{ev} = \\ &\frac{\mathcal{N}_{sc}}{RT}\,\Big(\frac{\mathcal{N}^{\rm el}_{ev}}{\mathcal{N}_{sc}} + (\frac{\mathcal{N}^{\rm el}_{ev}}{\mathcal{N}_{sc}} + 1)\,E_4\,E\Big)\,d\overline{\mathcal{G}}_{\rm 3S} - \frac{\mathcal{N}_{sc}}{RT}\,(\frac{\mathcal{N}^{\rm el}_{ev}}{\mathcal{N}_{sc}} + 1)\,E_4\,E\,d\overline{\mathcal{G}}_{\rm 4S}\,.\end{aligned} \tag{C.7}$$

The derivative of the elastic coefficient κ due to the dependence in electric charge is as follows

$$\kappa = \kappa(\ldots, \mathcal{N}^{\rm el}_{ev}) = \tilde\kappa(\ldots, \overline{\mathcal{G}}_{\rm 3S}, \overline{\mathcal{G}}_{\rm 4S}) \Rightarrow d\kappa = \ldots + \frac{\partial\kappa}{\partial\mathcal{N}^{\rm el}_{ev}}\,d\mathcal{N}^{\rm el}_{ev} = \ldots + \frac{\partial\kappa}{\partial\mathcal{N}^{\rm el}_{ev}}\,\Big(\frac{d\mathcal{N}^{\rm el}_{ev}}{d\overline{\mathcal{G}}_{\rm 3S}}\,d\overline{\mathcal{G}}_{\rm 3S} + \frac{d\mathcal{N}^{\rm el}_{ev}}{d\overline{\mathcal{G}}_{\rm 4S}}\,d\overline{\mathcal{G}}_{\rm 4S}\Big)\,. \tag{C.8}$$

The derivative $\partial\kappa/\partial\mathcal{N}_{ev}^{\rm el} = \mathcal{N}_{\rm c} \times \partial\kappa/\partial\xi_{ev}$ is provided in Appendix B4, and the derivatives $d\mathcal{N}_{ev}^{\rm el}/d\overline{\mathcal{G}}_{3\rm S}$ and $d\mathcal{N}_{ev}^{\rm el}/d\overline{\mathcal{G}}_{4\rm S}$ by eqn (C.7).

A single acid-base mechanism:

When a single mechanism of acid-base reaction is used, the latter inversion is modified as follows:

3. $\mathcal{N}_{3\rm S}^{\rm el} = \mathcal{N}_{3\rm S}^{\rm el}(\overline{\mathcal{G}}_{3\rm S}) \Rightarrow \mathcal{N}_{ev}^{\rm el} = 2\,\mathcal{N}_{3\rm S}^{\rm el} = \mathcal{N}_{ev}^{\rm el}(\overline{\mathcal{G}}_{3\rm S})$.

The inversion can not be made in explicit form. One may proceed as follows. First, let

$$a = \frac{F^2\,V_0}{G_e RT}\mathcal{N}_{sc}, \quad b = a\,\frac{\mathcal{N}_{ep}}{\mathcal{N}_{sc}} + \frac{F}{RT}\,\phi_{\rm W} - \frac{F(\overline{p})}{RT}\,\frac{\partial\kappa}{\partial\mathcal{N}_{ev}^{\rm el}}\,, \tag{C.9}$$

and

$$E = \exp(a\,\frac{\mathcal{N}_{ev}^{\rm el}}{\mathcal{N}_{sc}}), \quad E_3 = \exp\Big(-\frac{\overline{\mathcal{G}}_{3\rm S} - \mathcal{G}_{3\rm S}^0}{RT} + 2\,b\Big)\,. \tag{C.10}$$

Using (F.12), the number of electrical variable charges per unit initial volume $\mathcal{N}_{ev}^{\rm el} \in [-\mathcal{N}_{sc},\ \mathcal{N}_{sc}]$ can be shown to be solution of the implicit equation [9]

$$\frac{\mathcal{N}_{ev}^{\rm el}}{\mathcal{N}_{sc}} = \frac{1 - E_3\,E^2}{1 + E_3\,E^2}\,. \tag{C.11}$$

Thus

$$\Big(1 + a\,(1 - (\frac{\mathcal{N}_{ev}^{\rm el}}{\mathcal{N}_{sc}})^2)\Big)\,d\mathcal{N}_{ev}^{\rm el} = \frac{1}{2}\,\frac{\mathcal{N}_{sc}}{RT}(1 - (\frac{\mathcal{N}_{ev}^{\rm el}}{\mathcal{N}_{sc}})^2)\,d\overline{\mathcal{G}}_{3\rm S}\,. \tag{C.12}$$

The derivative of the elastic coefficient $\tilde{\kappa}$ due to the dependence in electric charge is as follows

$$\kappa = \kappa(\ldots, \mathcal{N}_{ev}^{\rm el}) = \tilde{\kappa}(\ldots, \overline{\mathcal{G}}_{3\rm S}) \Rightarrow d\kappa = \ldots + \frac{\partial\kappa}{\partial\mathcal{N}_{ev}^{\rm el}}\,d\mathcal{N}_{ev}^{\rm el} = \ldots + \frac{\partial\kappa}{\partial\mathcal{N}_{ev}^{\rm el}}\,\frac{d\mathcal{N}_{ev}^{\rm el}}{d\overline{\mathcal{G}}_{3\rm S}}\,d\overline{\mathcal{G}}_{3\rm S}\,. \tag{C.13}$$

The derivative $\partial\kappa/\partial\mathcal{N}_{ev}^{\rm el} = \mathcal{N}_{\rm c} \times \partial\kappa/\partial\xi_{ev}$ is provided in Appendix B4, and the derivative $d\mathcal{N}_{ev}^{\rm el}/d\overline{\mathcal{G}}_{3\rm S}$ by eqn (C.12).

Warning: since $\mathcal{N} = N/V_0$, then $d\mathcal{N} = dN/V_0$.

[9] The definition of site numbers per unit initial volume for surface complexation $\mathcal{N}_{sc} = N_{sc}/V_0$ excludes now the inert sites SOH, see eqn (F.6).

Appendix D: Chemical interpolations for the plastic coefficients λ and M in terms of $\overline{\mathcal{G}}_{\rm S}$

Since the chemical effects on these two coefficients are assumed to be similar, we just consider one of them, say $\lambda = \lambda(\overline{\mathcal{G}}_{\rm S})$. Formally, a dependence in $\mathcal{N}_{\rm S}^{\rm el}$ similar to that of the elastic coefficient is sought through the partial inversion $\mathcal{N}_{\rm S}^{\rm el}(\overline{\mathcal{G}}_{\rm S})$ exposed in Appendix C that defines the functions $\phi^{(1)}$ ... [10]

D1. Interpolation over individual ionic planes of $\mathcal{I}_{ie}$

We consider in turn the two hypothetical extreme situations where the molar fraction of one cation, say cation $Na^{+(2)}$, overweighs the other in both phases. We may get measures or approximations of the values of $\lambda_{\rm Na}^{\rm dw}$ and $\lambda_{\rm Na}^{\rm sat}$ corresponding respectively to a deionised and salt-saturated pore water. Then the chemical effect on λ, noted $\lambda_{\rm Na}$, is introduced through interpolation between these two situations, for example

$$\lambda_{\rm Na}(\overline{\mathcal{G}}_{\rm 1S}) = \lambda_{\rm 1Na}\,\Phi(\,\lambda_{\rm 3Na}\,\tilde{\theta}_{\rm Na}(\overline{\mathcal{G}}_{\rm 1S})\,) + \lambda_{\rm 2Na}\,, \tag{D.1}$$

where the $\lambda_{i\rm Na}$'s, $i = 1, 3$, are constants. The hyperbolic tangent is taken as the interpolation function, i.e. $\Phi(y) = \tanh(y)$ and

$$\tilde{\theta}_k(\overline{\mathcal{G}}_{\rm 1S}) = \frac{\phi^{(1)}(\overline{\mathcal{G}}_{\rm 1S}) - \phi^{(1)}(\overline{\mathcal{G}}_{\rm 1S}^{\rm dw})}{\phi^{(1)}(\overline{\mathcal{G}}_{\rm 1S}^{\rm sat}) - \phi^{(1)}(\overline{\mathcal{G}}_{\rm 1S}^{\rm dw})}\,. \tag{D.2}$$

Then

$$\lambda_{\rm 1Na} = \frac{\lambda_{\rm Na}^{\rm sat} - \lambda_{\rm Na}^{\rm dw}}{\Phi(\lambda_{\rm 3Na})}, \quad \lambda_{\rm 2Na} = \lambda_{\rm Na}^{\rm dw}. \tag{D.3}$$

The constant $\lambda_{\rm 3Na}$ can be obtained from the slope $d\lambda/d\overline{\mathcal{G}}_{\rm 1S}$ estimated at $\overline{\mathcal{G}}_{\rm 1S} = \overline{\mathcal{G}}_{\rm 1S}^{\rm dw}$, indeed

$$\frac{\lambda_{\rm 3Na}}{\tanh(\lambda_{\rm 3Na})} = \frac{\phi^{(1)}(\overline{\mathcal{G}}_{\rm 1S}^{\rm sat}) - \phi^{(1)}(\overline{\mathcal{G}}_{\rm 1S}^{\rm dw})}{\lambda_{\rm Na}^{\rm sat} - \lambda_{\rm Na}^{\rm dw}}\,\frac{d\lambda_{\rm Na}}{d\overline{\mathcal{G}}_{\rm 1S}}\,\Big(\frac{d\phi^{(1)}}{d\overline{\mathcal{G}}_{\rm 1S}}\Big)^{-1}. \tag{D.4}$$

The same procedure is followed to define the coefficients$\lambda_{i\rm H}$, $i = 1, 3$.

D2. Interpolation over the ions of $\mathcal{I}_{ie}$

A second interpolation is performed that weighs the relative number of moles of the ions in $\mathcal{I}_{ie}$,

$$\lambda = \lambda_1\,\Phi(\lambda_3\,\tilde{\theta}) + \lambda_2, \tag{D.5}$$

with

$$\lambda_1 = \sum_{k\in\mathcal{I}_{ie}} \tilde{\omega}_k\,\lambda_{1k}, \quad \lambda_2 = \sum_{k\in\mathcal{I}_{ie}} \tilde{\omega}_k\,\lambda_{2k}, \quad \lambda_3\,\tilde{\theta} = \sum_{k\in\mathcal{I}_{ie}} \tilde{\omega}_k\,\lambda_{3k}\,\tilde{\theta}_k\,. \tag{D.6}$$

The weights $\tilde{\omega}_{\rm Na}$ and $\tilde{\omega}_{\rm H}$, with sum equal to 1, are defined as follows,

$$\tilde{\omega}_{\rm Na}(\overline{\mathcal{G}}_{\rm 2S}) = 1 - \tilde{\omega}_{\rm H}(\overline{\mathcal{G}}_{\rm 2S}) = \frac{1}{1+\phi^{(2)}(\overline{\mathcal{G}}_{\rm 2S})}\,. \tag{D.7}$$

D3. Interpolation over the electric charge of the clay particle

The mineral electrical charge is characterized by the variable relative charge $\xi_{ev} = N_{ev}^{\rm el}/N_{sc}$ which is viewed as depending on the electro-chemical affinities $\overline{\mathcal{G}}_{\rm 3S}$ and $\overline{\mathcal{G}}_{\rm 4S}$ as described in Appendix C, that is below $\xi_{ev} = \xi_{ev}(\overline{\mathcal{G}}_{\rm 3S}, \overline{\mathcal{G}}_{\rm 4S})$. The complete expression of the elastic-plastic coefficient λ is obtained mimicking the interpolation for the elastic coefficient κ.

D4. Useful derivatives

two acid-base mechanisms:

$$d\xi_{ev} = \frac{1}{\mathcal{N}_{sc}}\Big(\underbrace{\frac{\partial\mathcal{N}_{ev}^{\rm el}}{\partial\overline{\mathcal{G}}_{\rm 3S}}}_{(C.7)}\,d\overline{\mathcal{G}}_{\rm 3S} + \underbrace{\frac{\partial\mathcal{N}_{ev}^{\rm el}}{\partial\overline{\mathcal{G}}_{\rm 4S}}}_{(C.7)}\,d\overline{\mathcal{G}}_{\rm 4S}\Big)$$

single acid-base mechanism:

$$d\xi_{ev} = \frac{1}{\mathcal{N}_{sc}}\,\underbrace{\frac{\partial\mathcal{N}_{ev}^{\rm el}}{\partial\overline{\mathcal{G}}_{\rm 3S}}}_{(C.12)}\,d\overline{\mathcal{G}}_{\rm 3S}\,. \tag{D.8}$$

Derivatives for $\lambda(\overline{\mathcal{G}}_{\rm S})$:

[10] I note $f(\mathcal{N}_{\rm S}^{\rm el}) = \tilde{f}(\overline{\mathcal{G}}_{\rm S})$, for $f = \kappa, \theta, \omega$.

$$d\lambda = \overbrace{Z \underbrace{d\lambda_{(\mathrm{a})}}_{(D.10)}}^{\text{mechanisms 1,2}} + \overbrace{\lambda_{(\mathrm{a})} \underbrace{\frac{\partial Z}{\partial \xi_{ev}} d\xi_{ev}}_{(D.13)}}^{\text{mechanisms 3,4}} \tag{D.9}$$

$$d\lambda_{(\mathrm{a})} = \Big(\sum_{k\in\mathcal{I}_{ie}} B_k \Big)\, d\overline{\mathcal{G}}_{1\mathrm{S}} + (A_{\mathrm{H}} - A_{\mathrm{Na}})\, \tilde{\omega}_{\mathrm{Na}}\, \tilde{\omega}_{\mathrm{H}} \underbrace{\frac{d\mathrm{Ln}\phi^{(2)}(\overline{\mathcal{G}}_{2\mathrm{S}})}{d\overline{\mathcal{G}}_{2\mathrm{S}}}}_{=1/RT,(C.2)} d\overline{\mathcal{G}}_{2\mathrm{S}}\,, \tag{D.10}$$

$$\frac{d\tilde{\theta}_k}{d\overline{\mathcal{G}}_{1\mathrm{S}}} = \frac{d\tilde{\theta}_k}{d\phi^{(1)}} \frac{d\phi^{(1)}}{d\overline{\mathcal{G}}_{1\mathrm{S}}} = \underbrace{\frac{1}{(x^{\mathrm{el}}_{\mathrm{wS}})^{k\mathrm{sat}} - (x^{\mathrm{el}}_{\mathrm{wS}})^{k\mathrm{dw}}}}_{(D.2)} \underbrace{\frac{x^{\mathrm{el}}_{\mathrm{wS}}}{RT}}_{(C.1)}, \quad k \in \mathcal{I}_{ie}\,. \tag{D.11}$$

$$A_k = \lambda_{1k}\Phi(\lambda_3\tilde{\theta}) + \lambda_{2k} + \lambda_1\lambda_{3k}\,\tilde{\theta}_k\,\Phi'(\lambda_3\tilde{\theta}), \quad B_k = \lambda_1\lambda_{3k} \underbrace{\frac{d\tilde{\theta}_k}{d\overline{\mathcal{G}}_{1\mathrm{S}}}}_{(D.11)} \tilde{\omega}_k\,\Phi'(\lambda_3\tilde{\theta})\,, \quad k \in \mathcal{I}_{ie}\,, \tag{D.12}$$

$$Z(\xi_{ev}) \equiv (1 - z(\xi_{ev}))\, R + z(\xi_{ev}), \quad \frac{\partial Z}{\partial \xi_{ev}} = (1-R) \underbrace{\frac{dz}{d\xi_{ev}}}_{\text{Sect. B3}}, \quad \underbrace{R \equiv \frac{\lambda_{(\mathrm{b})}}{\lambda_{(\mathrm{a})}}}_{(B.11)}. \tag{D.13}$$

Thus altogether

$$d\lambda = \sum_{n=1,3/4} \frac{\partial \lambda}{\partial \overline{\mathcal{G}}_{n\mathrm{S}}}\, d\overline{\mathcal{G}}_{n\mathrm{S}}\,, \tag{D.14}$$

$$\frac{\partial \lambda}{\partial \overline{\mathcal{G}}_{n\mathrm{S}}} = \underbrace{Z}_{(D.13)} \underbrace{(\sum_{k\in\mathcal{I}_{ie}} B_k)}_{(D.12)}\, I_{n1} + \underbrace{Z}_{(D.13)} \underbrace{\frac{A_{\mathrm{H}} - A_{\mathrm{Na}}}{RT}}_{(D.12)} \underbrace{\tilde{\omega}_{\mathrm{Na}}\,\tilde{\omega}_{\mathrm{H}}}_{(D.7)}\, I_{n2} + \lambda_{(\mathrm{a})} \underbrace{\frac{\partial Z}{\partial \xi_{ev}}}_{(D.13)} \underbrace{\frac{d\xi_{ev}}{\partial \overline{\mathcal{G}}_{n\mathrm{S}}}}_{(D.8)}, \quad n \in [1, 3/4]\,, \tag{D.15}$$

Derivatives for $\tilde{\kappa} = \tilde{\kappa}(\overline{\mathcal{G}}_{\mathrm{S}})$:

$$\tilde{\kappa}_{(\mathrm{a})} = \kappa_1\,\Phi(\kappa_3\,\tilde{\theta}) + \kappa_2, \quad \kappa_1 = \sum_{k\in\mathcal{I}_{ie}} \overbrace{\tilde{\omega}_k}^{(D.7)}\, \kappa_{1k}, \quad \kappa_2 = \sum_{k\in\mathcal{I}_{ie}} \overbrace{\tilde{\omega}_k}^{(D.7)}\, \kappa_{2k}, \quad \kappa_3\tilde{\theta} = \sum_{k\in\mathcal{I}_{ie}} \overbrace{\tilde{\omega}_k}^{(D.7)}\, \kappa_{3k}\, \overbrace{\tilde{\theta}_k}^{(D.2)} \tag{D.16}$$

$$A_k = \kappa_{1k}\Phi(\kappa_3\tilde{\theta}) + \kappa_{2k} + \kappa_1\kappa_{3k}\, \overbrace{\tilde{\theta}_k}^{(D.2)}\, \Phi'(\kappa_3\tilde{\theta}), \quad B_k = \kappa_1\kappa_{3k}\, \overbrace{\frac{d\tilde{\theta}_k}{d\overline{\mathcal{G}}_{1\mathrm{S}}}}^{(D.11)}\, \overbrace{\tilde{\omega}_k}^{(D.7)}\, \Phi'(\kappa_3\tilde{\theta})\,, \quad k \in \mathcal{I}_{ie}\,. \tag{D.17}$$

$$\tilde{\kappa} = \tilde{\kappa}_{(\mathrm{a})}\, Z(\xi_{ev}), \quad Z(\xi_{ev}) \equiv (1 - z(\xi_{ev}))\, R + z(\xi_{ev}), \quad \frac{\partial Z}{\partial \xi_{ev}} = (1-R) \underbrace{\frac{dz}{d\xi_{ev}}}_{\text{Sect. B3}}, \quad \underbrace{R \equiv \frac{\tilde{\kappa}_{(\mathrm{a})}}{\tilde{\kappa}_{\mathrm{iso}}}}_{(B.11)}, \tag{D.18}$$

Thus altogether

$$d\tilde{\kappa} = \sum_{n=1,3/4} \frac{\partial \tilde{\kappa}}{\partial \overline{\mathcal{G}}_{n\mathrm{S}}}\, d\overline{\mathcal{G}}_{n\mathrm{S}}\,, \tag{D.19}$$

$$\frac{\partial \tilde{\kappa}}{\partial \overline{\mathcal{G}}_{n\mathrm{S}}} = \underbrace{Z}_{(D.18)} \underbrace{(\sum_{k\in\mathcal{I}_{ie}} B_k)}_{(D.17)}\, I_{n1} + \underbrace{Z}_{(D.18)} \underbrace{\frac{A_{\mathrm{H}} - A_{\mathrm{Na}}}{RT}}_{(D.17)} \overbrace{\tilde{\omega}_{\mathrm{Na}}\,\tilde{\omega}_{\mathrm{H}}}^{(D.7)}\, I_{n2} + \kappa_{(\mathrm{a})} \underbrace{\frac{\partial Z}{\partial \xi_{ev}}}_{(D.18)} \underbrace{\frac{d\xi_{ev}}{\partial \overline{\mathcal{G}}_{n\mathrm{S}}}}_{(D.8)}, \quad n \in [1, 3/4]\,, \tag{D.20}$$

D5. Detailed analysis of chemo-plastic coupling

In order to analyze the chemical influence on p_c, let us consider temporarily a simplified setting. The functions $\tilde{\theta}_k$, k=Na,H, eqn (D.2), which introduce the dependence with respect to the chemical potential of absorbed water $\overline{\mathcal{G}}_{1S}$, are taken to be the same for both cations, that is, in agreement with (D.6),

$$\tilde{\kappa}_{3k} = \kappa_3, \quad \lambda_{3k} = \lambda_3, \quad \theta_k(\overline{\mathcal{G}}_{1S}) = \theta(\overline{\mathcal{G}}_{1S}) \quad \text{for } k = \text{Na, H.} \tag{D.21}$$

Moreover the dependence in electrical charge of the clay particle is also assumed to be described by the same function Z, i.e. the same function z and the same ratio R, as detailed in Appendices B and D.

The dependence of $\lambda - \tilde{\kappa}$ with respect to the chemical potential of absorbed water and to the chemical affinity of exchangeable ions can be identified via (D.2)-(D.7),

$$d(\lambda - \tilde{\kappa}) = \frac{\partial(\lambda - \tilde{\kappa})}{\partial \overline{\mathcal{G}}_{1S}}\, d\overline{\mathcal{G}}_{1S} + \frac{\partial(\lambda - \tilde{\kappa})}{\partial \overline{\mathcal{G}}_{2S}}\, d\overline{\mathcal{G}}_{2S}, \tag{D.22}$$

where, by (D.10), (D.12) and (D.17),

$$\frac{\partial(\lambda - \tilde{\kappa})}{\partial \overline{\mathcal{G}}_{1S}} = \Big(\lambda_1\, \lambda_3\, \Phi'(\lambda_3\theta) - \kappa_1\, \kappa_3\, \Phi'(\kappa_3\theta) \Big)\, \frac{d\theta}{d\overline{\mathcal{G}}_{1S}}\,, \tag{D.23}$$

and, to within the multiplicative factor $\tilde{\omega}_H\, \tilde{\omega}_{Na}/RT$, with help of (D.3),

$$\begin{aligned} \frac{\partial(\lambda - \tilde{\kappa})}{\partial \overline{\mathcal{G}}_{2S}} \quad &\sim \quad (\lambda_{1H} - \lambda_{1Na})\, \Phi(\lambda_3\theta) - (\kappa_{1H} - \kappa_{1Na})\, \Phi(\kappa_3\theta) + (\lambda_{2H} - \lambda_{2Na}) - (\kappa_{2H} - \kappa_{2Na}) \\ &\sim \quad \Big((\lambda_H^{sat} - \lambda_H^{dw}) - (\lambda_{Na}^{sat} - \lambda_{Na}^{dw}) \Big)\, \frac{\Phi(\lambda_3\theta)}{\Phi(\lambda_3)} - \Big((\kappa_H^{sat} - \kappa_H^{dw}) - (\kappa_{Na}^{sat} - \kappa_{Na}^{dw}) \Big)\, \frac{\Phi(\kappa_3\theta)}{\Phi(\kappa_3)} \\ &+ \quad (\lambda_H^{dw} - \lambda_{Na}^{dw}) - (\kappa_H^{dw} - \kappa_{Na}^{dw})\,. \end{aligned} \tag{D.24}$$

Then the coefficient of the chemical affinity in (D.22) vanishes, and only the chemical potential of absorbed water influences p_c, if the material coefficients satisfy the following restrictions,

$$\lambda_{Na}^{sat} - \kappa_{Na}^{sat} = \lambda_H^{sat} - \kappa_H^{sat}, \quad \lambda_{Na}^{dw} - \kappa_{Na}^{dw} = \lambda_H^{dw} - \kappa_H^{dw}, \quad \lambda_{3Na} = \lambda_{3H} = \kappa_{3Na} = \kappa_{3H}. \tag{D.25}$$

If in addition, λ_1=κ_1, that is, again with help of (D.3) if

$$\lambda_{Na}^{sat} - \kappa_{Na}^{sat} = \lambda_H^{sat} - \kappa_H^{sat} = \lambda_{Na}^{dw} - \kappa_{Na}^{dw} = \lambda_H^{dw} - \kappa_H^{dw}, \quad \lambda_{3Na} = \lambda_{3H} = \kappa_{3Na} = \kappa_{3H}, \tag{D.26}$$

there is no chemical influence any longer on p_c and therefore chemical loadings and unloadings at constant effective stress are reversible, if $\overline{p}_\lambda$=$\overline{p}_\kappa$.

D6. Elastic-plastic stiffness n=3/4 single/two acid-base mechanisms

Let the generalized stress and strain vectors to be defined as (vector notation)

$$\Sigma = \begin{bmatrix} -\overline{p} \\ \overline{\mathcal{G}}_{1\mathrm{S}} \\ \overline{\mathcal{G}}_{2\mathrm{S}} \\ \overline{\mathcal{G}}_{3\mathrm{S}} \\ \overline{\mathcal{G}}_{4\mathrm{S}} \end{bmatrix}, \quad E^{\mathrm{el}} = \begin{bmatrix} \mathrm{tr}\boldsymbol{\epsilon}^{\mathrm{el}} \\ \mathcal{N}^{\mathrm{el}}_{1\mathrm{S}} \\ \mathcal{N}^{\mathrm{el}}_{2\mathrm{S}} \\ \mathcal{N}^{\mathrm{el}}_{3\mathrm{S}} \\ \mathcal{N}^{\mathrm{el}}_{4\mathrm{S}} \end{bmatrix}, \quad E = \begin{bmatrix} \mathrm{tr}\boldsymbol{\epsilon} \\ \mathcal{N}_{1\mathrm{S}} \\ \mathcal{N}_{2\mathrm{S}} \\ \mathcal{N}_{3\mathrm{S}} \\ \mathcal{N}_{4\mathrm{S}} \end{bmatrix}. \tag{D.27}$$

The elastic and elastic-plastic behavior may be written,

$$\delta\Sigma = \underbrace{\mathbb{E}^{\mathrm{el}}}_{(B.23)}\,\delta E^{\mathrm{el}}\,, \quad \delta E^{\mathrm{el}} = \delta E - \underbrace{\delta\Lambda\,\frac{\partial g}{\partial \Sigma}}_{(7.3)}\,. \tag{D.28}$$

Plastic consistency implies

$$df = \frac{\partial f}{\partial \Sigma}\,d\Sigma + \frac{\partial f}{\partial \mathrm{tr}\boldsymbol{\epsilon}^{\mathrm{pl}}}(-\delta\Lambda\,\frac{\partial g}{\partial \overline{p}}) = 0\,, \tag{D.29}$$

hence

$$\delta\Lambda = \frac{1}{H}\,\frac{\partial f}{\partial \Sigma}\,\mathbb{E}^{\mathrm{el}}\,\delta E, \quad H = \underbrace{\frac{\partial f}{\partial \mathrm{tr}\boldsymbol{\epsilon}^{\mathrm{pl}}}\,\frac{\partial g}{\partial \overline{p}}}_{=h,\ (D.33)} + \Big(\frac{\partial f}{\partial \Sigma}\Big)^T\,\mathbb{E}^{\mathrm{el}}\,\frac{\partial g}{\partial \Sigma}\,. \tag{D.30}$$

Consequently

$$\delta\Sigma = \Big[\mathbb{E}^{\mathrm{el}} - \frac{1}{H}\,\mathbb{E}^{\mathrm{el}}\frac{\partial g}{\partial \Sigma}\,\frac{\partial f}{\partial \Sigma}\,\mathbb{E}^{\mathrm{el}}\Big]\,\delta E\,. \tag{D.31}$$

For $q = 0$, the yield function and hardening law are

$$\underbrace{f = g = \overline{p} - p_{\mathrm{c}}}_{(7.4)}, \quad \underbrace{(\lambda - \tilde{\kappa})\,\frac{\delta p_{\mathrm{c}}}{p_{\mathrm{c}}} = -\delta\mathrm{tr}\,\boldsymbol{\epsilon}^{\mathrm{pl}} + \mathrm{Ln}\,\frac{\overline{p}_\lambda}{p_{\mathrm{c}}}\,\delta\lambda - \mathrm{Ln}\,\frac{\overline{p}_\kappa}{p_{\mathrm{c}}}\,\delta\tilde{\kappa}}_{(7.6)}\,, \tag{D.32}$$

so that

$$h = \frac{\partial f}{\partial \mathrm{tr}\boldsymbol{\epsilon}^{\mathrm{pl}}}\,\frac{\partial g}{\partial \overline{p}} = \frac{p_{\mathrm{c}}}{\lambda - \tilde{\kappa}}\,, \tag{D.33}$$

and

$$\frac{\partial g}{\partial \Sigma} = \begin{bmatrix} -1 \\ \partial g/\partial \overline{\mathcal{G}}_{1\mathrm{S}} \\ \partial g/\partial \overline{\mathcal{G}}_{2\mathrm{S}} \\ \partial g/\partial \overline{\mathcal{G}}_{3\mathrm{S}} \\ \partial g/\partial \overline{\mathcal{G}}_{4\mathrm{S}} \end{bmatrix}, \quad \frac{\partial g}{\partial \overline{\mathcal{G}}_{n\mathrm{S}}} = -\frac{p_{\mathrm{c}}}{\lambda - \tilde{\kappa}}\Big(\mathrm{Ln}\,\frac{\overline{p}_\lambda}{p_{\mathrm{c}}}\,\underbrace{\frac{\partial \lambda}{\partial \overline{\mathcal{G}}_{n\mathrm{S}}}}_{(D.15)} - \mathrm{Ln}\,\frac{\overline{p}_\kappa}{p_{\mathrm{c}}}\,\underbrace{\frac{\partial \tilde{\kappa}}{\partial \overline{\mathcal{G}}_{n\mathrm{S}}}}_{(D.20)}\Big), \quad n \in [1, 3/4]\,. \tag{D.34}$$

Appendix E: Electroneutrality of the acid-base reactions with schemes (B)

In the acidification process according to scheme (B), Fig. 4, the charged site SOH_2^+ produced by the reaction (5.9) is subsequently neutralized by a chlorine ion, which sorbs to the site,

$$\underbrace{SOH_2^+ - Cl^-}_{\text{clay mineral}} \rightleftharpoons \underbrace{SOH_2^+}_{\text{clay site}} + \underbrace{Cl^-}_{\text{fluid phase}} \quad . \tag{E.1}$$

The work done in the volume V_0 during the reaction is,

$$g^{\rm ec}_{SOH_2Cl}\,\delta N_{SOH_2Cl} + g^{\rm ec}_{SOH_2}\,\delta N_{SOH_2} + g^{\rm ec}_{ClW}\,\delta \hat{N}_{ClW} = \overbrace{(g^{\rm ec}_{SOH_2Cl} - g^{\rm ec}_{SOH_2} - g^{\rm ec}_{ClW})}^{\mathcal{G}_{\underline{3}}}\,\delta N_{SOH_2Cl}\,, \tag{E.2}$$

since $\delta N_{SOH_2Cl} = -\delta N_{SOH_2} = -\delta \hat{N}_{ClW}$. A linear rate of transfer rule defined by a characteristic time $\tau_{\underline{3}}$ and an equilibrium constant $K_{\underline{3}}^{eq}$ can thus be expressed as,

$$\frac{\delta N_{SOH_2Cl}}{\delta t} = -\frac{1}{\tau_{\underline{3}}}\,{\rm Ln}\,\frac{\{SOH_2Cl\}}{\{SOH_2\}}\,\frac{K_{\underline{3}}^{eq}}{x_{ClW}}\,\exp^{-\frac{F[\phi]}{RT}}\,, \tag{E.3}$$

and

$$\delta\{SOH_2Cl\} = -\delta\{SOH_2\} = \delta N_{SOH_2Cl}/A_c\,. \tag{E.4}$$

In order to restore electroneutrality, the two propositions delineated for scheme (A) are now reconsidered.

A very fast second submechanism is physically difficult to motivate as the chlorine ions have to transfer close to the clay site. Moreover, this is mathematically impossible as it would overdetermine the electrical potential, as explained earlier in reference to scheme A.

The second possibility of re-uniting the two submechanisms with equal transfer times requires that the transfer relations (5.12) and (E.3) be equivalent to

$$\frac{\delta \hat{N}_{HW}}{\delta t} = \frac{\delta \hat{N}_{ClW}}{\delta t} = \frac{1}{2\,\tau_3}\,{\rm Ln}\,\frac{\{SOH_2Cl\}}{\{SOH\}}\,\frac{K_3^{eq}}{x_{HW}}\,\frac{K_{\underline{3}}^{eq}}{x_{ClW}}\,, \tag{E.5}$$

which is seen to correspond to the electrically neutral physico-chemical reaction,

$$\underbrace{SOH_2^+ - Cl^-}_{\text{clay mineral}} \rightleftharpoons \underbrace{SOH}_{\text{clay site}} + \underbrace{H^+ + Cl^-}_{\text{fluid phase}}\,. \tag{E.6}$$

Let us now consider the second submechanism of the alkalinization process. The site SO^- produced by the reaction (5.15) is subsequently neutralized by a sodium ion, which sorbs to the charged site,

$$\underbrace{SO^- - Na^+}_{\text{clay mineral}} \rightleftharpoons \underbrace{SO^-}_{\text{clay site}} + \underbrace{Na^+}_{\text{fluid phase}} \quad . \tag{E.7}$$

Since $\delta N_{SONa} = -\delta N_{SO} = -\delta \hat{N}_{NaW}$, the work done in the volume V_0 during the submechanism is,

$$g^{\rm ec}_{SONa}\,\delta N_{SONa} + g^{\rm ec}_{SO}\,\delta N_{SO} + g^{\rm ec}_{NaW}\,\delta \hat{N}_{NaW} = \overbrace{(g^{\rm ec}_{SONa} - g^{\rm ec}_{SO} - g^{\rm ec}_{NaW})}^{\mathcal{G}_{\underline{4}}}\,\delta N_{SONa}\,. \tag{E.8}$$

A linear transfer law, expressed in terms of a characteristic time $\tau_{\underline{4}}$ and an equilibrium constant $K_{\underline{4}}^{eq}$, takes the form,

$$\frac{\delta N_{SONa}}{\delta t} = -\frac{1}{\tau_{\underline{4}}}\,{\rm Ln}\,\frac{\{SONa\}}{\{SO\}}\,\frac{K_{\underline{4}}^{eq}}{x_{NaW}}\,\exp^{\frac{F[\phi]}{RT}}\,, \tag{E.9}$$

and

$$\delta\{SONa\} = -\delta\{SO\} = \delta N_{SONa}/A_c\,. \tag{E.10}$$

Electroneutrality can be established, exactly as for the acidification mechanism, by requiring the rates relations (5.18) and (E.9) to be equivalent.

Appendix F: Single acid-base mechanism

If the number of sites S–OH changes much less than those of the two other sites, acid-base equilibrium is controlled by a single mechanism. The reaction is defined as, Fig. 17,

$$\underbrace{\mathrm{S-OH_2^+}}_{\text{clay site}} \rightleftharpoons \underbrace{\mathrm{S-O^-}}_{\text{clay site}} + \underbrace{2\,\mathrm{H^+}}_{\text{fluid phase}} \quad . \tag{F.1}$$

The work done in the volume V_0 during these exchanges is,

$$\begin{aligned} &\text{in the solid phase}: \ g^{\rm ec}_{\rm SOH_2}\delta N_{\rm SOH_2} + g^{\rm ec}_{\rm SO}\delta N_{\rm SO} = (g^{\rm ec}_{\rm SOH_2} - g^{\rm ec}_{\rm SO})\,\delta N_{\rm SOH_2}\,, \\ &\text{in the fluid phase}: \ g^{\rm ec}_{\rm HW}\delta \hat{N}^{(3)}_{\rm HW}\,. \end{aligned} \tag{F.2}$$

Let $N_{3\rm S} \equiv N_{\rm SOH_2}$. Since $\delta N_{\rm SOH_2} = -\delta N_{\rm SO} = -\frac{1}{2}\,\delta \hat{N}^{(3)}_{\rm HW}$, the dissipation due to this mechanism expresses as $-\mathcal{G}_3\,\delta N_{3\rm S}$ via the electro-chemical affinity $\mathcal{G}_3$,

$$\mathcal{G}_3 = g^{\rm ec}_{\rm SOH_2} - g^{\rm ec}_{\rm SO} - 2\,g^{\rm ec}_{\rm HW}\,. \tag{F.3}$$

In line with (5.1), a linear transfer law for the rate of variation of the mole number of sites $\rm SOH_2$ involves the transfer time $\tau_3 > 0$ and the equilibrium constant K_3^{eq},

$$\frac{\delta N_{3\rm S}}{\delta t} = -\frac{1}{\tau_3}\,\mathrm{Ln}\,\frac{\{\rm SOH_2\}}{\{\rm SO\}}\frac{K_3^{eq}}{x^2_{\rm HW}}e^{\frac{2\,F[\phi]}{RT}}\,, \tag{F.4}$$

with $[\phi]$ as defined by (5.13), and

$$\delta\{\rm SOH_2\} = -\delta\{\rm SO\} = \delta N_{3\rm S}/A_{\rm c}\,. \tag{F.5}$$

Indeed, surface complexation includes now the sites SO and $\rm SOH_2$ only,

$$\begin{aligned} N_{\rm SOH_2} + N_{\rm SO} &= N_{sc}\,, \\ N_{\rm SOH_2} - N_{\rm SO} &= N_{ev}\,, \end{aligned} \tag{F.6}$$

so that

$$\delta N_{ev} = 2\,\delta N_{3\rm S}\,. \tag{F.7}$$

The relations (5.30) are modified as follows,

$$\delta N_{3\rm S} \equiv \delta N_{\rm SOH_2} = -\delta N_{\rm SO} = \frac{1}{2}\delta N^{(3)}_{\rm HS} = -\frac{1}{2}\delta \hat{N}^{(3)}_{\rm HW} = \frac{1}{2}\delta N_{\rm ClS} = -\frac{1}{2}\delta \hat{N}_{\rm ClW}\,, \tag{F.8}$$

while the relations (5.31) become

$$\begin{aligned} \delta \hat{N}_{\rm wW} &= -\delta N_{1\rm S}\,, \\ \delta \hat{N}_{\rm HW} &= -\delta N_{2\rm S} - 2\,\delta N_{3\rm S}\,, \\ \delta \hat{N}_{\rm OHW} &= 0\,, \\ \delta \hat{N}_{\rm NaW} &= \delta N_{2\rm S}\,, \\ \delta \hat{N}_{\rm ClW} &= -\delta N_{\rm ClS} = -2\,\delta N_{3\rm S}\,. \end{aligned} \tag{F.9}$$

The mole content of the variable electrical charge $\mathcal{N}_{ev} = N_{ev}/V_0$ is given by (F.7) as $2\,\mathcal{N}_{3\mathrm{S}}$.

The index n runs from 1 to 3, and $\underline{v}_3 = 2\underline{v}_{\mathrm{H}} + 2\underline{v}_{\mathrm{Cl}}$.

The chemical part of the elastic potential is now

$$\begin{aligned}\varphi_{\mathrm{ch}}(\mathcal{N}_{\mathrm{S}}^{\mathrm{el}}) = RT/V_0 \Big(\quad & N_{\mathrm{S}}\,\mathrm{Ln}N_{\mathrm{S}} - N_{\mathrm{c}}\,\mathrm{Ln}N_{\mathrm{c}} - N_{\mathrm{wS}}\,\mathrm{Ln}N_{\mathrm{wS}} \\ & -N_{\mathrm{HS}}^{(2)}\,\mathrm{Ln}N_{\mathrm{HS}}^{(2)} - N_{\mathrm{NaS}}^{(2)}\,\mathrm{Ln}N_{\mathrm{NaS}}^{(2)} \\ & -N_{\mathrm{SOH_2}}\,\mathrm{Ln}N_{\mathrm{SOH_2}} - N_{\mathrm{SO}}\,\mathrm{Ln}N_{\mathrm{SO}}\Big)\,.\end{aligned} \tag{F.10}$$

The total number of moles N_{S} is defined as

$$N_{\mathrm{S}} = N_{\mathrm{c}} + \underbrace{N_{\mathrm{wS}}}_{=N_{1\mathrm{S}}} + \underbrace{N_{\mathrm{HS}}^{(2)} + N_{\mathrm{NaS}}^{(2)}}_{=N_{ie}} + \underbrace{N_{\mathrm{SOH_2}} + N_{\mathrm{SO}}}_{=N_{sc}}\,, \tag{F.11}$$

and the relation (6.10) still holds.

The mechanism 4 disappears and the mechanism 3 becomes

$$\overline{\mathcal{G}}_{3\mathrm{S}} = \mathcal{G}_{3\mathrm{S}}^{0} - 2\,F(\overline{p})\,\frac{\partial\kappa}{\partial\mathcal{N}_{ev}} + RT\,\mathrm{Ln}\,\frac{\{\mathrm{SOH_2}\}}{\{\mathrm{SO}\}} + 2\,F\,\phi_{\mathrm{S}}\,. \tag{F.12}$$

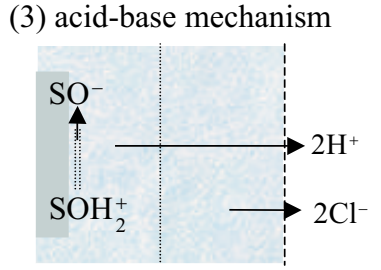

Figure 17 As an alternative to Fig. 4, a single mechanism (3) describes the acid-base reactions.